OFFICE OF ADVANCED RESEARCH AND TECHNOLOGY
SPACE VEHICLES DIVISION

PROCEEDINGS OF CONFERENCE ON

HEAT TRANSFER COMPUTER PROGRAMS

MAY 7, 1964

NASA

NASA HEADQUARTERS

WASHINGTON, D.C.

FOR NASA INTERNAL USE ONLY

TABLE OF CONTENTS

Introduction

On May 7, 1964, at the invitation of Dr. Raymond L. Bisplinghoff, Associate Administrator for Advanced Research and Technology, a conference was held in NASA Headquarters, on the subject "Heat Transfer Computer Programs." The conference was one of several held in Headquarters during the first half of 1964 for review and planning of NASA's research program on space vehicle thermal radiation and temperature control.

The conference brought about a useful interchange of information between the NASA Centers, including JPL, on computer programs which had been developed for the thermal design of spacecraft. The conferees concluded that in addition to our annual conference in this area, a useful continuing exchange of information could be through the establishment of a quarterly newsletter issued from Headquarters describing current efforts. Such a newsletter, on heat transfer computer programs, has been established and it is hoped that the publication of the present proceedings will be a further milestone in advancing the technology of using electronic computers as a tool in the thermal design of space vehicles.

The present volume includes all of the formal presentations made by staff members of the various NASA Centers. Their cooperation, which led to a highly successful conference, is greatly appreciated.

Conrad P. Hook
NASA Headquarters (Code RV-1)
Washington, D.C.

MSFC COMPUTER PROGRAMS UTILIZED IN THE THERMAL DESIGN AND ANALYSIS OF SATELLITES

William C. Snoddy
MSFC

MSFC Computer Programs Utilized in the Thermal Design and Analysis of Satellites

William C. Snoddy
MSFC

INTRODUCTION

Three IBM 7094 computer programs used in the thermal design of spacecraft will be discussed. The first program is one used for integrating spectral reflectance or emittance data to obtain total reflectance or emittance. The second program calculates the percent time a satellite spends in the earth's shadow during a revolution about the earth. And the third program is called our General Space Thermal Program and is used to calculate satellite temperatures throughout a revolution about the earth.

SPECTRAL INTEGRATION PROGRAM

This program integrates spectral radiometric data with respect to blackbody radiation at any temperature or with respect to the Johnson solar radiation curve. One of the advantages of this program over similar programs is the simplicity of data input. Only those data points are needed which together with linear interpolation between points will define the spectral data curve. For example, the curves shown in figure 1 were entered into the computer by reading only those points marked on the curves. These points were chosen because it can be seen that if they are connected by straight lines (which the computer does when it interpolates linearly) the result will closely follow the original curves. Thus, for much spectral data it is necessary to enter only four or five points into the computer.

Figure 2 is the computer printout for the data taken from the upper curve in figure 1. First is given the identification of the sample and then the input data is printed out. Given any two of the following, (1) emittance, (2) reflectance, and (3) transmittance, the computer will calculate the third using Kirchoff's Law. In this case the sample was opaque so that the transmittance was assumed to be zero and thus the emittance was calculated. The integration of this data with respect to solar-type radiation was of interest and therefore this integration was performed with respect to a blackbody curve at 5800°K and 6000°K (for other temperatures it is only necessary to input the temperatures themselves) and also with respect to the Johnson solar curve which is stored in the computer.. The column on the right gives the percent of the energy outside the region covered by the data (in this case less than 0.32 microns and greater than 3.0 microns). The center three columns give the integrated emittance (which is equal to the absorptance by Kirchoff's Law) for each of the three cases of interest and for various means of extrapolation to cover the wavelengths outside the data region. In the first of these

columns the integrated value is shown where a "straight" extrapolation is used. That is the radiometric values for the two end data points are used as the extrapolated values. In the next column results are given for an extrapolation made by fitting a curve to the data. And in the next column the results are shown for the case where no extrapolation is made or it can be thought of as an extrapolation made such that it does not alter the value of the integration. It might be noted that in this case, depending on the solar model (blackbody or Johnson) and manner of extrapolation, a solar absorptance ranging from 0.32 to 0.39 was obtained.

The 7094 computer together with a S.C. 4020 also plots the data as shown in figure 3 (reflectance) and figure 4 (emittance or absorptance).

The lower curve in figure 1 was integrated to obtain total emittance with respect to various blackbody temperatures and by mistake the Johnson solar curve. These results are given in figure 5 where the results for the Johnson curve indicates problems caused by extrapolation over large regions. Plots of the spectral reflectance and emittance are given in figures 6 and 7 respectively. By using the results of this program and fitting a curve to the total emittance as a function of temperature the variation of emittance with respect to temperature could easily be included in thermal computer programs.

SHADOW-SUNLIGHT PROGRAM

In this program information regarding the passage of a satellite through the earth's shadow (figure 8) is obtained for use in satellite thermal design and analysis work. The effect that variations in the percent of the time that a satellite spends in the earth's shadow per revolution can have on temperature of a satellite is shown in figure 9 where a close correlation between this parameter and the internal temperature of Explorer VII during 320 days of orbiting can be seen.

Great pains have been taken with this program to simplify data input as much as possible. For prelaunch studies it is usually convenient to input the data shown in figure 10 and for postlaunch calculations the alternate form of data input given in figure 11 may be used, since these parameters are usually readily available for any orbiting satellite. From this input the program calculates, among other things, the orbital positions where the satellite enters and leaves the earth's shadow, and the percent time spent in the shadow. Calculations are also made for successive days by extrapolation of the orbital elements considering perturbations caused by the oblateness of the earth. To avoid having to load the position of the sun into the computer from the ephemeris, equations were derived and included in the program which calculate the right ascension and declination of the sun considering such parameters as leap years.

Some of the results of the program are shown in figure 12. The top curve is the percent of time spent in the sunlight per revolution as a

function of days after launch for the Explorer VII satellite. This curve was obtained in one computer run consisting of 365 complete calculations and required about one minute of machine time giving a running time of about 1/6 second per calculation. The orbital parameters were extrapolated for the entire year and it was later determined that these extrapolated results were in good agreement with results obtained using actual orbital parameters. In the lower part of figure 12 is plotted additional computer output, namely, the orbital position of ingress into the earth's shadow, egress from the shadow, and perigee relative to the ascending node and as a function of days after launch. The position is given in terms of time (in minutes) required for the satellite to travel from the ascending node to the point of interest and an error analysis indicates accuracy to less than 10 seconds. This accuracy was further verified by visual observations of Echo I.

This type of graph is especially useful in determining what part of the orbit a given tracking station will be able to "see" and thus aid in planning tracking and performing data analysis. This is accomplished by the fact that a tracking station at some fixed geographical latitude can at best "see" only a certain part of the satellite's orbit on any given day. In the case of Explorer VII and the Huntsville station, that part of the orbit approximately between the two lines on the graph in figure 12 could be tracked at some time during the day. Thus initially Huntsville could track only during the daylight portions of the orbit. On about 20 days after launch we could catch the satellite as it went into the earth's shadow and around 50 days after launch we could track it as it was leaving the shadow. Knowing this information ahead of time, tracking at the Huntsville station was coordinated throughout the year such that special effort could be made to obtain data at times of particular interest such as ingress, egress, and maximum and minimum sunlight conditions.

GENERAL SPACE THERMAL PROGRAM

MSFC has been involved in the thermal design of several spacecraft including Explorers I, III, IV, VII, VIII, and XI; Pioneers III and IV; Saturn SA-V Payload; and the Meteoroid Measurement Satellite to be flown on Saturn around the end of this year. Some of these spacecraft are shown in figure 13. It was found that weeks and even months were often required to set up and debug each of the computer programs used for the thermal design and evaluation of each of the spacecraft. Thus was born the idea of a computer program which could be utilized to minimize the time and effort involved in obtaining theoretical results and at the same time maximize the degree of sophistication which can be efficiently used for such calculations.

The basic general equation used in the General Space Thermal Program is given in figure 14. The equation is a first order fourth degree differential equation representing the instantaneous heat flow into and out of a section of the spacecraft the temperature of which is assumed to be such that it can be represented by one "effective temperature." The computer

will automatically set up "n" such equations depending on how many sections the spacecraft must be divided in order that the resulting set of equations will serve sufficiently as an analytical model. The first term on the right in the equation represents the solar flux absorbed by the section, the next term is the earth albedo flux absorbed, next the earth infrared radiation term, then radiation away from the surface to space, internal heat generation, and finally conduction and radiation exchange with all the other sections. The bracketed factors are treated as separate functions which are dependent on the specific makeup of each section.

The manner in which the program is organized is shown in figure 15. The program includes many special subroutines which can be used in calculating the separate functions (A's and Q's). Each of the subroutines are discussed briefly below.

"D" = determines whether the satellite is in the earth's shadow at each calculation point in the orbit

"PS" = determines the angle between perigee and the sun in the plane of the orbit

"$F_{s/p}$" = calculates the geometry factor between a flat plate or the sides of a cylinder and the earth as a function of altitude and orientation.

"g" = calculates the geometry factor between a sphere and the earth as a function of altitude

"h" = calculates the altitude of the satellite as a function of position in orbit

MAS = determines the angle between M, a vector defining the orientation of a section of the spacecraft, and S, a vector toward the sun

RAM = calculates the angle between the radius vector to the satellite and the vector M as a function of position in orbit

RAS = calculates the angle between the radius vector and a vector toward the sun

The F subroutine might be of particular interest and its derivation is as follows: The geometry for planetary thermal radiation to a cylinder is shown in figure 16. The geometry factors for various orientation and altitudes were calculated using a lengthly numerical progress by Ballinger, et.al. (references 1 and 2) and part of their results is shown in figure 17. In order to most efficiently enter these results into the program with an overall accuracy of better than two percent, a two variable curve fit was made such all the information in figure 17 is contained in one fifth degree polynomial the coefficients of which are each fourth degree polynomials (figure 18). Such an efficient means of calculating the geometry factor allows the luxury of being able to combine the flux calculations directly

into the general program itself and thus reduce data handling and overall time required to obtain results.

It was further found that the albedo flux could be calculated for the sides of a cylinder (or a flat plate) simply by multiplying the infrared geometry factor (F_{jA}) by the cosine of RAS and ignoring variations in the "azimuth" angle ϕ (figure 19) and the fact that the flux is actually a very complicated function of RAS. This process gives maximum errors of around 5% as shown in figure 20 where the dashed curves represent the results obtained by this method and the solid curves represent the "true" results from references 1 and 2. It might be noted that during a complete revolution about the earth the errors tend to cancel out.

The method used to integrate the set of "n" first order differential equation is the Kutta-Simpson one-third rule illustrated in figure 21. In order to reduce running time a method of varying the integration time step throughout a run was incorporated. This prevents the program from "blowing up" and decreasing computation times by factors of 10 or more in some cases.

As an example of the simplicity of using this program the case of a space-fixed hollow cube in orbit was considered (figure 22). The only information needed to set up the program is given in figure 23 and input data for a run is shown in figures 24 and 25. The conduction and radiation coefficients between sections are entered by use of a matrix (figure 25) and each value is given twice (i.e. $R_{ij} = R_{ji}$) allowing the computer to perform a check on data input. The results for this case are shown in figure 26.

Thus by use of this program it is possible to set up and obtain fairly sophisticated theoretical results from a computer program within 24 hours in many cases.

REFERENCES

1. Ballinger, J. C., Elizalda, J. C., Garcia-Varela, R. M., and Christensen, E. H.: "Environmental Control Study of Space Vehicles," Part II (Thermal Environment of Space), Convair (Astronautics) Division, General Dynamics Corporation, November 1960.

2. Ballinger, J. C. and Christensen, E. H.: "Environmental Control Study of Space Vehicles," Part II, Supplement A, Convair (Astronautics) Division, General Dynamics Corporation, January 1961.

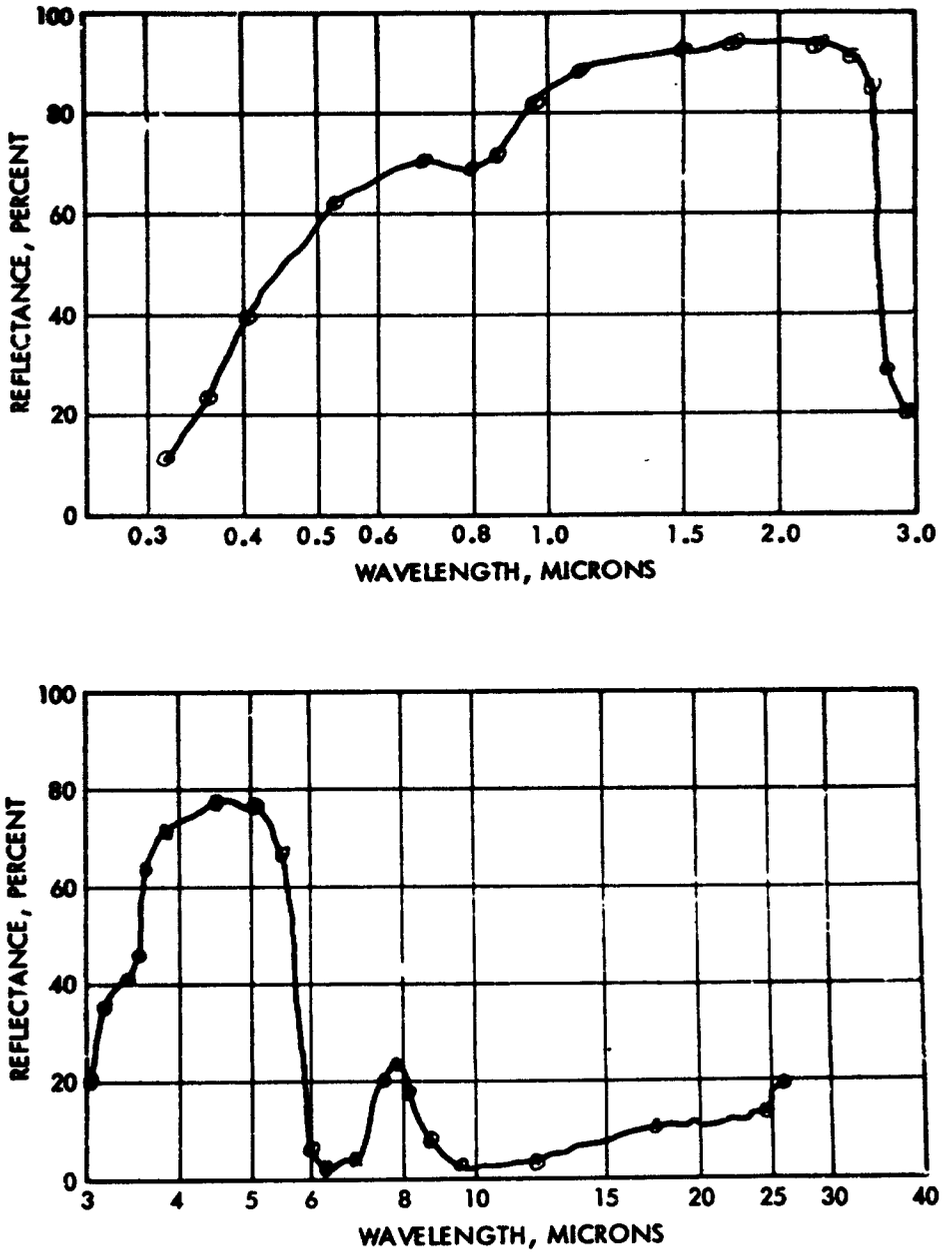

5557 Aluminum Alloy, Oxalic Acid Electrolyte
(Table III-7, Sample No. 13)

Figure 1

5557 ALUMINUM ALLOY, OXALIC ACID ELECTROLYTE (SOLAR)

WAVE LENGTH	EMITTANCE	REFLECTANCE	TRANSMITTANCE
0.320	0.900	0.100	0.
0.360	0.780	0.220	0.
0.400	0.600	0.400	0.
0.530	0.380	0.620	0.
0.700	0.300	0.700	0.
0.800	0.320	0.680	0.
0.880	0.290	0.710	0.
0.980	0.180	0.820	0.
1.100	0.110	0.890	0.
1.500	0.080	0.920	0.
1.800	0.070	0.930	0.
2.300	0.080	0.920	0.
2.600	0.100	0.900	0.
2.800	0.150	0.850	0.
2.900	0.710	0.290	0.
3.000	0.800	0.200	0.

T	STRAIGHT EXTRAPOLATION	CURVED EXTRAPOLATION	NB EXTRAPOLATION	PCT. BLACK BODY NOT COVERED	FILM PRINTED
5000.	0.36	0.38	0.32	7	
6000.	0.37	0.39	0.33	7	
JOHNSON SOLAR CURVE	0.34	0.36	0.32	4	

Figure 2

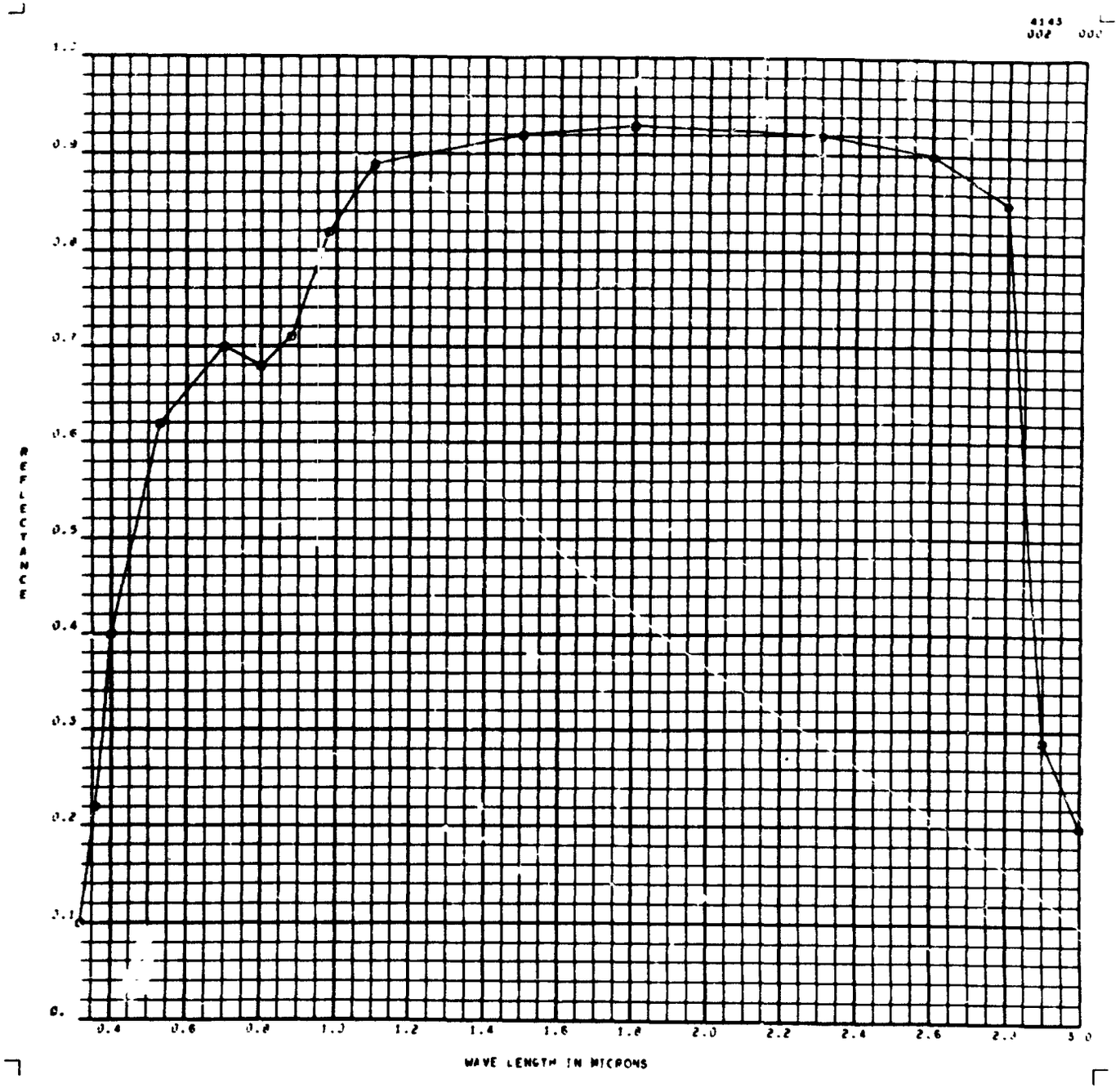
4143
0.9
0.8
0.7
0.6
0.5
0.4
0.3
0.2
0.1
0.
REFLECTANCE
0.4
0.6
0.8
1.0
1.2
1.4
1.6
1.8
2.0
2.2
2.4
2.6
WAVE LENGTH IN MICRONS

Figure 3

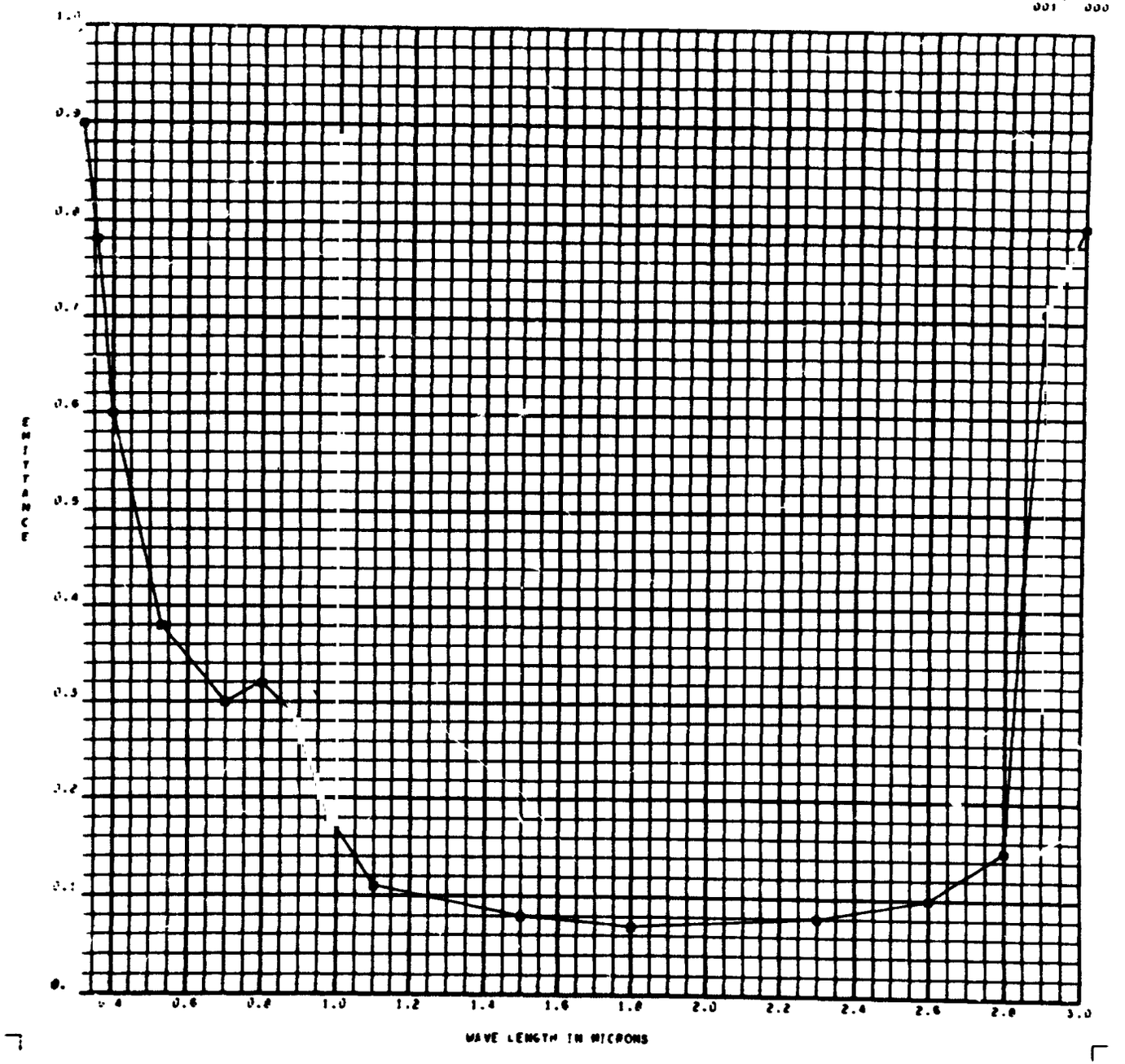

Figure 4

5557 ALUMINUM ALLOY, OXALIC ACID ELECTROLYTE (1R)

WAVE LENGTH	EMITTANCE	REFLECTANCE	TRANSMITTANCE
3.000	0.800	0.200	0.
3.200	0.630	0.370	0.
3.400	0.590	0.410	0.
3.600	0.550	0.450	0.
3.800	0.360	0.640	0.
4.000	0.280	0.720	0.
4.500	0.210	0.790	0.
5.100	0.220	0.780	0.
5.500	0.330	0.670	0.
6.000	0.950	0.050	0.
6.500	0.980	0.020	0.
7.000	0.960	0.040	0.
7.600	0.800	0.200	0.
7.900	0.780	0.220	0.
8.100	0.810	0.190	0.
8.700	0.920	0.080	0.
9.600	0.980	0.020	0.
12.500	0.970	0.030	0.
17.500	0.900	0.100	0.
24.500	0.860	0.140	0.
26.000	0.810	0.190	0.

T	STRAIGHT EXTRAPOLATION	CURVED EXTRAPOLATION	NB EXTRAPOLATION	PCT. BLACK BODY NOT COVERED FILM PRINTED
200.	0.88	0.66	0.91	34
300.	0.89	0.81	0.90	15
400.	0.84	0.80	0.84	8
500.	0.78	0.76	0.77	5
JOHNSON SOLAR CURVE	0.79	0.99	0.41	98

Figure 5

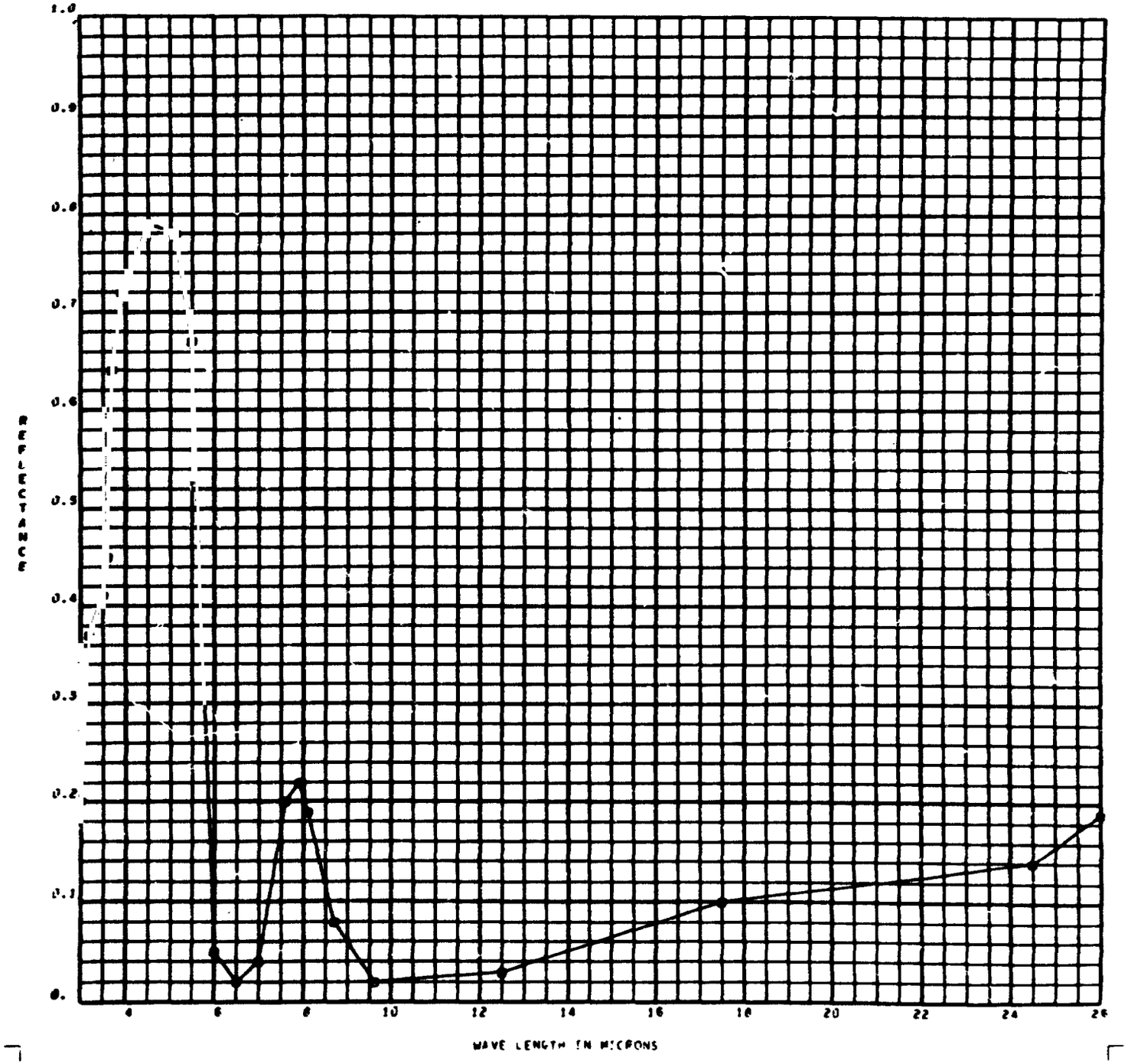
1.0
0.9
0.8
0.7
0.6
0.5
0.4
0.3
0.2
0.1
0.
REFLECTANCE
4
6
8
10
12
14
16
18
20
22
24
26
WAVE LENGTH IN MICRONS

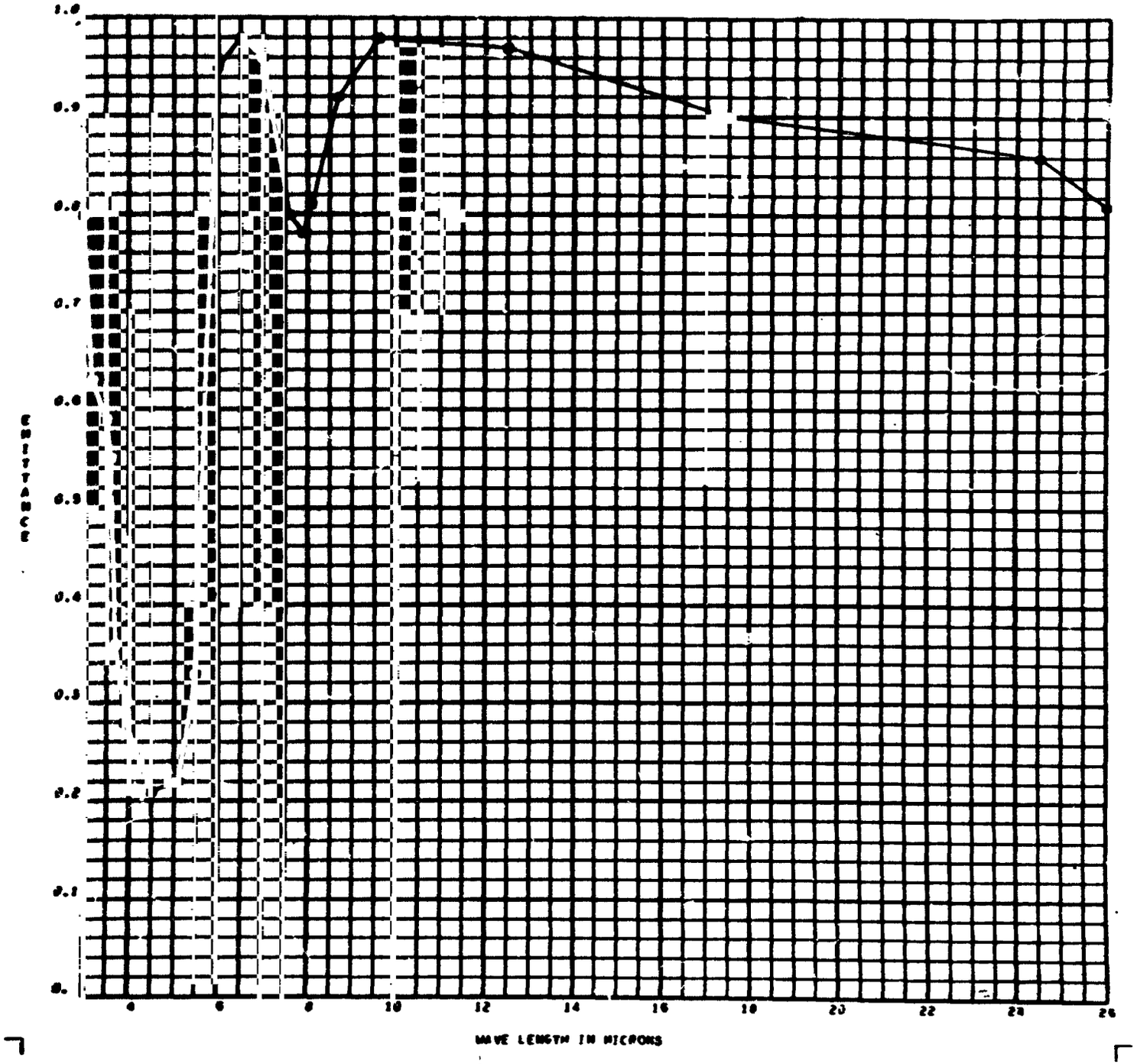
4143
001 000
1.0
0.9
0.8
0.7
0.6
0.5
0.4
0.3
0.2
0.1
0.
4
6
8
10
12
14
16
18
20
22
24
26
WAVE LENGTH IN MICRONS

Figure 7

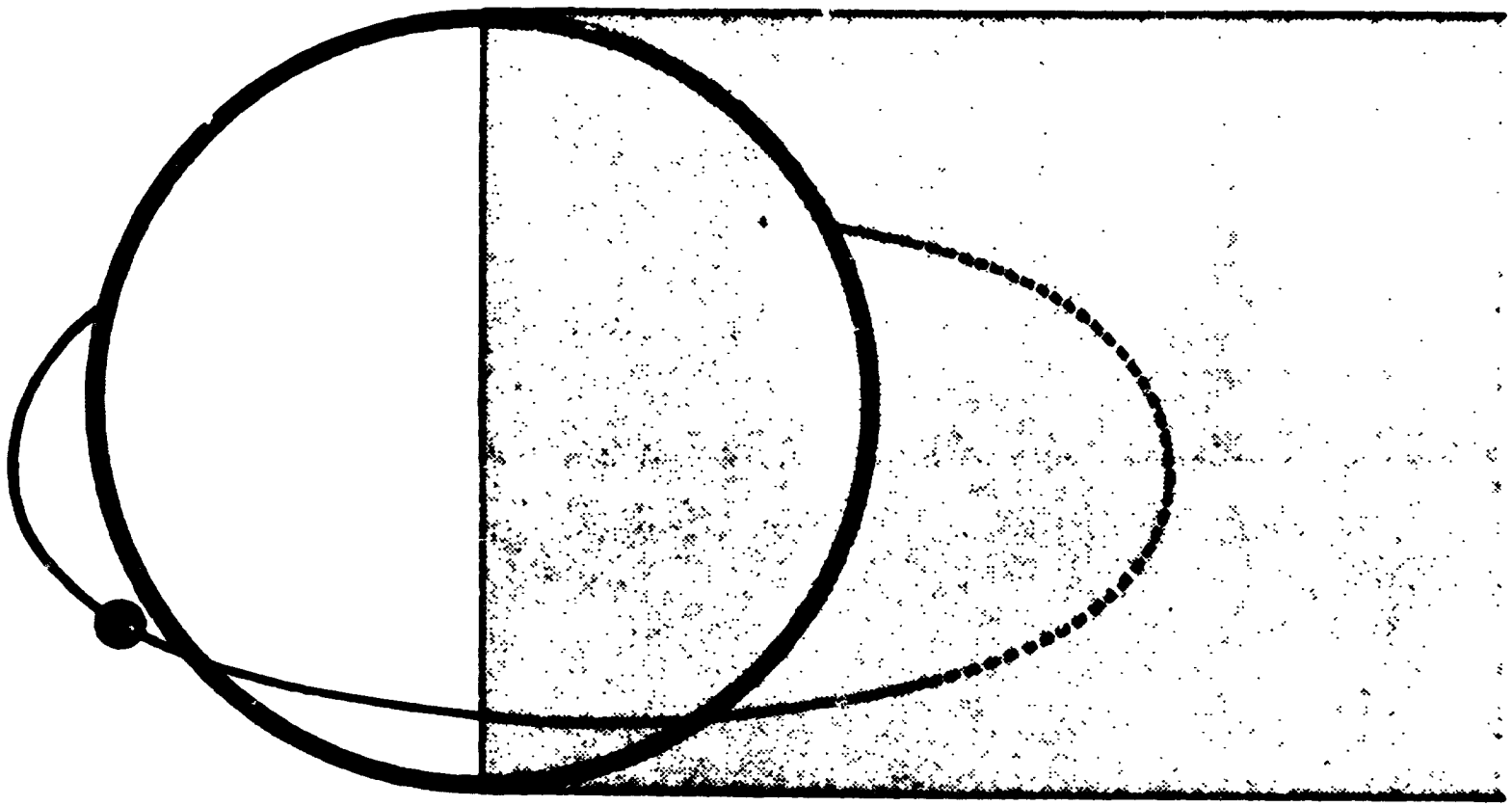

Satellite orbit showing passage through shadow.

Figure 8

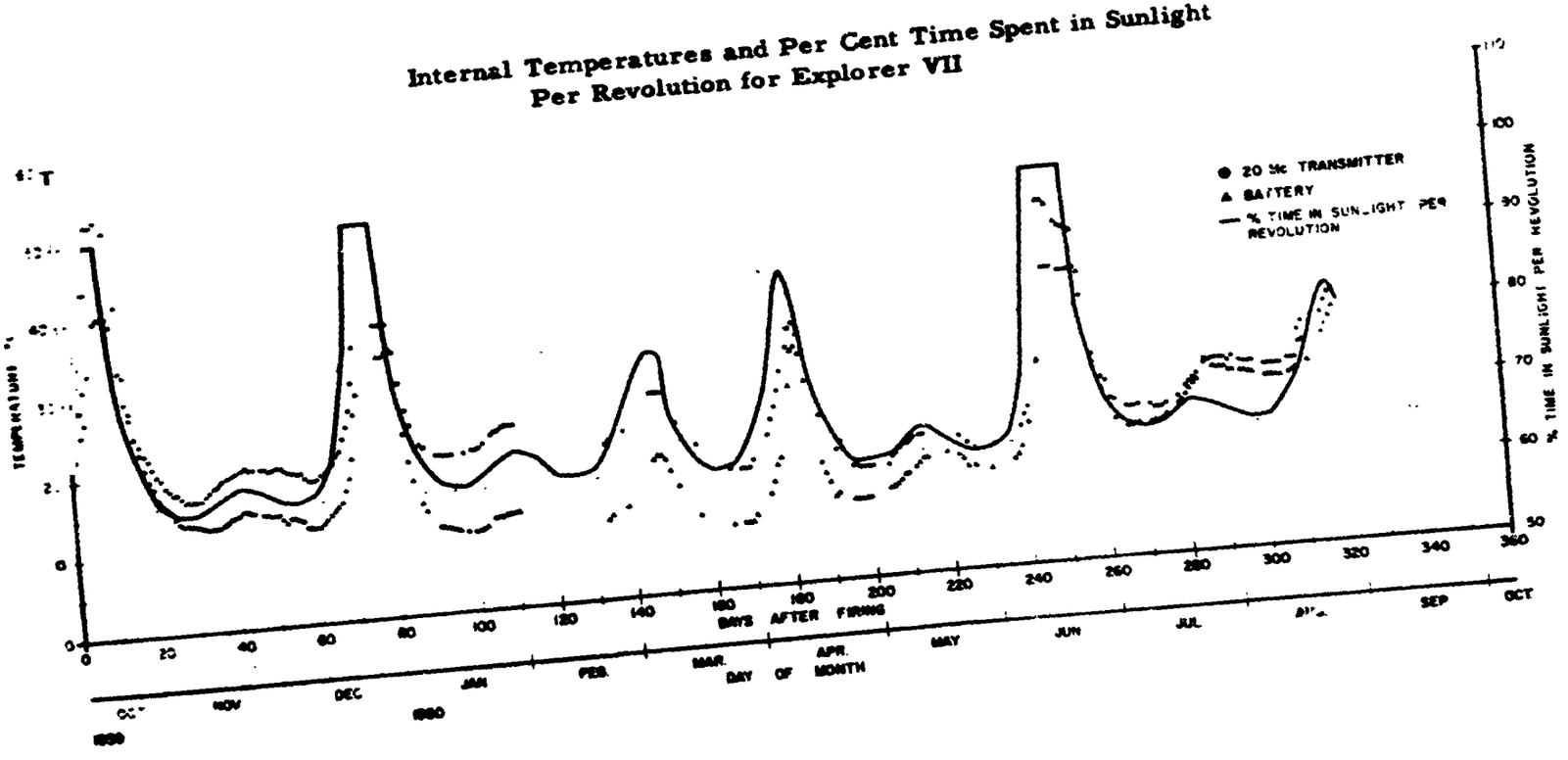
Internal Temperatures and Per Cent Time Spent in Sunlight
Per Revolution for Explorer VII
20 Mc TRANSMITTER
BATTERY
% TIME IN SUNLIGHT PER REVOLUTION
TEMPERATURE °F
% TIME IN SUNLIGHT PER REVOLUTION
DAYS AFTER FIRING
DAY OF MONTH
OCT
NOV
DEC
JAN
FEB.
MAR.
APR.
MAY
JUN
JUL
SEP
OCT
1959
1960

Figure 9

DATA INPUT FOR SHADOW-SUNLIGHT PROGRAM

1. Universal time during initial perigee passage
2. Number of days after vernal equinox
3. Eccentricity of orbit
4. Longitude of initial perigee
5. Latitude of initial perigee
6. Inclination of orbit
7. Altitude of perigee
8. North or South at initial perigee
9. Year

Figure 10

ALTERNATE FORM OF DATA INPUT

1. Anomalistic period
2. Argument of perigee
3. Longitude of ascending node
4. Inclination of orbit
5. Ratio of orbital semimajor axis to earth's radius
6. Time of ascending node crossing
7. Number of days after vernal equinox
8. Eccentricity of orbit
9. Year

Figure 11

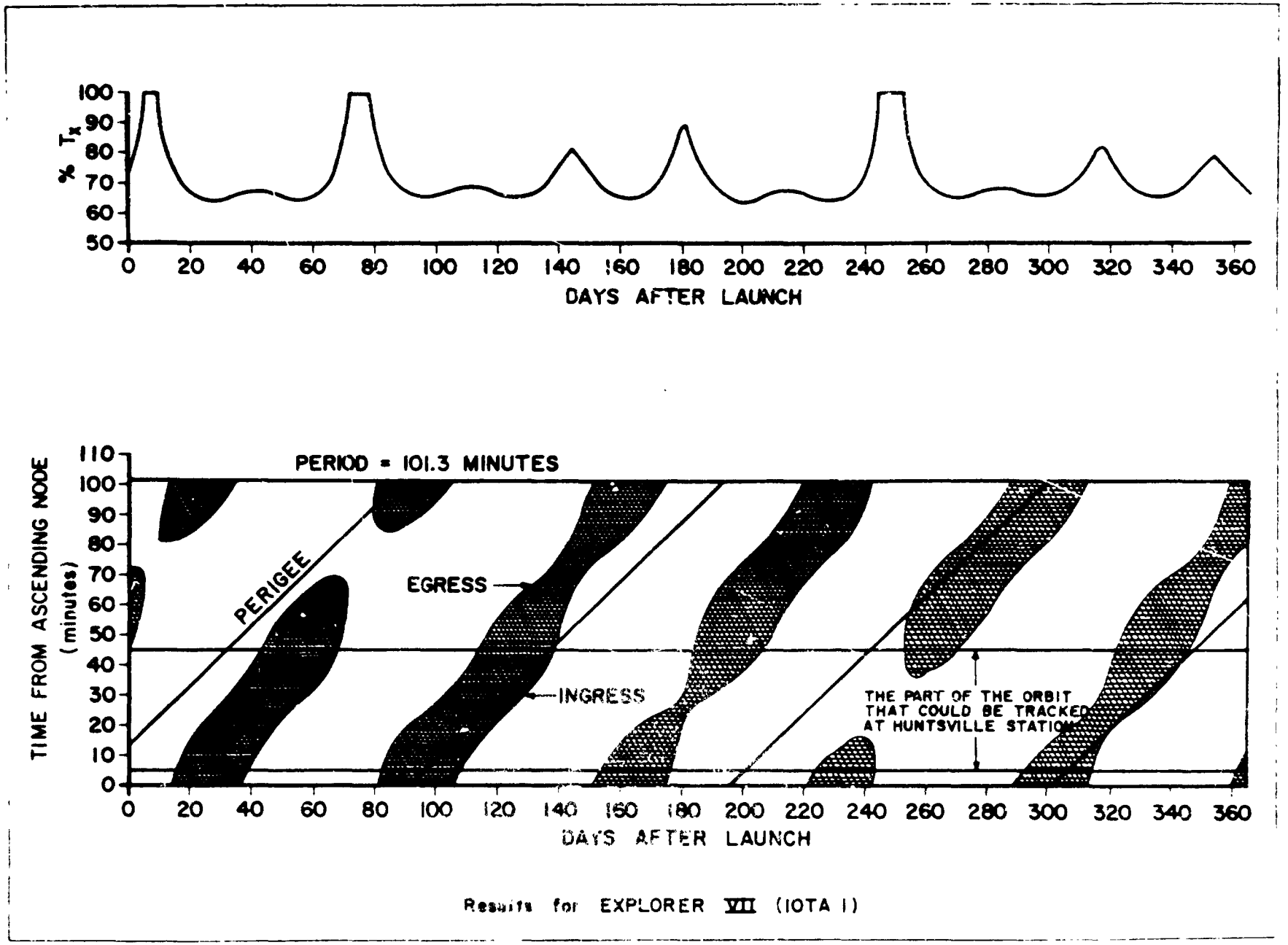

Results for EXPLORER VII (IOTA I)

Figure 12



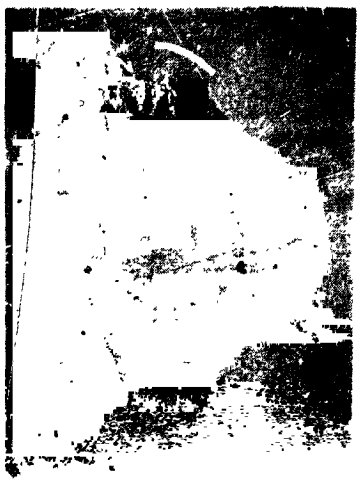



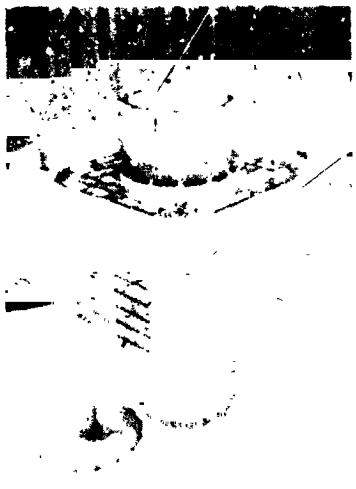

BASIC EQUATIONS

$$\dot{T}_i H_i = \{A_{1i}\} \alpha_i S + \{A_{2i}\} \alpha_i B S + \{A_{3i}\} \epsilon_i E S - \{A_{4i}\} \epsilon_i \sigma T_i^4 + \{Q_i\} + \sum_{j=1}^{n} \left[C_{ij} (T_j - T_i) + R_{ij} (T_j^4 - T_i^4) \right]$$

where $i = 1, 2, 3, \ldots, n$

GENERAL SPACE THERMAL PROGRAM

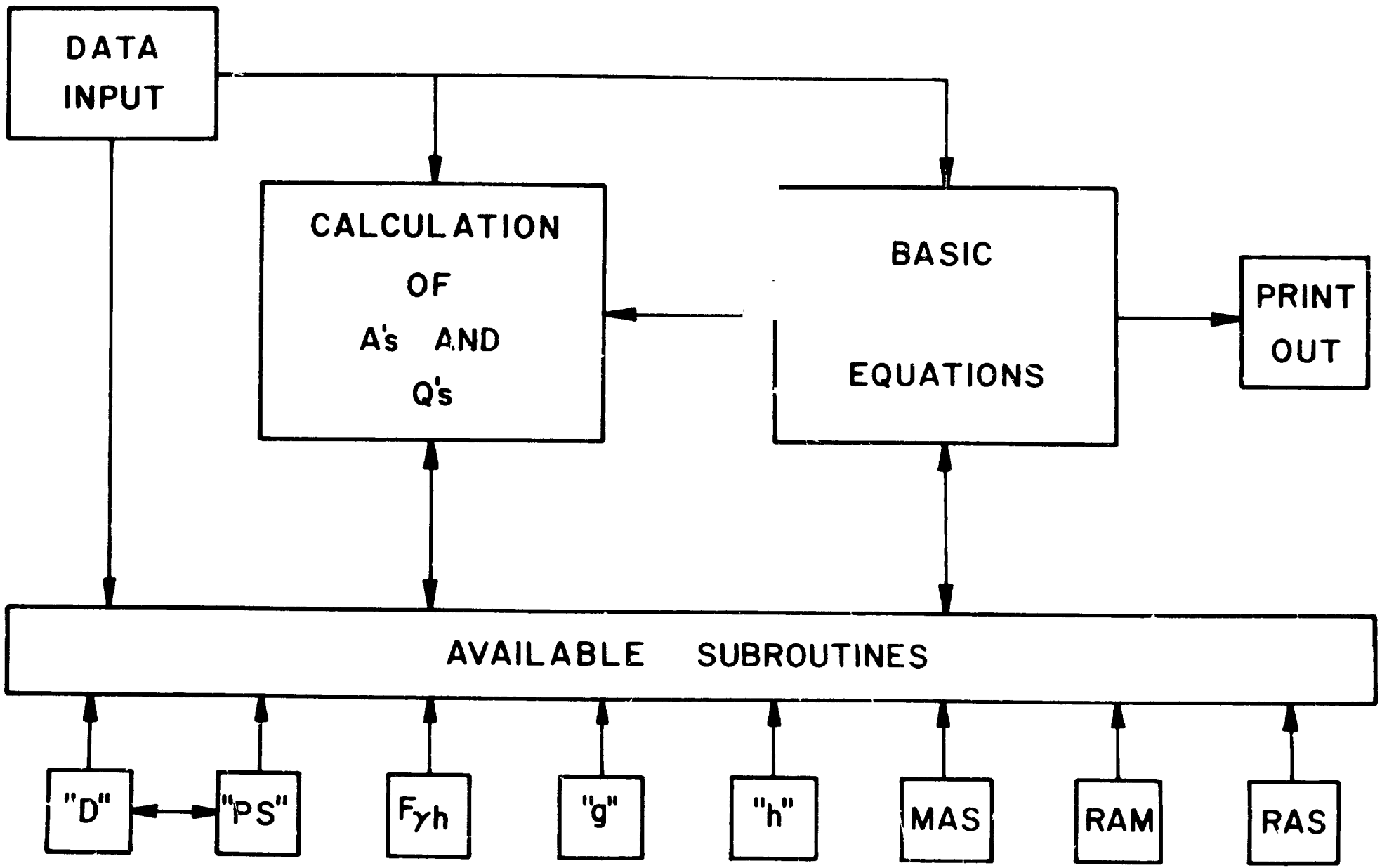

Figure 15

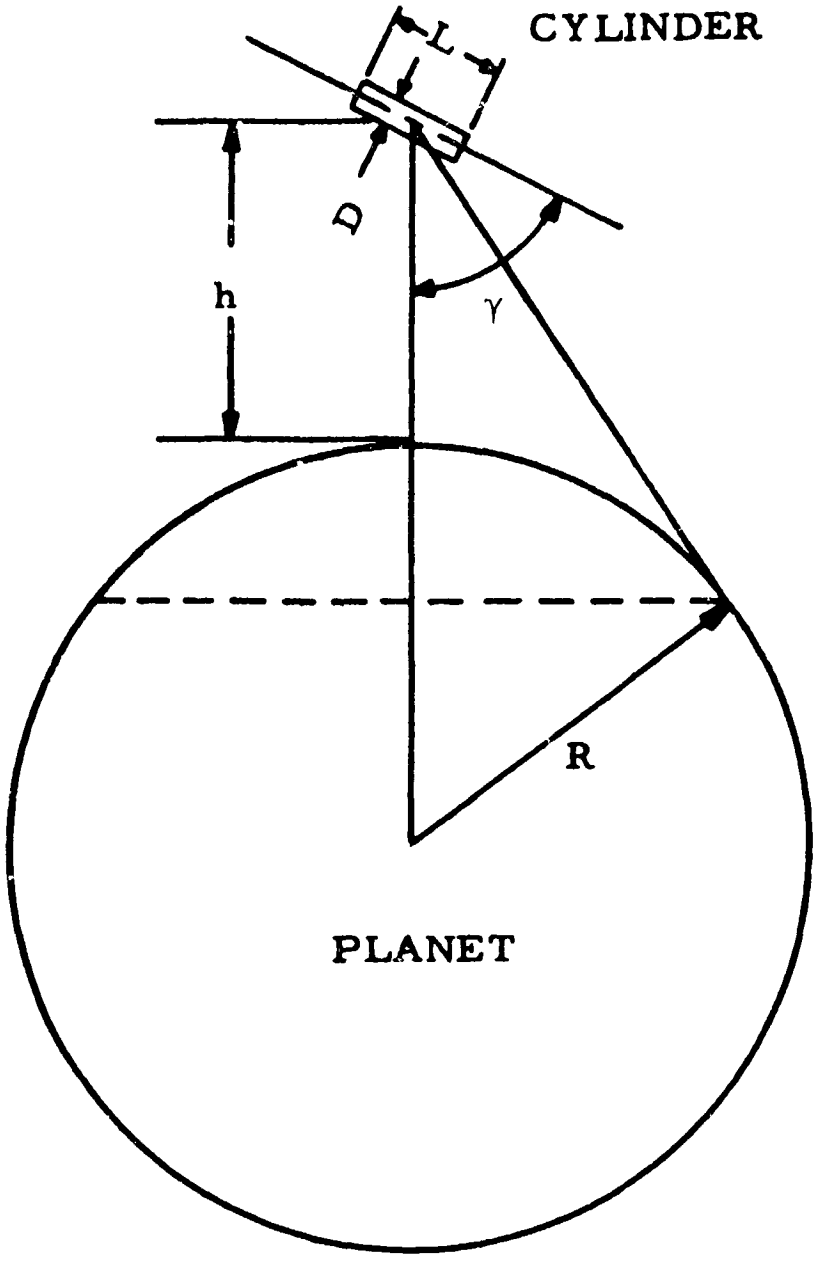

Geometry for Planetary Thermal Radiation to a Cylinder

Figure 16

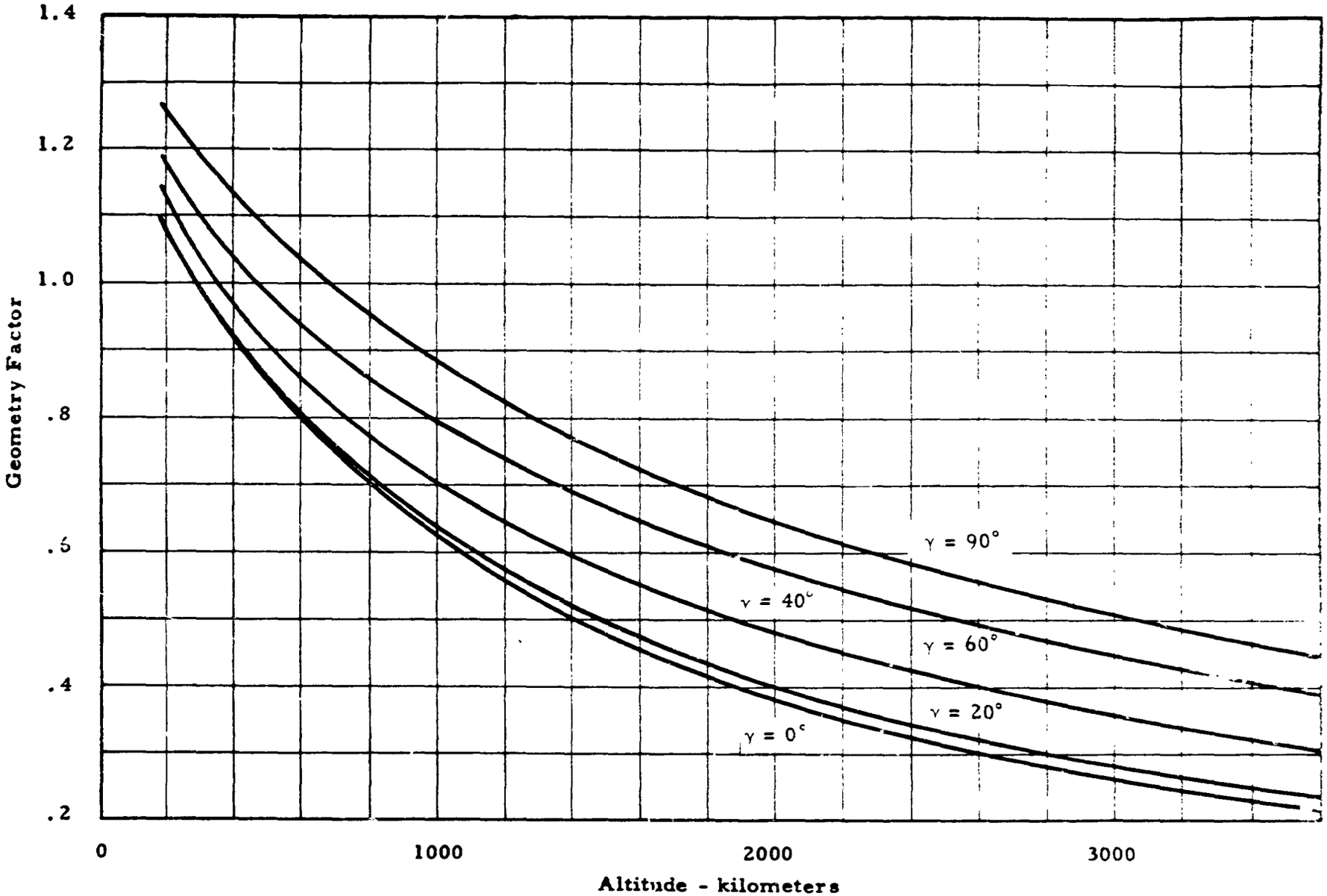

Geometry Factor vs. Altitude for
IR to a Cylinder

Figure 17

LEAST SQUARE CURVE FIT IN TWO VARIABLES

$$F_{\gamma, r} = \sum_{i=0}^{5} \left(\sum_{j=0}^{4} A_{ij} \gamma^{j} \right) h^{i}$$

Figure 18

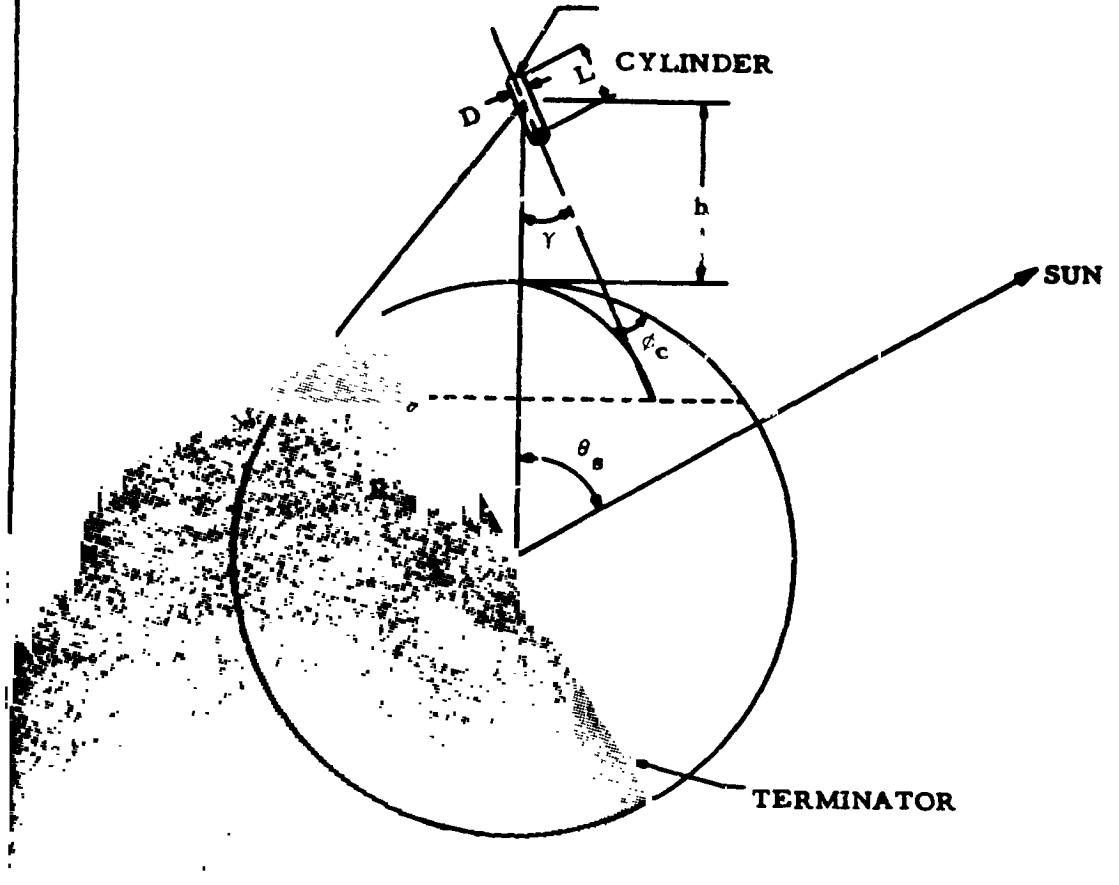

Geometry for Planetary Albedo
to a Cylinder

Figure 19

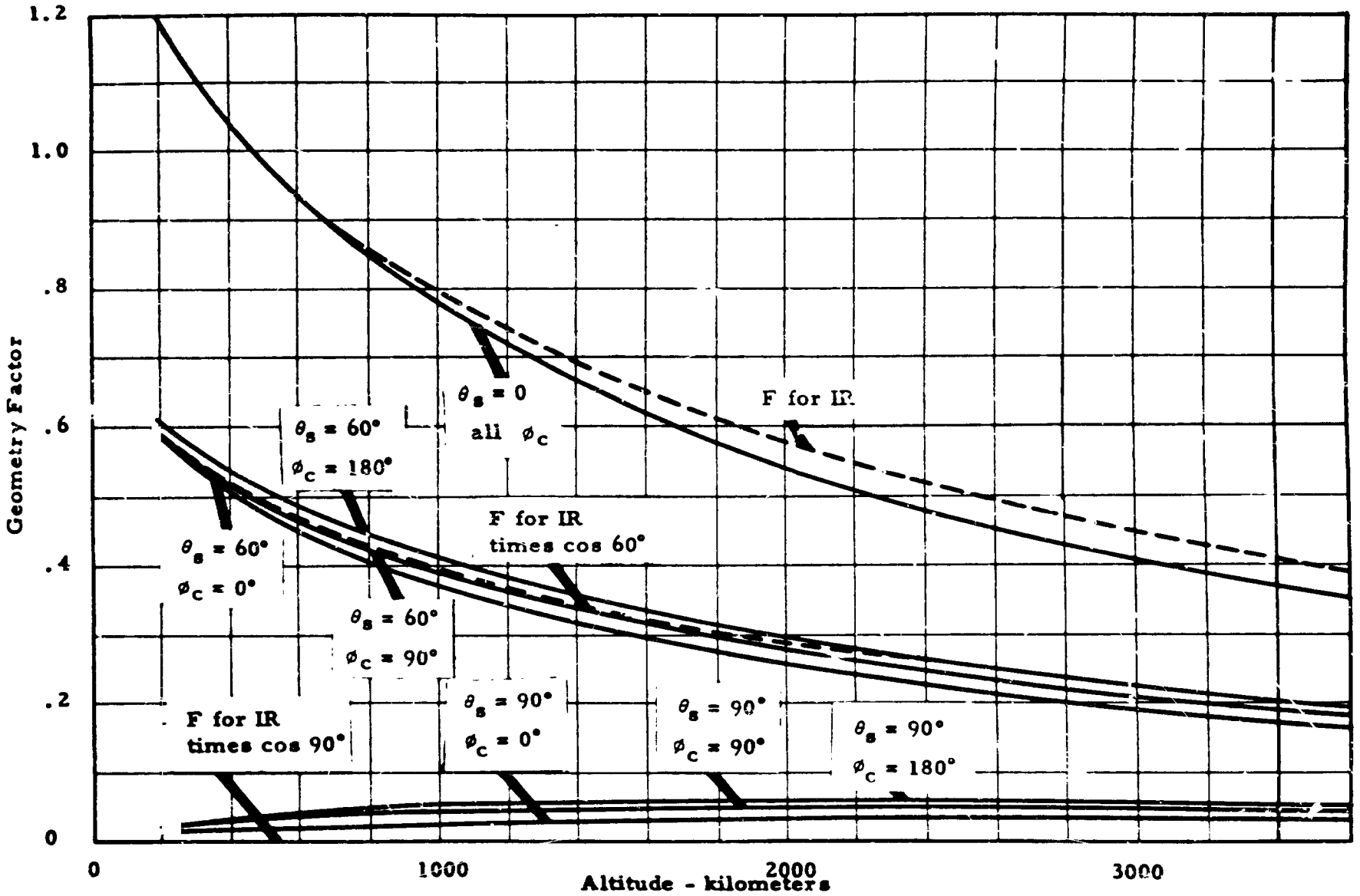

Geometry Factor vs. Altitude for Albedo to a Cylinder ($\gamma = 60°$)

Figure 20

NUMERICAL INTEGRATION BY KUTTA-SIMPSON ONE-THIRD RULE

$$T_{i\,new} = T_{i\,old} + \frac{1}{6}\left(\Delta^1 T_i + 2\,\Delta^2 T_i + 2\,\Delta^3 T_i + \Delta^4 T_i\right)$$

where

$$\Delta^1 T_i = \Delta t\; f\left(t_o,\; T_{io},\; T_{jo}\right)$$

$$\Delta^2 T_i = \Delta t\; f\left(t_o + \frac{1}{2}\Delta t,\; T_i + \frac{1}{2}\Delta^1 T_i,\; T_j + \frac{1}{2}\Delta^1 T_j\right)$$

$$\Delta^3 T_i = \Delta t\; f\left(t_o + \frac{1}{2}\Delta t,\; T_i + \frac{1}{2}\Delta^2 T_i,\; T_j + \frac{1}{2}\Delta^2 T_j\right)$$

$$\Delta^4 T_i = \Delta t\; f\left(t_o + \Delta t,\; T_i + \Delta^3 T_i,\; T_j + \Delta^3 T_j\right)$$

Figure 21

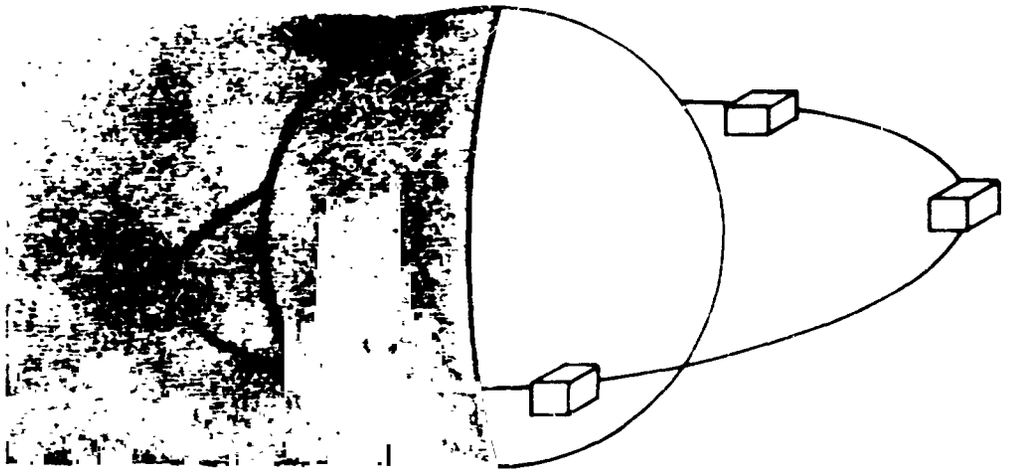

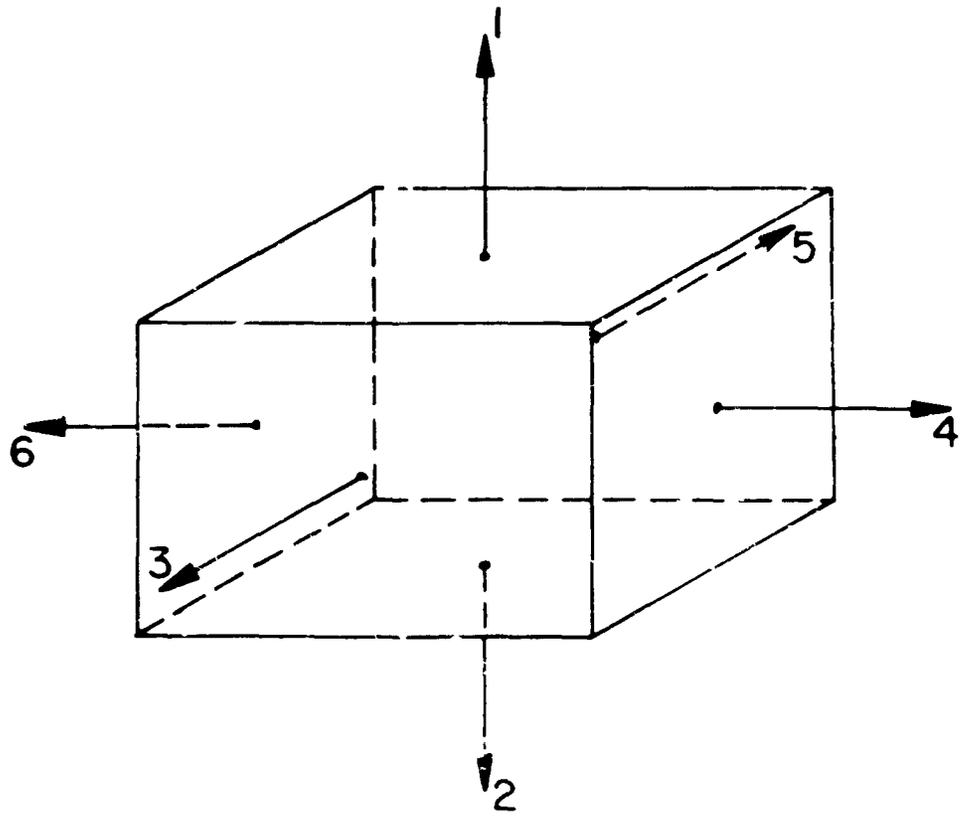
1
2
3
4
5
6

INFORMATION NEEDED TO SET UP PROGRAM

$n = 6$

$A_{1i} = A_{4i} \cos (MAS)_i \; D$

$A_{2i} = A_{4i} F_{\gamma_i h} \cos (RAS)_i \; \gamma_i = 180^\circ - (RAM)_i$

$A_{3i} = A_{4i} F_{\gamma_i h}$

$A_{4i} =$ Constant

$Q_i = 0$

$H_i =$ Constant

INPUT DATA NEEDED TO MAKE A RUN

$T_{io} = 300^{\circ}K$

$H_i = 1.13 \times 10^5$ Joules/$^{\circ}K$

$\alpha_i = 0.80$

$\epsilon_i = 0.55$

$S = 1400$ watts/m^2

$B = 0.39$

$E = 0.174$

C_{ij} = see matrix

R_{ij} = see matrix

$A_{4i} = 1\ m^2$

$\sigma = 5.67 \times 10^{-8}$

$\gamma_{mi} = 0^{\circ}, 0^{\circ}, 0^{\circ}, 90^{\circ}, 180^{\circ}, 270^{\circ}$

$\delta_{mi} = +90^{\circ}, -90^{\circ}, 0^{\circ}, 0^{\circ}, 0^{\circ}, 0^{\circ}$

$a_S = 90^{\circ}$

$\delta_S = 23.5^{\circ}$

$R_o = 6371$ km

$R_p = 6671$ km

$e = 0.1$

$T_x = 70^{\circ}$

$\Omega = 0^{\circ}$

$i = 40^{\circ}$

$\omega = 120^{\circ}$

Figure 24

C_{ij}

i \ j	1	2	3	4	5	6
1	0	0	.76	.76	.76	.76
2	0	0	.76	.76	.76	.76
3	.76	.76	0	.76	0	.76
4	.76	.76	.76	0	.76	0
5	.76	.76	0	.76	0	.76
6	.76	.76	.76	0	.76	0

$R_{ij} \times 10^{-8}$

i \ j	1	2	3	4	5	6
1	0	1.245	1.150	1.150	1.150	1.150
2	1.245	0	1.150	1.150	1.150	1.150
3	1.150	1.150	0	1.150	1.245	1.150
4	1.150	1.150	1.150	0	1.150	1.245
5	1.150	1.150	1.245	1.150	0	1.150
6	1.150	1.150	1.150	1.245	1.150	0

Figure 25

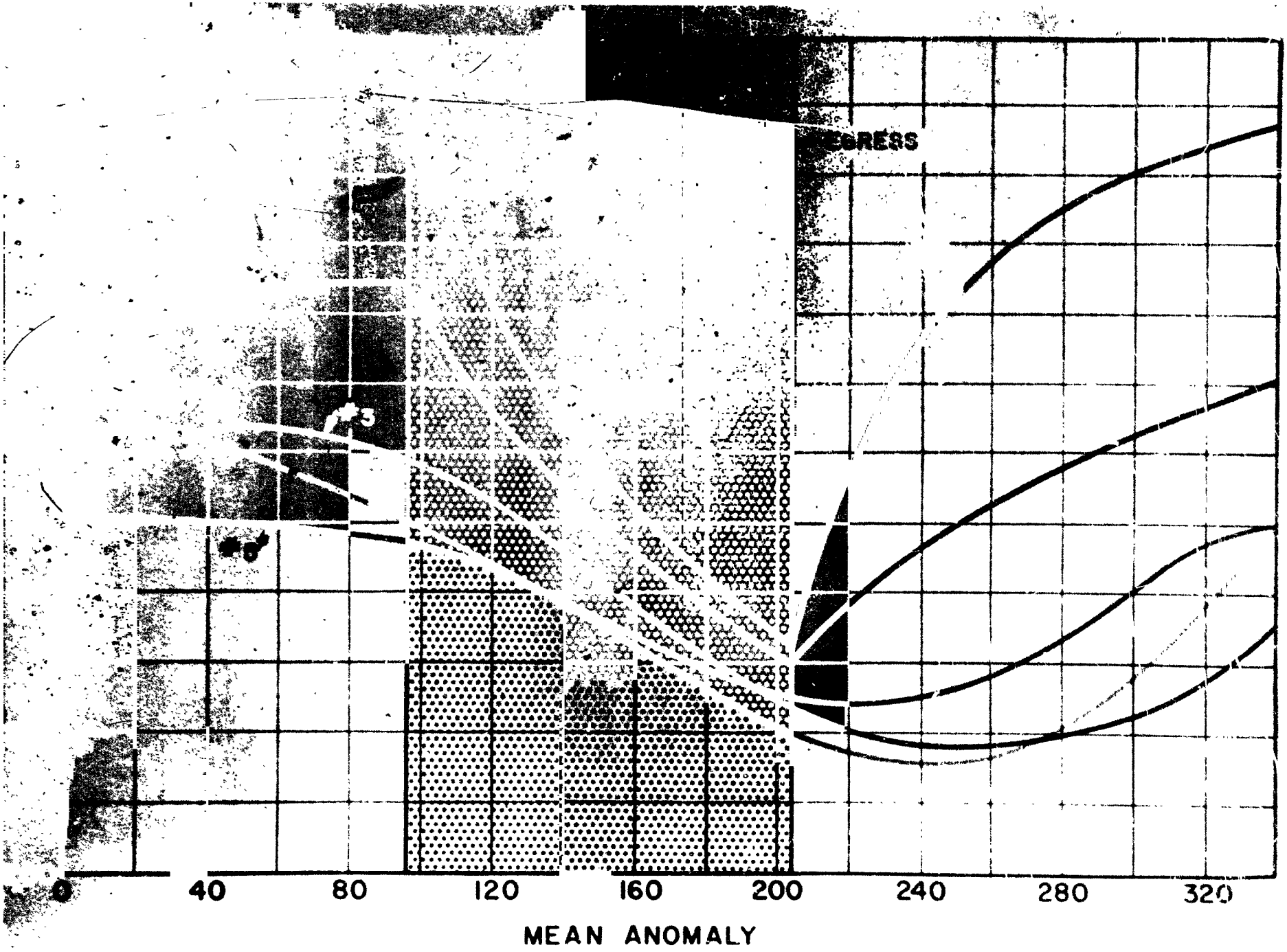

Figure 26

SATELLITE HEAT TRANSFER PROGRAMS

by

Edward I. Powers
NASA Goddard Space Flight Center
Greenbelt, Maryland

Computer Programs for Spacecraft Thermal Design at Goddard Space Flight Center

The thermal design of an earth satellite requires an accurate knowledge of both thermal radiation inputs and internal temperature distribution. The use of the IBM-7094 as an analytical tool to determine these functions is now widely employed.

At Goddard Space Flight Center, two programs are used extensively. One determines the thermal radiation (i.e., direct solar radiation, earth emitted radiation, and albedo) to a spinning flat plate. The program is geared toward the analysis of spin-stabilized spacecraft, but can be applied to non-spinning plates either earth or space oriented. The second program determines the temperature distribution and net heat flow, provided the appropriate conductances, radiation view factors, and thermal properties are known.

A detailed discussion of these programs is presented below.

THERMAL RADIATION TO A FLAT SURFACE ROTATING ABOUT AN ARBITRARY AXIS IN AN ELLIPTICAL EARTH ORBIT: APPLICATION TO SPIN-STABILIZED SATELLITES

by
Edward I. Powers
Goddard Space Flight Center

SUMMARY

The derivation of total thermal radiation incident upon a flat plate rotating about an arbitrary axis is presented. The functional relationships between position in an elliptical earth orbit and direct solar radiation, earth-reflected solar radiation (albedo), and earth-emitted radiation (earthshine) are included. The equations have been programmed for the IBM 7090 digital computer, resulting in solutions which relate the incident radiation to spin axis orientation and orbital position. Several representative orbits for a typical geometrical configuration were analyzed and are presented as examples.

CONTENTS

THERMAL RADIATION TO A FLAT SURFACE ROTATING ABOUT AN ARBITRARY AXIS IN AN ELLIPTICAL EARTH ORBIT: APPLICATION TO SPIN-STABILIZED SATELLITES

by
Edward I. Powers
Goddard Space Flight Center

INTRODUCTION

The satisfactory operation of an artificial satellite depends upon maintaining the payload temperature within prescribed limits. For example, the standard batteries employed in present-day spacecraft generally restrict the temperature limits to 0° and 40°C. Often experiments located within the satellite structure further restrict this variation.

The temperature level of a satellite may be determined by solving the instantaneous energy balance

$$P + S\alpha_s A_p + q_{alb} + q_{es} - \sigma\epsilon A_s \bar{T}^4 + WC_p \frac{dT}{dt} ,$$

where

P = internal power dissipation,

S = solar constant,

α_s = solar absorptance,

A_p = instantaneous projected area for sunlight,

q_{alb} = reflected solar radiation (albedo),

q_{es} = earth-emitted radiation (earthshine),

σ = Stefan-Boltzmann constant,

ϵ = infrared emittance,

A_s = total surface area,

$\bar{T}^4$ = mean fourth power, surface temperature,

WC_p = heat capacity of the satellite,

$\frac{dT}{dt}$ = time rate of change of satellite temperature.

If the average orbital temperature is being computed, the last term is dropped. In this case all heat input terms represent integrated orbital values.

It should be noted that the above equation, as a representation of the entire satellite, is greatly oversimplified. The values for ϵ and α_s generally vary over the surface and great fluctuations in skin temperature may exist. In practice the thermal analysis consists of the development of a thermal model which represents a fine mesh of interconnected isothermal nodes. The appropriate relationship between nodes in regard to thermal conduction and radiation interchange must be established.

The energy balance for each node of a thermal model may be written

$$P_n + S\alpha_{s_n} A_{p_n} + q_{alb_n} + q_{es_n} + \sum_m C_{nm} (T_m - T_n) + \sigma \sum_m E_{nm} F_{nm} (T_m^4 - T_n^4) = \sigma \epsilon A_{s_n} T_n^4 + (WC_p)_n \frac{dT_n}{dt} ,$$

where

C_{nm} = conductance between nodes n and m,

E_{nm} = effective emissivity between nodes n and m,

F_{nm} = shape factor-area product between nodes n and m.

Since the major interest at present is to determine the satellite temperature level and not the gradients within, a discussion of the terms in the first equation is in order.

For most passive controlled satellites P is relatively small compared with the total radiation input and does not have a significant effect on the satellite mean temperature. The magnitude of this effect, however, depends upon the ϵ of the surface (e.g. a surface with a low absolute ϵ may raise the internal temperature significantly because the skin has a limited capacity for re-radiation).

The remaining three heat sources, direct solar heating, earth-reflected solar heating (albedo), and earth-emitted radiation (earthshine), represent the significant inputs to the satellite. It is apparent that an adequate thermal design is predicated upon a reasonably accurate knowledge of these thermal radiation inputs. The major source of energy—direct solar radiation—is fortunately the most accurately obtained. Since the sun's rays impinging upon the satellite are virtually

parallel, the problem is simply one of determining the instantaneous orientation of each external face with respect to the solar vector.

The calculation of earthshine is considerably less precise, requiring fundamental assumptions to reduce the complexity of computation. These include the assumptions that the earth is a diffusely emitting blackbody and that the surface temperature is uniform at 450°R. This permits direct calculation of energy input from all visible positions on the earth. Since all locations supply varying inputs, an integral equation must be solved to obtain the total incident energy.

The albedo determination involves a similar integration. The earth in this case is assumed to be a diffusely reflecting sphere. In addition, the source intensity is a function of the satellite location relative to the sunlit portion of the earth.

For a nonrotating satellite whose orientation is "fixed in space" the calculation of the thermal radiation fluxes is performed at any interval during the orbit. At each orbital position a particular flat surface may or may not "see" the entire part of the earth's cap visible from the satellite. In the latter case integration for albedo and earthshine must exclude the shaded portion of the cap. Spin-stabilized satellites which rotate uniformly about the spin axis greatly complicate the analysis. The rotation around an arbitrary axis means in general that the heat fluxes vary, since the visible portion of the earth is a function of this rotation.

The analysis presented herein is based upon the energy impinging upon a flat surface whose orientation is defined in vector notation (by the normal vector), and which is rotating about an arbitrary axis. This has a much broader application than may be realized at first. Although the obvious application is for spin-stabilized satellites, the results apply to any body of revolution. Here the interest lies in the variation of flux about the axis rather than an average value per spin. Thus, with the orientation of a single flat plate, the impinging fluxes on cylinders and cones are obtained. A sphere or a shape with a variable surface curvature along its axis requires several or many such plates, depending upon the precision required. It can be seen that the thermal radiation to the entire satellite surface may be found by simply considering a handful of appropriately oriented flat plates.

The purpose of this paper is to present, in general form, the derivation of the governing equations for the radiation energy sources as stated. The equations refer specifically to a flat surface rotating about an axis whose orientation is arbitrary. The dependence upon orbital position is included; the results of the numerical integration of these equations, encompassing a suitable range of applicable orbits, is presented.

COORDINATE SYSTEMS AND VECTOR REPRESENTATION

The primary coordinate system is fixed with respect to the orbit (Figure 1). The XY plane lies in the plane of the orbit with the X axis coincident with the line connecting the center of the earth (the focus of the ellipse) and perigee.

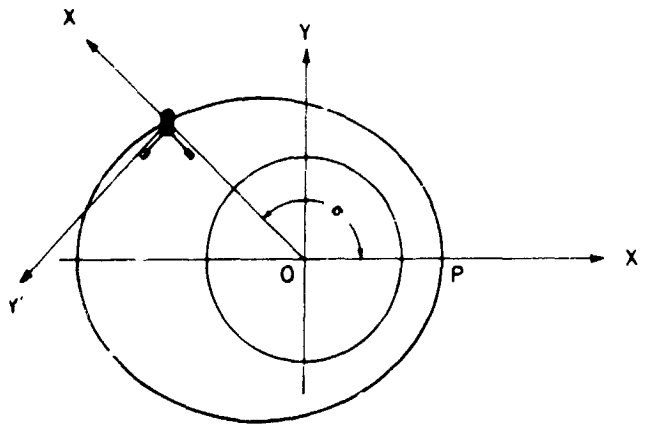

LEGEND
O-EARTH CENTER
P-PERIGEE

Figure 1—Coordinate systems.

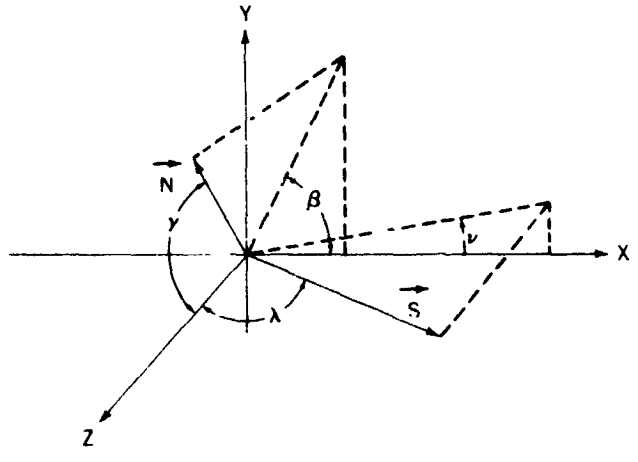

Figure 2—Orientation of normal and solar vectors.

As the satellite traverses the orbit, the instantaneous location is defined by the angle α. The altitude, therefore, may be determined at any instant by

$$A(\alpha) = \frac{(P + R_e)(1 + e)}{1 + e \cos \alpha} - R_e \qquad (1)$$

where

$A(\alpha)$ = altitude,

P = altitude at perigee,

R_e = radius of the earth,

e = eccentricity of the orbit.

The orientation of the unit vectors (Figure 2) representing the normals to the flat plates, N, and the solar vector, S, are specified by the following angles:

β = angle between the projection of N on the XY plane and the X axis,

γ = angle between N and the Z axis,

ν = angle between the projection of S on the XY plane and the X axis,

λ = angle between S and the Z axis.

The vectorial representations in the fixed coordinate system are thus

$$\mathbf{N} = \cos\beta \sin\gamma\, \mathbf{i} + \sin\beta \sin\gamma\, \mathbf{j} + \cos\gamma\, \mathbf{k} \qquad (2)$$

and

$$\mathbf{S} = \cos\nu \sin\lambda\, \mathbf{i} + \sin\nu \sin\lambda\, \mathbf{j} + \cos\lambda\, \mathbf{k} \; . \qquad (3)$$

It is convenient to introduce an instantaneous coordinate system (X' Y' Z') whose origin is fixed in the satellite (Figure 1). The X'Y' plane lies in the orbital plane with the X' axis coincident with the line from the earth's center to the satellite. Z' and Z have the same orientation.

The vectors N and S in the primed system are

$$\mathbf{N} = \cos(\beta - \alpha) \sin\gamma\, \mathbf{i}' + \sin(\beta - \alpha) \sin\gamma\, \mathbf{j}' + \cos\gamma\, \mathbf{k}' \; , \qquad (4)$$

$$\mathbf{S} = \cos(\nu - \alpha) \sin\lambda\, \mathbf{i}' + \sin(\nu - \alpha) \sin\lambda\, \mathbf{j}' + \cos\lambda\, \mathbf{k}' \; . \qquad (5)$$

In a similar manner the expression for the spin axis vector A may be shown to be

$$\mathbf{A} = \cos(\delta - \alpha)\sin\mu\,\mathbf{i}' + \sin(\delta - \alpha)\sin\mu\,\mathbf{j}' + \cos\mu\,\mathbf{k}' \tag{6}$$

where

δ = angle between the projection of A on the XY plane and the X axis,

μ = angle between A and the Z axis.

PLATE ROTATING ABOUT THE SPIN AXIS

For spin-stabilized satellites the normal vectors N, which represent the orientation of the exterior surfaces, rotate about the spin axis. In determining both instantaneous and average heat fluxes, the orientation of N as a function of this rotation with respect to the primed coordinate system (X' Y' Z') must be known. This is accomplished by defining a third coordinate system X'' Y'' Z'' (Figure 3). The X'' axis is coincident with the spin axis A. Y'' is defined so that it lies in the plane formed by X'' and an arbitrary fixed position of the normal vector N_o.*

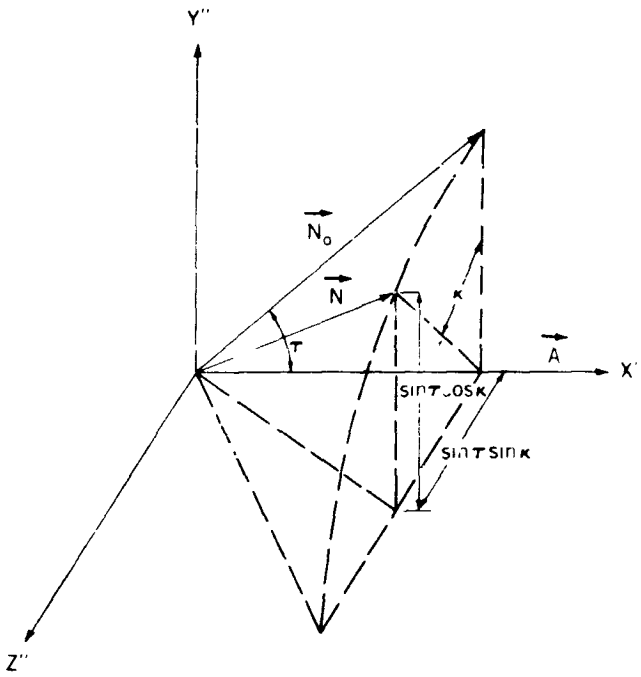

Figure 3—Double-primed coordinate system.

In Figure 3, the following terms may be evaluated:

$$\cos\tau = \cos(\beta - \alpha)\sin\gamma\cos(\delta - \alpha)\sin\mu + \sin(\beta - \alpha)\sin\gamma\sin(\delta - \alpha)\sin\mu + \cos\gamma\cos\mu\,, \tag{7}$$

$$\sin\tau = \sqrt{1 - \cos^2\tau}\,,$$

$$\mathbf{N} = \cos\tau\,\mathbf{i}'' + \sin\tau\cos\kappa\,\mathbf{j}'' + \sin\tau\sin\kappa\,\mathbf{k}'' \tag{8}$$

It can be seen that the angle between the spin axis and N_o can be computed only in the first and second quadrants of the X''Y'' plane. This has little effect since κ varies from 0 to 2π (a rotation). [If the vector N_o lies in the third quadrant (of the X''Y'' plane) the initial position for rotation remains in the second quadrant.] The objective now is to relate the double-primed unit vectors to the primed vectors in order to determine N in the primed system.

*Since a complete rotation occurs, the orientation of N_o merely indicates the starting point.

The projections of $\mathbf{j}''$ and $\mathbf{k}''$ in the primed coordinate system are found in the following manner: The value for the unit vector $\mathbf{k}''$ is

$$\mathbf{k}'' = \frac{\mathbf{A} \times \mathbf{N}_o}{|\mathbf{A} \times \mathbf{N}_o|} = \frac{g\mathbf{i}' + h\mathbf{j}' + l\mathbf{k}'}{\sqrt{g^2 + h^2 + l^2}} , \tag{9}$$

where

$$g = \sin(\delta - \alpha) \sin\mu \cos\gamma - \cos\mu \sin(\beta - \alpha) \sin\gamma ,$$

$$h = \cos\mu \cos(\beta - \alpha) \sin\gamma - \cos(\delta - \alpha) \sin\mu \cos\gamma ,$$

$$l = \cos(\delta - \alpha) \sin\mu \sin(\beta - \alpha) \sin\gamma$$

$$- \sin(\delta - \alpha) \sin\mu \cos(\beta - \alpha) \sin\gamma$$

similarly

$$\mathbf{j}'' = \frac{(\mathbf{A} \times \mathbf{N}_o) \times \mathbf{A}}{|(\mathbf{A} \times \mathbf{N}_o) \times \mathbf{A}|} = \frac{m\mathbf{i}' + n\mathbf{j}' + o\mathbf{k}'}{\sqrt{m^2 + n^2 + o^2}} \tag{10}$$

where

$$m = h\cos\mu - l \sin(\delta - \alpha) \sin\mu ,$$

$$n = l \cos(\delta - \alpha) \sin\mu - g\cos\mu ,$$

$$o = g \sin(\delta - \alpha) \sin\mu - h\cos(\delta - \alpha) \sin\mu .$$

N may now be determined in the primed coordinate system (X' Y' Z'). By rewriting the double-primed unit vectors,

$$\left.\begin{aligned} \mathbf{i}'' &= p\mathbf{i}' + q\mathbf{j}' + r\mathbf{k}' \\ \mathbf{j}'' &= s\mathbf{i}' + t\mathbf{j}' + u\mathbf{k}' \\ \mathbf{k}'' &= v\mathbf{i}' + w\mathbf{j}' + x\mathbf{k}' \end{aligned}\right\} . \tag{11}$$

where

$$p = \cos(\delta - \alpha) \sin\mu ,$$

$$q = \sin(\delta - \alpha) \sin\mu ,$$

$$r = \cos\mu ,$$

$$s = \frac{m}{\sqrt{m^2 + n^2 + o^2}} ,$$

$$t = \frac{n}{\sqrt{m^2 + n^2 + o^2}} ,$$

$$u = \frac{o}{\sqrt{m^2 + n^2 + o^2}} ,$$

$$v = \frac{g}{\sqrt{g^2 + h^2 + l^2}} ,$$

$$w = \frac{h}{\sqrt{g^2 + h^2 + l^2}} ,$$

$$x = \frac{l}{\sqrt{g^2 + h^2 + l^2}} .$$

By substituting for i'', j'', and k'' in Equation 8

$$N = ai' + bj' + ck' , \tag{12}$$

where

$$a = p\cos\tau + s\sin\tau\cos\kappa + v\sin\tau\sin\kappa ,$$

$$b = q\cos\tau + t\sin\tau\cos\kappa + w\sin\tau\sin\kappa ,$$

$$c = r\cos\tau + u\sin\tau\cos\kappa + x\sin\tau\sin\kappa ,$$

where κ is the angle of rotation. N may now be evaluated at any position during rotation throughout the orbit in the primed system (X' Y' Z').

DETERMINATION OF EARTHSHINE

The general expression for the radiation intensity dq, from a diffusely emitting source dA_e, impinging upon a unit area, is as follows:

$$dq = \frac{I\cos\omega\cos\eta\, dA_e}{D^2} , \tag{13}$$

where

I = source intensity,

ω = angle between the line connecting the unit area with dA_e and the normal to dA_e (N_e),

η = angle between the line connecting dA_e with the unit area and the normal to the unit area,

D = distance between the unit area and dA_e.

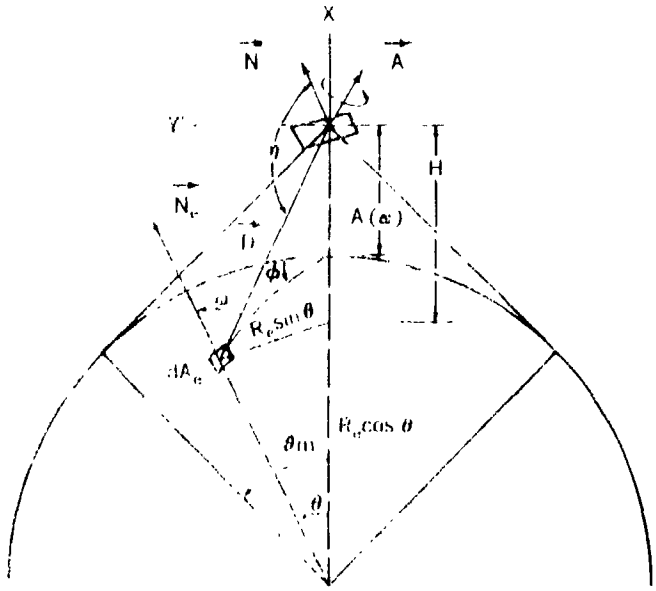

Figure 4—Earth's cap visible from satellite ($\phi = 0$ when coincident with r').

With the application of this equation to a flat plate of unit area at an altitude $A(\alpha)$, the radiation intensity impinging upon the plate is

$$q_E = \frac{\sigma T_e^4}{\pi} \int_0^{\theta_m} \int_0^{2\pi} \frac{\cos\alpha \cos\eta \, dA_e}{D^2} \qquad (14)$$

where

σ = Stefan-Boltzmann constant,

T_e = mean black body temperature of the earth's surface,

σT_e^4 = the heat flux leaving the source dA_e.

From the geometry of Figure 4 (which is similar to a sketch used by Katz*) and the vector notation presented, the terms in the equation may be defined more specifically:

$$\mathbf{D} = -H\mathbf{i}' + R_e \sin\theta \cos\phi \, \mathbf{j}' + R_e \sin\theta \sin\phi \, \mathbf{k}' ,$$

$$= -\left[A(\alpha) + R_e (1-\cos\theta)\right] \mathbf{i}' + R_e \sin\theta \cos\phi \, \mathbf{j}' + R_e \sin\theta \sin\phi \, \mathbf{k}' ,$$

$$D^2 = \left[A(\alpha) + R_e(1-\cos\theta)\right]^2 + R_e^2 \sin^2\theta ,$$

$$\alpha = \theta + \tan^{-1}\left[\frac{R_e \sin\theta}{A(\alpha) + R_e (1-\cos\theta)}\right] ,$$

$$\cos\eta = \frac{\mathbf{D}\cdot\mathbf{N}}{|\mathbf{D}|} ,$$

$$= \left\{ a\left[A(\alpha) + R_e (1-\cos\theta)\right] + b R_e \sin\theta \cos\phi + c R_e \sin\theta \sin\phi \right\} \cdot$$

$$\cdot \frac{1}{\sqrt{\left[A(\alpha) + R_e (1-\cos\theta)\right]^2 + \left(R_e^2 \sin^2\theta\right)}} ,$$

$$\theta_m = \cos^{-1}\left[\frac{R_e}{A(\alpha) + R_e}\right] .$$

*Katz, A. J., "Determination of Thermal Radiation Incident upon the Surfaces of an Earth Satellite in an Elliptical Orbit," Grumman Aircraft Engineering Corp., Rept. XP 12.20, May 1960.

Equation 14 may now be written in the form

$$q_E = \frac{\sigma T_e^4}{\pi} \int_0^{\cos^{-1}\left[\frac{R_e}{A(\alpha)+R_e}\right]} \int_0^{2\pi} \cos\left\{\theta + \tan^{-1}\left[\frac{R_e \sin\theta}{A(\alpha) + R_e(1-\cos\theta)}\right]\right\} \cdot$$

$$\cdot \left\{a\left[-A(\alpha) + R_e(1-\cos\theta)\right] + b R_e \sin\theta\cos\phi + c R_e \sin\theta \sin\phi\right\} \cdot$$

$$\cdot \left\{\frac{1}{\left[A(\alpha) + R_e(1-\cos\theta)\right]^2 + R_e^2 \sin^2\theta}\right\}^{3/2} R_e^2 \sin\theta \, d\phi \, d\theta \, . \qquad (15)$$

The limits of integration are such that the part of the earth cap visible from the instantaneous location of the satellite is included. For most practical cases, at least a portion of the cap is not visible from a plate because of its orientation. Attempts to define the appropriate integration limits for such cases are extremely laborious. Since the equations cannot be solved without the aid of a high speed computer, an alternative approach is employed.* The numerical integration includes the entire visible part of the earth cap as stated, but the contributions of the elemental area that the plate does not see are deleted if the local value of $\cos\eta$ is negative.

Equation 15 represents the flux for the instantaneous orientation of the plate. Interest also lies in the determination of the flux for a complete rotation of the plate about the satellite spin axis. The average value for q_E is therefore

$$q_{E_{av.}} = \frac{1}{2\pi} \int_0^{2\pi} q_E \, d\kappa \qquad (16)$$

where κ is the rotational angle.

DETERMINATION OF ALBEDO

The calculation for the albedo input to an orbiting plate is similar to that for the earthshine but involves additional basic assumptions. The reflectance of the earth depends on what is the visible surface—land, water, snow, cloud cover, etc. Until precise data is available which indicates the functional relationship between the albedo and the visible surface, an approximate mean value of 35 percent appears satisfactory.

The reflected radiation is assumed to be diffuse. The local earth-reflected intensity varies with the cosine of the angle between the solar vector and the local normal. Since the input to the plate is a function of the source intensity of the visible elemental areas, the reflected radiation can be expressed by

*Katz, A. J., op. cit.

$$q_A = \frac{S\ alb}{\pi} \int_0^{\cos^{-1}\left[\frac{R_e}{A(\alpha)+R_e}\right]} \int_0^{2\pi} \cos\left\{\theta + \tan^{-1}\left[\frac{R_e \sin\theta}{A(\alpha) + R_e\,(1-\cos\theta)}\right]\right\} \cdot$$

$$\cdot \left\{a\left[-A(\alpha) + R_e\,(1-\cos\theta)\right] + b\,R_e \sin\theta\cos\phi + c\,R_e \sin\theta \sin\phi\right\} \cdot$$

$$\cdot \cos\psi \cdot \left\{\frac{1}{\left[A(\alpha) + R_e\,(1-\cos\theta)\right]^2 + R_e^2 \sin^2\theta}\right\}^{3/2} R_e^2 \sin\theta\, d\phi\, d\theta\,, \qquad (17)$$

where

S = solar constant (440 BTU/hr/ft^2)

alb = albedo factor (0.35)

ψ = angle between the solar vector S and the normal to dA_e, N_e,

Cos ψ may be obtained from:

$$\cos\psi = S \cdot N_e$$

$$= \cos(\nu-\alpha)\cos\theta \sin\lambda + \sin(\nu-\alpha)\sin\theta\cos\phi\sin\lambda + \cos\lambda\sin\theta\sin\phi\,. \qquad (18)$$

The area of the earth that contributes to the albedo input is the surface common to the sunlit part of the earth and the part of the cap visible from the plate. The remaining area visible from the plate but receiving no sunlight contributes nothing to the heat input. This is accounted for in the numerical integration by deleting inputs when cos ψ is negative.

The average albedo flux received by the plate per rotation about the spin axis is

$$q_{A_{av.}} = \frac{1}{2\pi}\int_0^{2\pi} q_A\, d\kappa\,. \qquad (19)$$

CALCULATION OF DIRECT SOLAR FLUX

The calculation of direct sunlight involves the determination of the instantaneous projected area of the plate with respect to the solar vector:

$$q_{SR} = S(S \cdot N)$$

$$= S\left[a\cos(\nu-\alpha)\sin\lambda + b\sin(\nu-\alpha)\sin\lambda + c\cos\lambda\right]\,, \qquad (20)$$

where S is the solar constant.

Because of its orientation the plate may or may not be facing the sun during a rotation. Negative values of $S \cdot N$ indicate that it is not facing the sun.

The average flux per spin is

$$q_{S R_{av.}} \quad \frac{1}{2\pi} \int_0^{2\pi} q_{S R} \, d\lambda \quad . \tag{21}$$

Because the orientation of the plate is fixed in space, the heat flux is constant throughout the sunlit portion of the orbit. To determine whether or not the satellite is within the earth's shadow at any orbital position requires two simple checks.* If both of the following expressions are satisfied, the satellite received no direct input from the sun:

$$\cos \Omega < 0 \quad ,$$

$$\left[R_e + A(\alpha)\right] \cdot | \sin \qquad \cdot R_e \quad ,$$

where Ω is the angle between the solar vector S and X',

$$\cos \Omega = S \cdot i' \quad ,$$

$$\cos \Omega = \cos (\nu - \alpha) \sin \lambda \quad .$$

APPLICATION

Hypothetical geometric configurations (Figure 5) have been chosen to illustrate the use of the equations. The external surfaces are represented by the indicated normal vectors.

*Katz, A. J., op. cit.

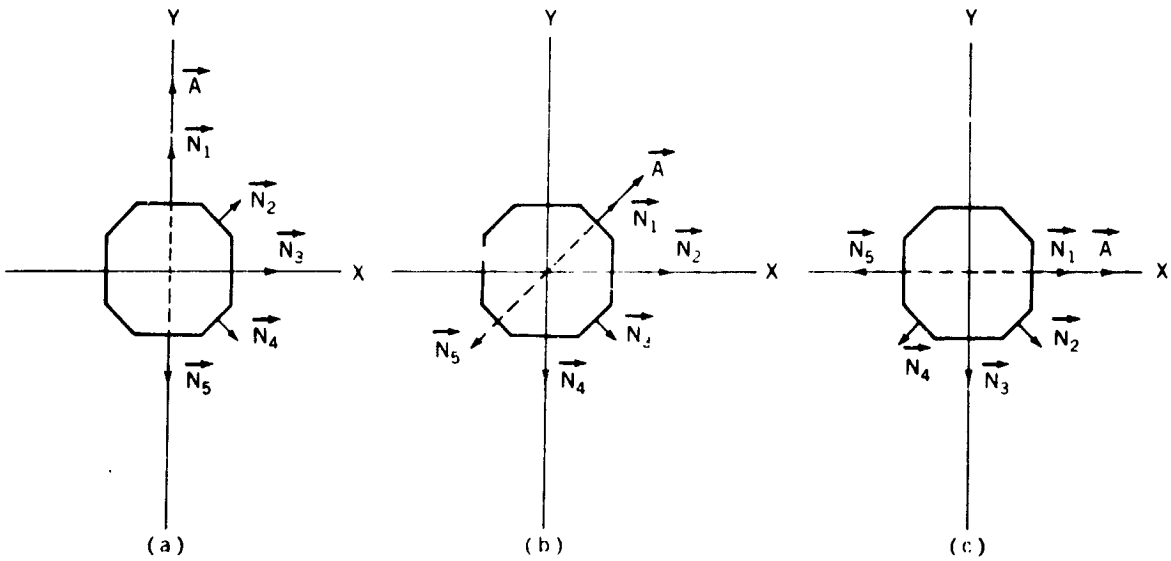

Figure 5—Geometrical configurations.

The three sketches represent three spin axis orientations.

Circular orbits of 150, 550, 1050, 2000, and 5000 statute miles, in which the solar vector lies in the plane of the orbit (minimum sunlight), were considered. Figures 6-35 indicate the orbital variation of earthshine and albedo.* These heat fluxes represent mean integrated values per rotation at the instantaneous orbital position. The direct solar flux is constant in sunlight for a specific orientation. Appropriate values are presented in Table 1.

Table 1

Mean Solar Heat Flux per Rotation*

δ (degrees)	β (degrees)	$Q_{SR_{av.}}$ (BTU/hr/ft^2)
90	90	0.0
90	45	99.0
90	0	140.0
90	315	99.0
90	270	0.0
45	45	311 0
45	0	220.0
45	315	99.0
45	270	0.0
45	225	0.0
0	0	440.0
0	315	311.0
0	270	0.0
0	225	0.0
0	180	0.0

*The data presented represent the instantaneous daylight heat flux impinging upon the rotating faces of the configuration in Figure 5. The sun in all cases is parallel to the X axis; μ, γ, and λ are 90 degrees.

ACKNOWLEDGMENTS

The author wishes to express gratitude to Mr. Frank Hutchinson and Mr. Henry Hartley for the IBM 7090 program and the data presentation, respectively.

*The mathematical model assumed the earth cap to be comprised of 512 elemental areas. The curves are based primarily on calculations made at 22.5 degree increments throughout the orbit. Because of this, the peaks in some of the albedo curves were estimated. It should be noted that, because of the configurations chosen, the orbital heat fluxes in several cases are identical except for angular displacement.

(Manuscript received June 26, 1963)

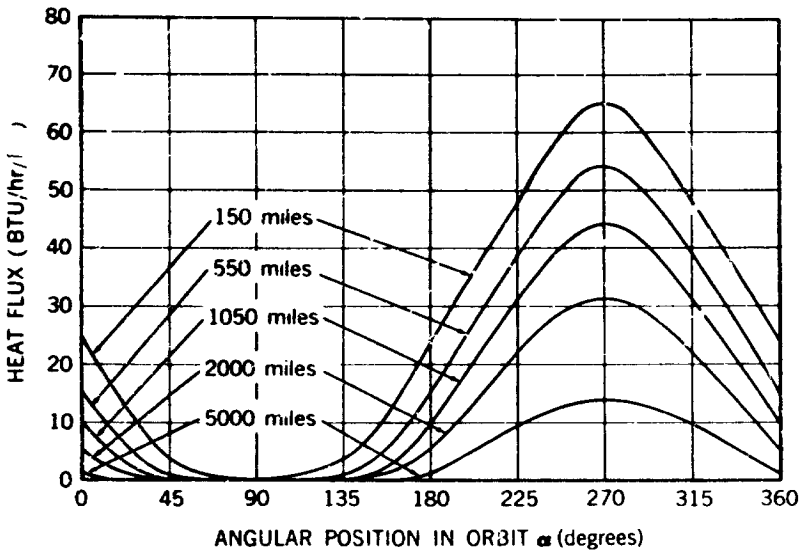

Figure 6—Earth-emitted radiation for circular orbits, δ = 90 degrees, β = 90 degrees.

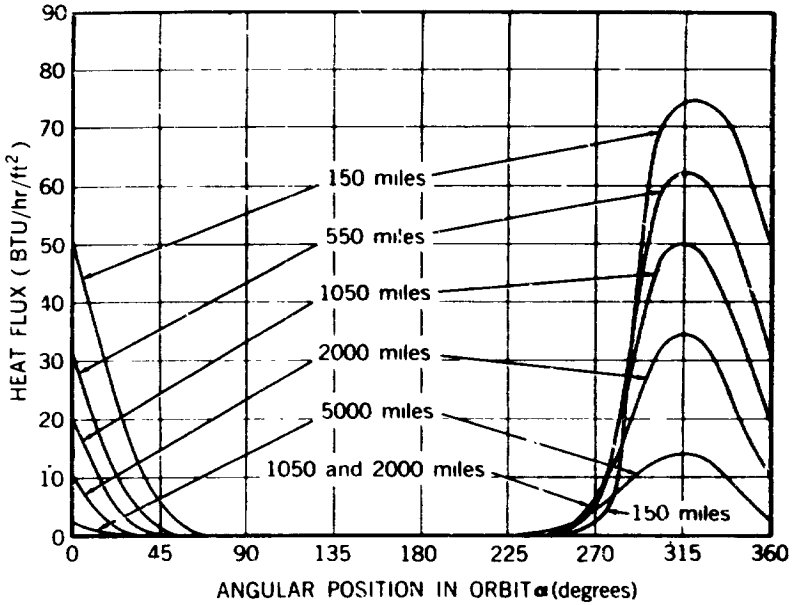

Figure 7—Albedo for minimum sunlit circular orbits, δ = 90 degrees, β = 90 degrees.

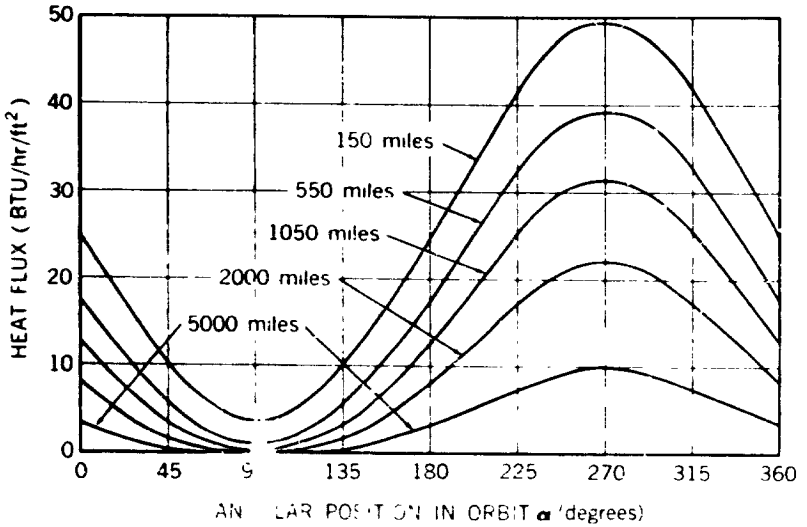

Figure 8—Earth-emitted radiation for circular orbits, δ = 90 degrees, β = 45 degrees.

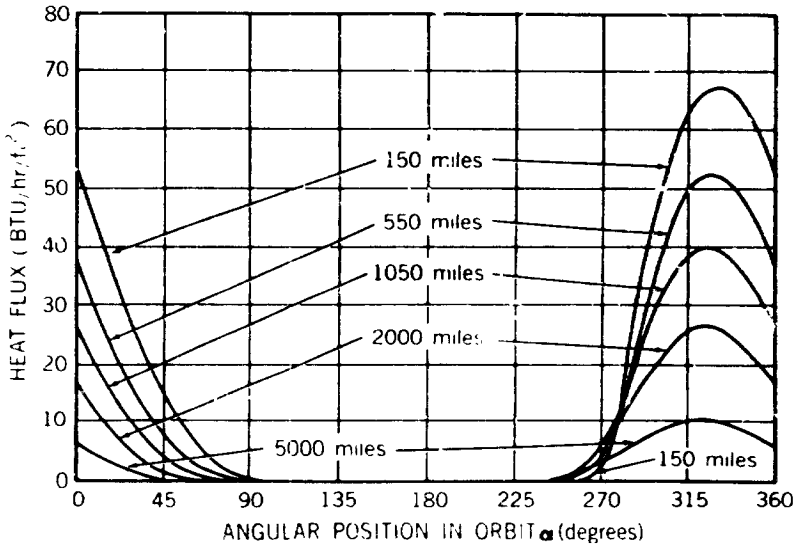

Figure 9—Albedo for minimum sunlit circular orbits, δ = 90 degrees, β = 45 degrees.

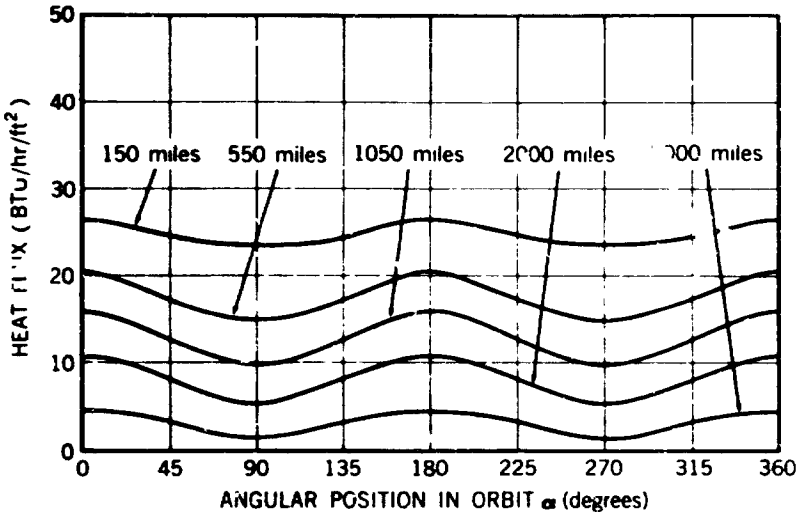

Figure 10—Earth-emitted radiation for circular orbits, δ = 90 degrees, β = 0 degrees.

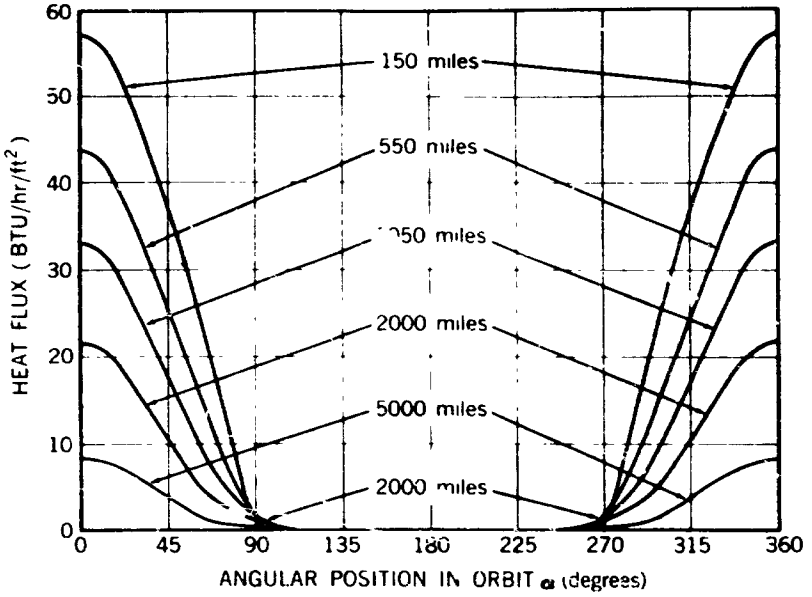

Figure 11—Albedo for minimum sunlit circular orbits, δ = 90 degrees, β = 0 degrees.

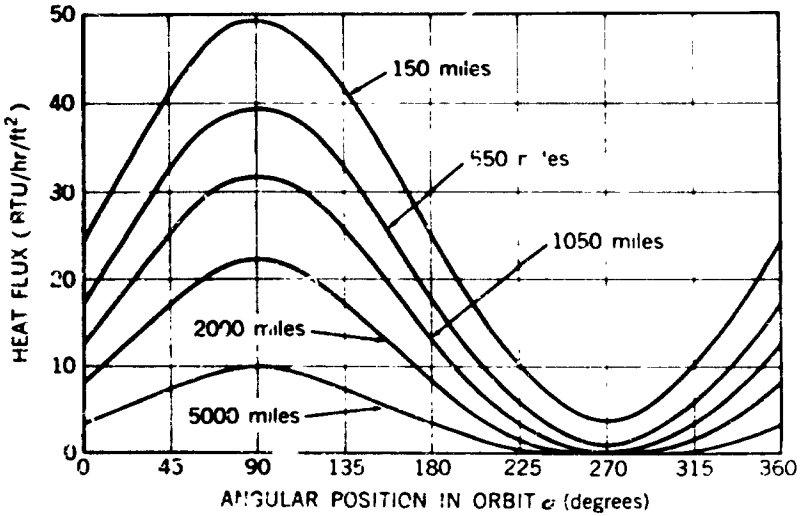

Figure 12—Earth-emitted radiation for circular orbits, δ = 90 degrees, β = 315 degrees.

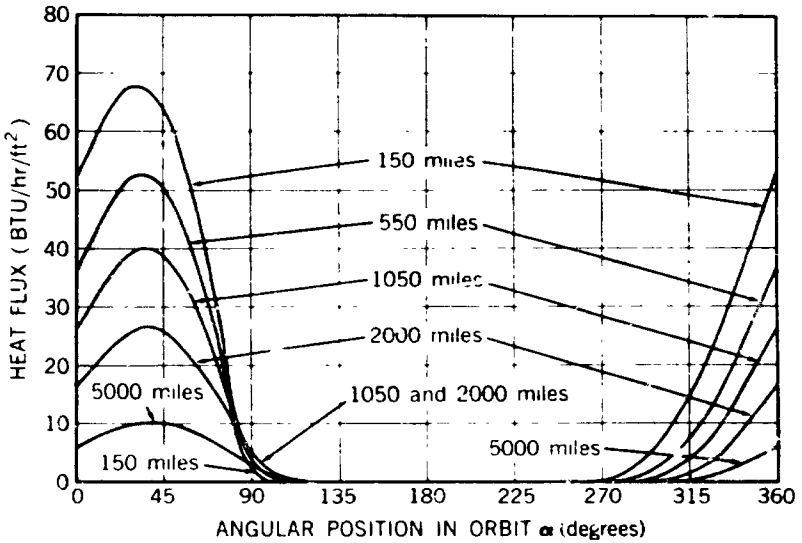

Figure 13—Albedo for minimum sunlit circular orbits, δ = 90 degrees, β = 315 degrees.

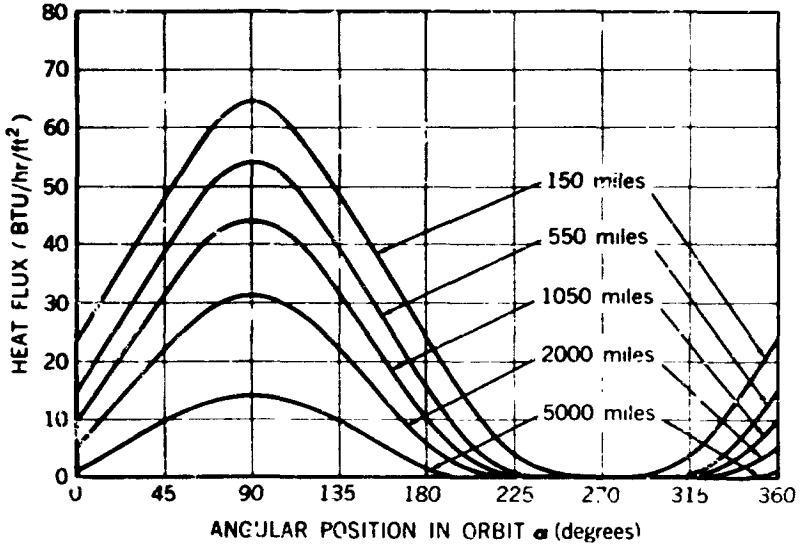

Figure 14—Earth-emitted radiation for circular orbits, δ = 90 degrees, β = 270 degrees.

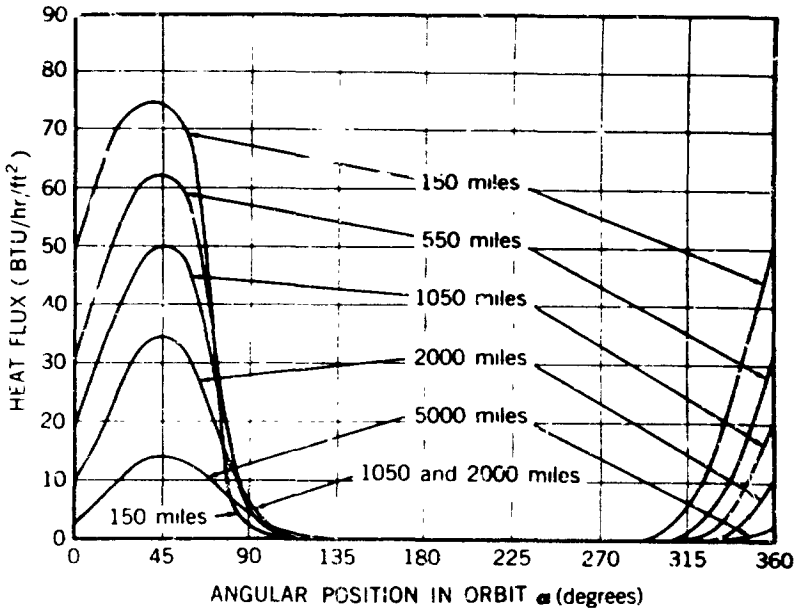

Figure 15—Albedo for minimum sunlit circular orbits, δ = 90 degrees, β = 270 degrees.

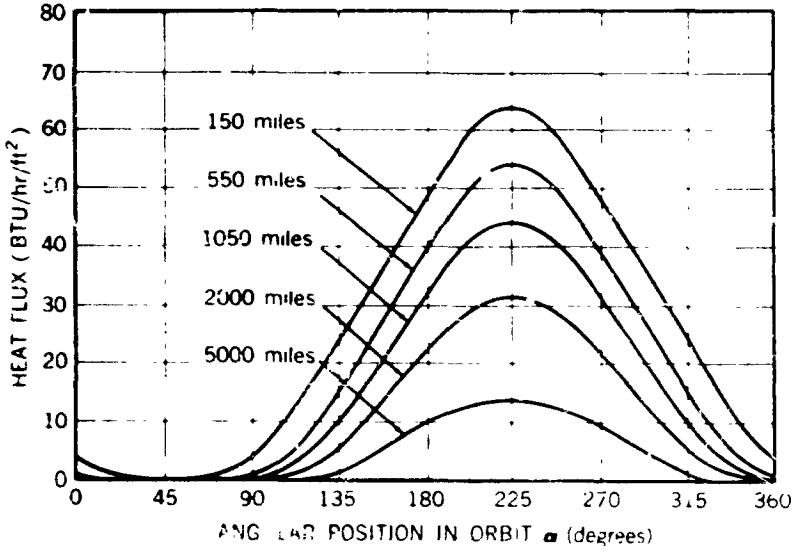

Figure 16—Earth-emitted radiation for circular orbits, δ = 45 degrees, β = 45 degrees.

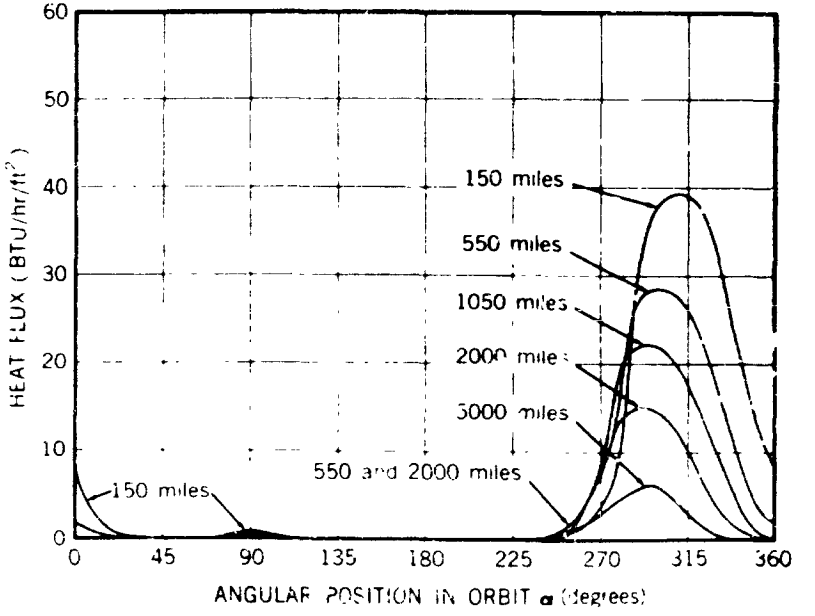

Figure 17—Albedo for minimum sunlit circular orbit, δ = 45 degrees, β = 45 degrees.

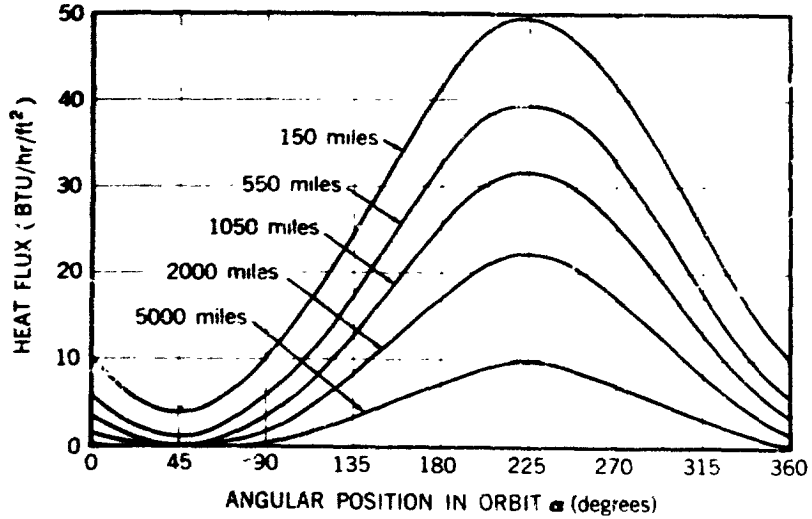

Figure 18—Earth-emitted radiation for circular orbits, δ = 45 degrees, β = 0 degrees.

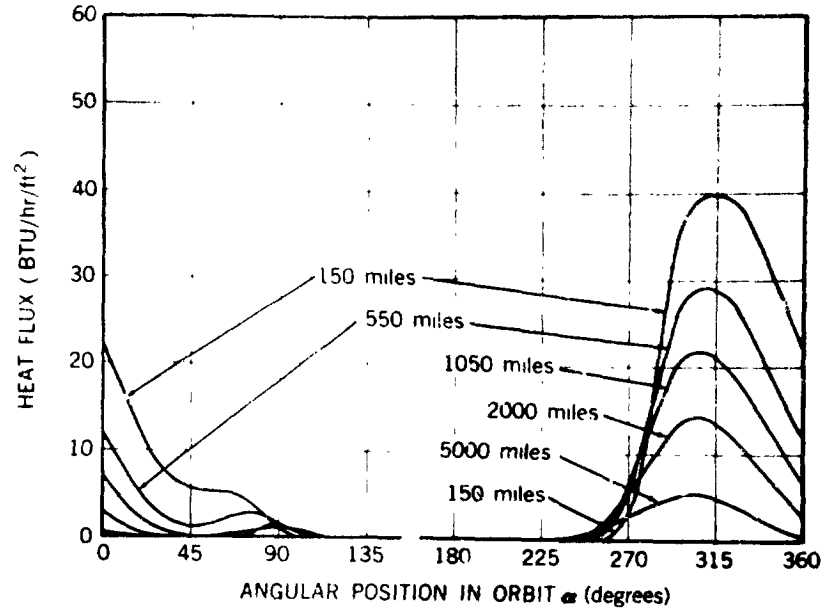

Figure 19—Albedo for minimum sunlit circular orbits, δ = 45 degrees, β = 0 degrees.

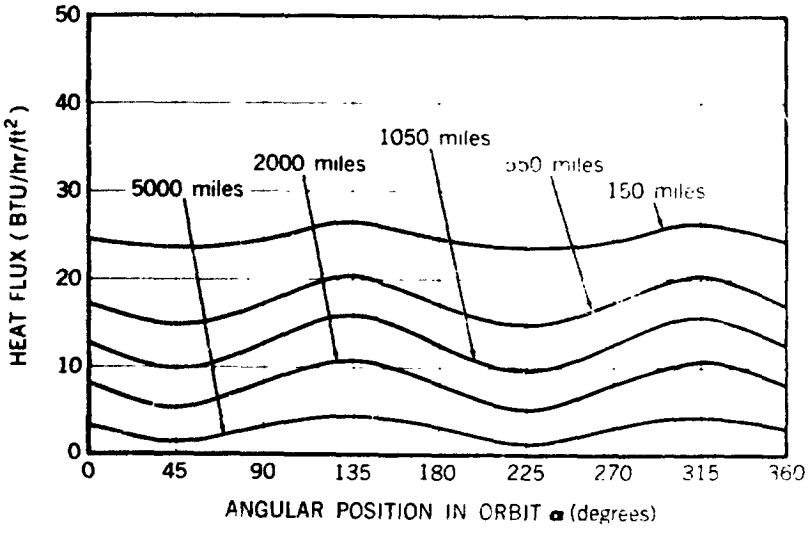

Figure 20—Earth-emitted radiation for circular orbits, δ = 45 degrees, β = 315 degrees.

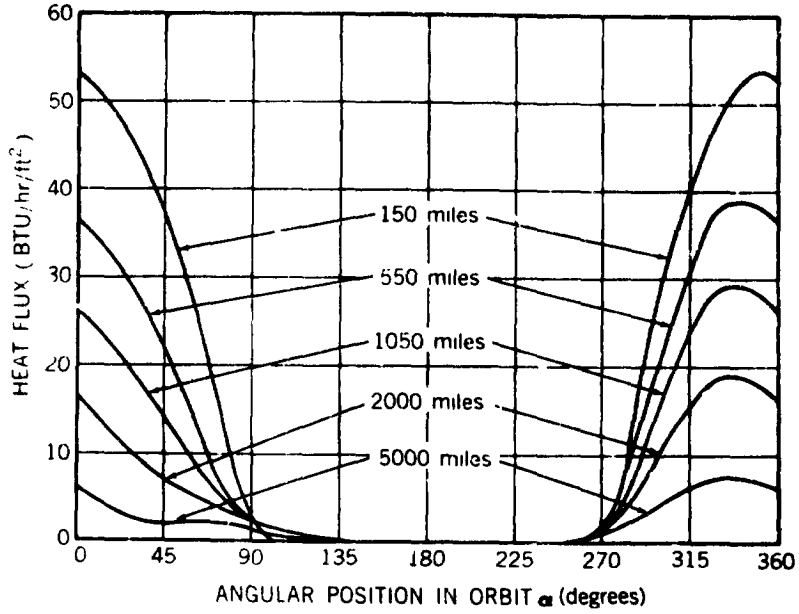

Figure 21—Albedo for minimum sunlit circular orbits, δ = 45 degrees, β = 315 degrees.

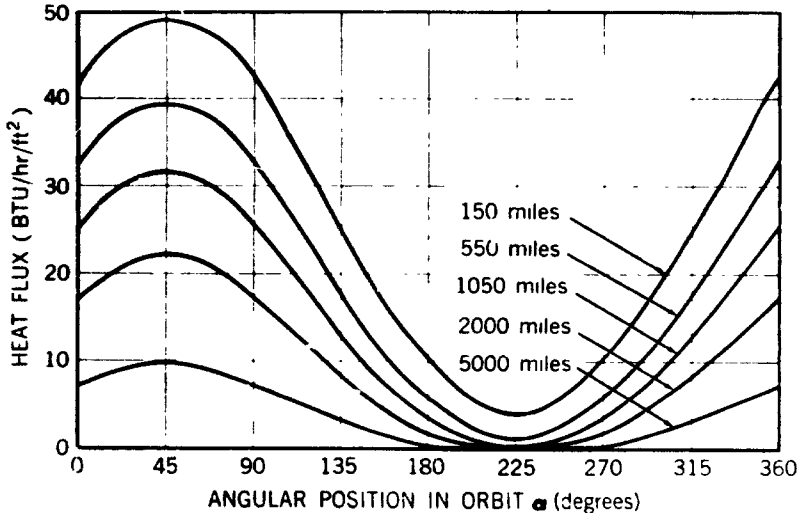

Figure 22—Earth-emitted radiation for circular orbits, δ = 45 degrees, β = 270 degrees.

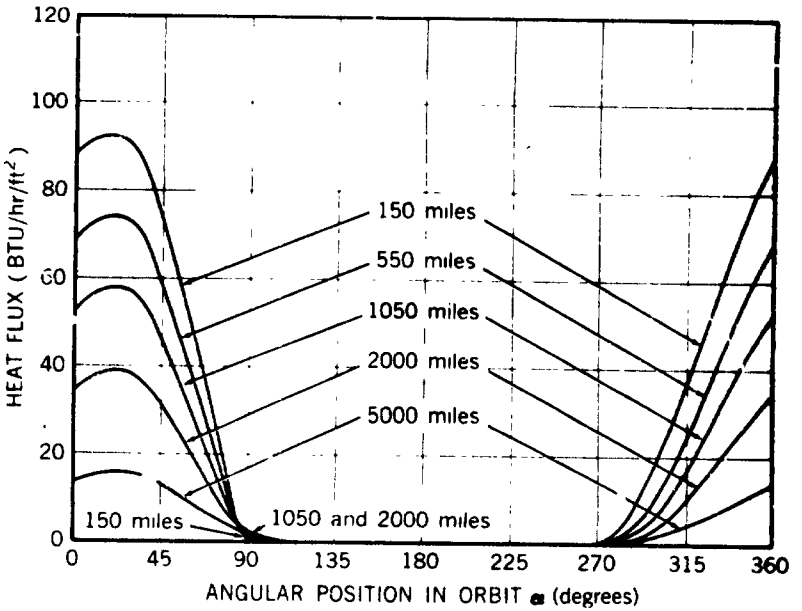

Figure 23—Albedo for minimum sunlit circular orbits, δ = 45 degrees, β = 270 degrees.

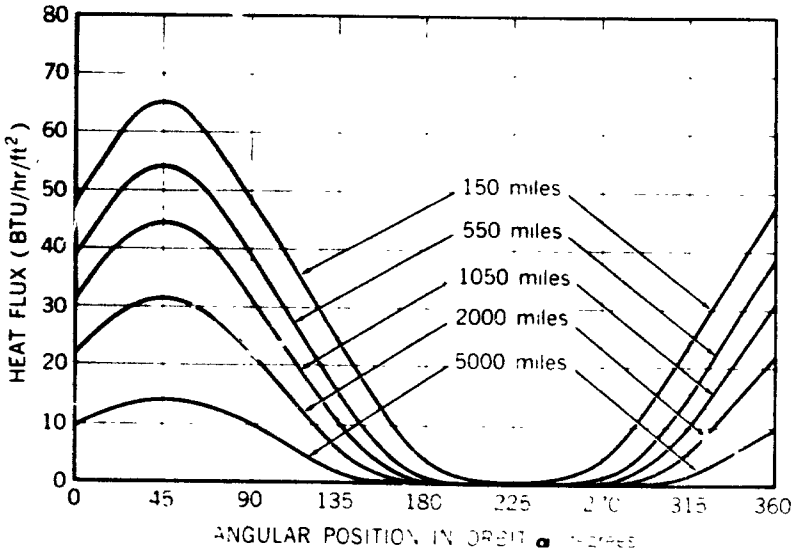

Figure 24—Earth-emitted radiation for circular orbits, δ = 45 degrees, β = 225 degrees.

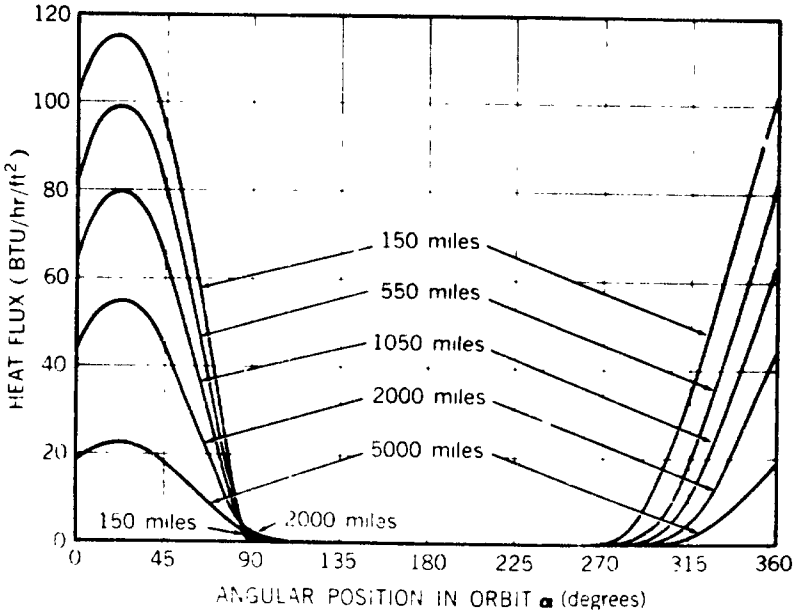

Figure 25—Albedo for minimum sunlit circular orbits, δ = 45 degrees, β = 225 degrees.

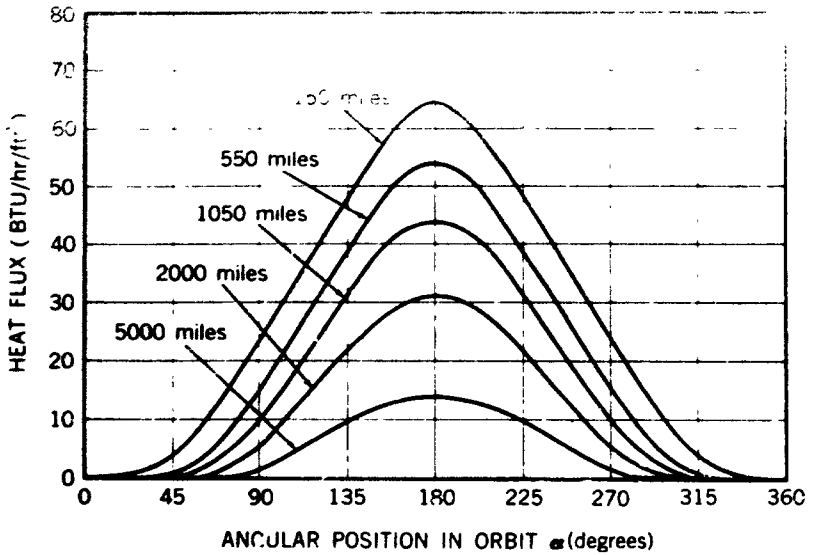

Figure 26—Earth-emitted radiation for circular orbits, δ = 0 degrees, β = 0 degrees.

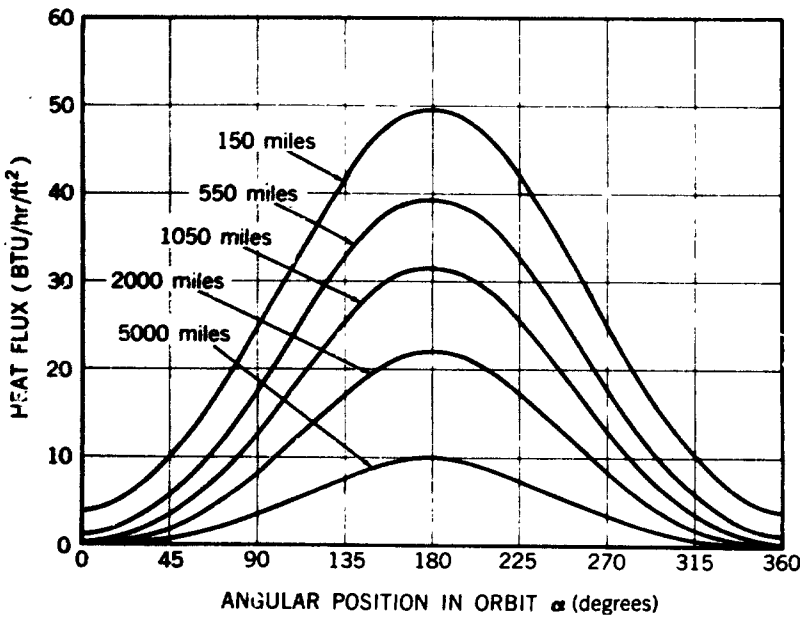

Figure 28—Earth-emitted radiation for circular orbits, δ = 0 degrees, β = 315 degrees.

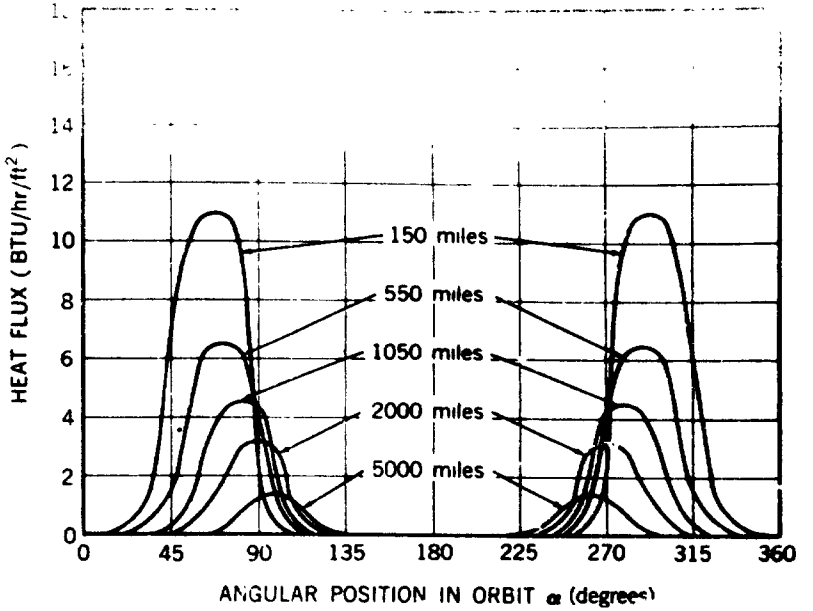

Figure 27—Albedo for minimum sunlit circular orbits, δ = 0 degrees, β = 0 degrees.

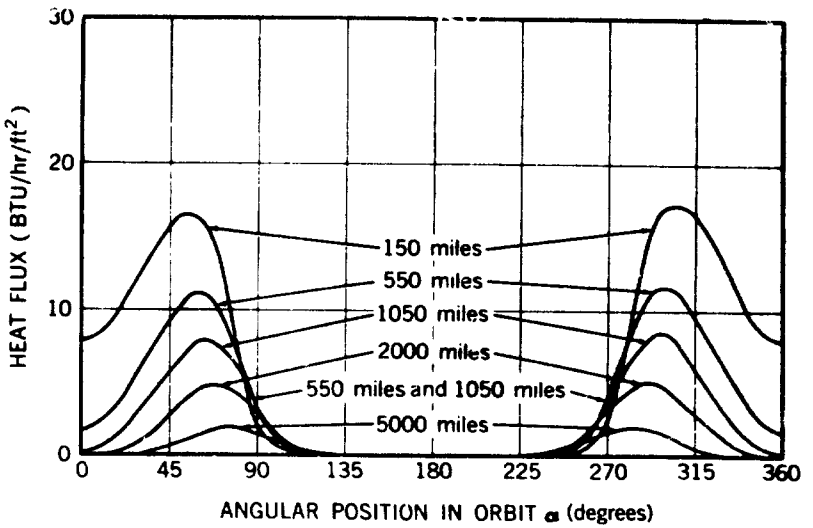

Figure 29—Albedo for minimum sunlit circular orbits, δ = 0 degrees, β = 315 degrees.

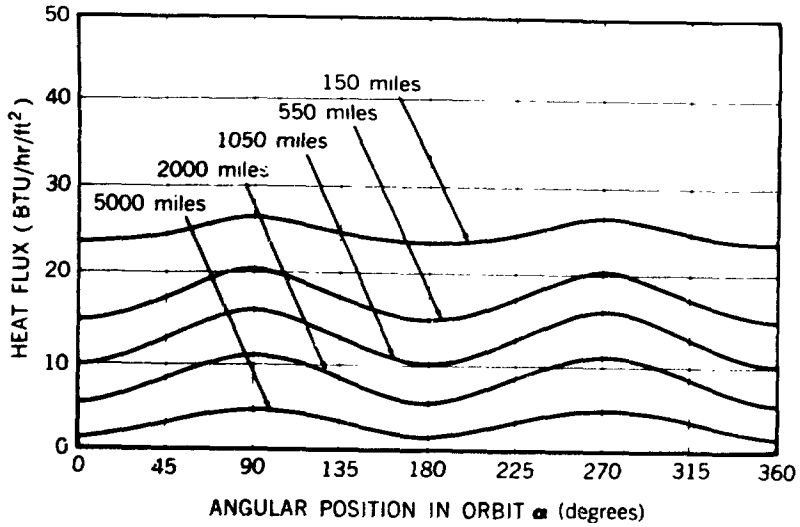

Figure 30—Earth-emitted radiation for circular orbits, δ = 0 degrees, β = 270 degrees.

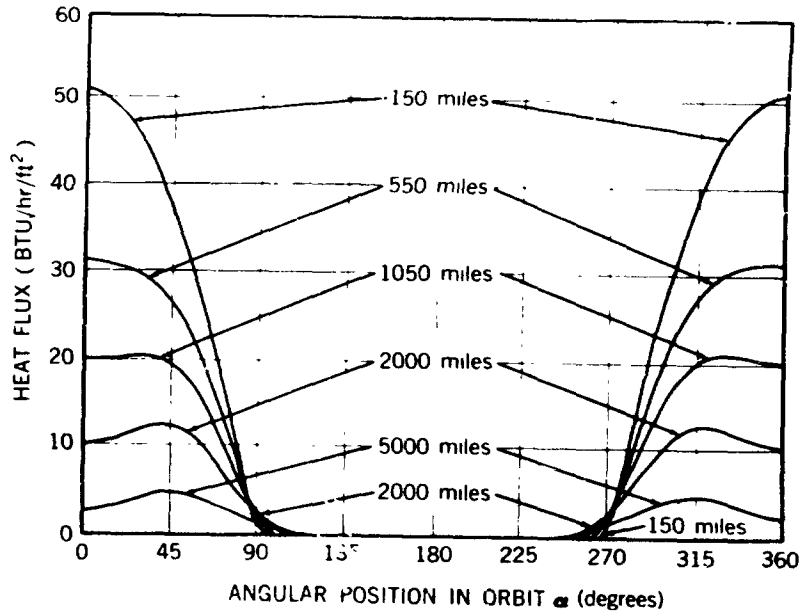

Figure 31—Albedo for minimum sunlit circular orbits, δ = 0 degrees, β = 270 degrees.

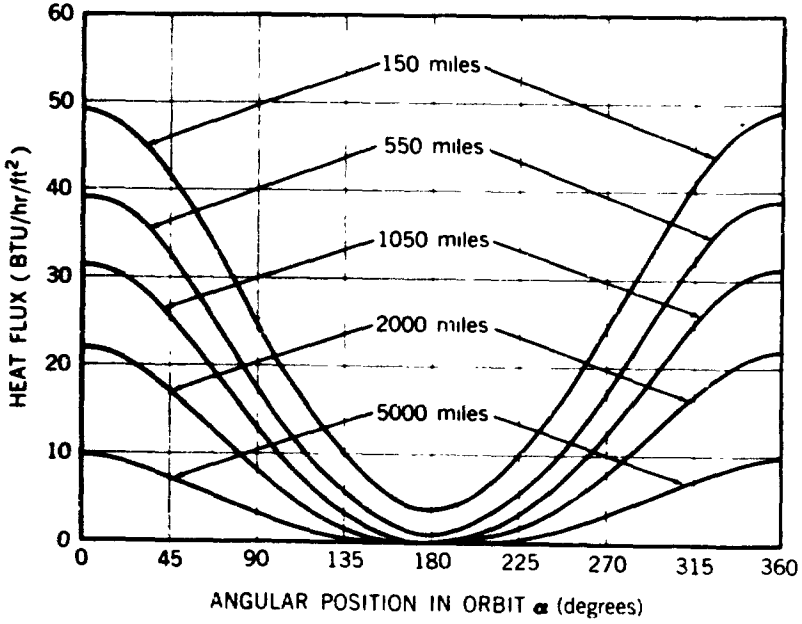

Figure 32—Earth-emitted radiation for circular orbits, δ = 0 degrees, β = 225 degrees.

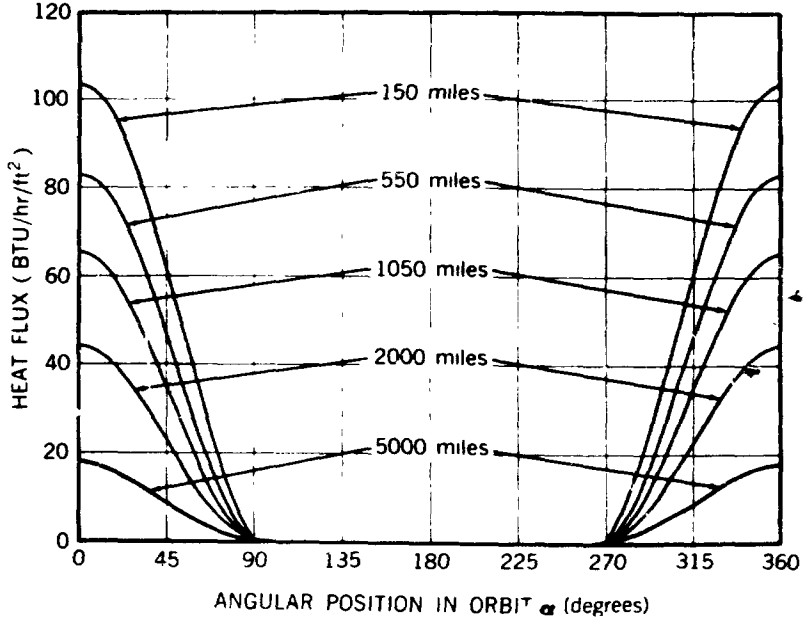

Figure 33—Albedo for minimum sunlit circular orbits, δ = 0 degrees, β = 225 degrees.

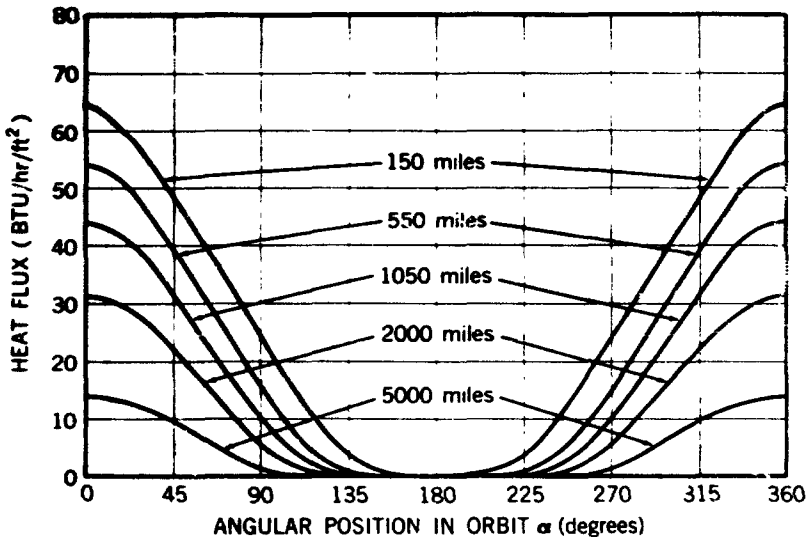

Figure 34—Earth-emitted radiation for circular orbits, δ = 0 degrees, β = 180 degrees.

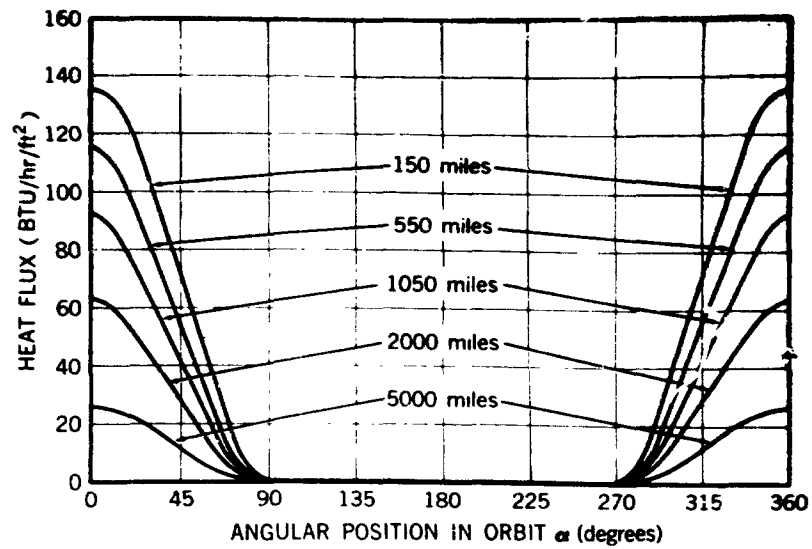

Figure 35—Albedo for minimum sunlit circular orbits, δ = 0 degrees, β = 180 degrees.

THREE DIMENSIONAL HEAT TRANSFER PROGRAM

TABLE OF CONTENTS

I. Summary

An IBM 7094, three dimensional, heat transfer program for satellite application is discussed. The program may be applied to all phases of spacecraft life, from launch to orbital quasi-steady state. Launch phase heating includes inputs by radiation from the hot fairing and free molecule flow heating after nose cone ejection. Orbital heat fluxes are accounted for by direct sunlight, earth-reflected sunlight, and earth-emitted input to the satellite.

Internal heat exchange by conduction and radiation is determined, provided the appropriate conductances, radiation view factors, and effective emittances are known.

A simplified analysis of an active thermal controlled spacecraft is incorporated into the program. One or more surfaces may contain shutter systems which have optical properties specified as a function of shutter opening. The program evaluates the feasibility of any configuration based upon maintaining an internal component within its tolerable temperature limits.

The program employs a matrix inversion subroutine (Gauss Elimination Method) to solve the heat balance equations.

II. General Discussion

In practice, the thermal analysis of a spacecraft consists of the development of the thermal model which represents a fine mesh of interconnected isothermal nodes. The appropriate relationship between nodes regarding thermal conduction and radiation interchange must be established.

The general energy balance for each node of a thermal model may be written

$$P_n + S\alpha_s Ap_n + q_{alb_n} + q_{es_n} + \sum_m C_{nm}(T_m - T_n) + \sum_m \sigma E_{nm} F_{nm} \cdot (T_m^4 - T_n^4) + q_{a_n} + q_{F_n} = \sigma \epsilon_n A s_n T_n^4 + W C p_n \frac{dT_n}{dt_n} \quad (1)$$

where

P_n	=	internal power dissipation of node n
S	=	solar constant
α_s	=	solar absorptance
Ap_n	=	instantaneous projected area for sunlight of node n
q_{alb_n}	=	absorbed earth-reflected solar radiation (albedo)
q_{es_n}	=	absorbed earth-emitted radiation (earthshine) by node n
σ	=	Stefan-Boltzmann constant
ϵ_n	=	infrared emittance of node n
As_n	=	surface area of node n
WCp_n	=	heat capacity of node n
dT/dt	=	time rate of change of node n temperature
C_{nm}	=	thermal conductance between nodes n and m
E_{nm}	=	effective emittance between nodes n and m
F_{nm}	=	shape factor area product between nodes n and m
q_{an}	=	free molecule flow heating to node n
q_{Fn}	=	radiation from fairing absorbed by node n (when fairing is present external radiation sources are 0)

The solution of the n simultaneous equations shown above is performed by the IBM 7094 digital computer with a matrix inversion routine (Gauss Elimination Method). However, since the inversion applies only to linear simultaneous equations, the fourth power temperature terms must be linearized. This is done by retaining the first two terms in the Taylor Expansion around T_n.

$$T_n^4 = (T_{in} + dT)^4 = T_{in}^4 + 4T_{in}^3 dT + \frac{4\cdot 3}{2!} T_{in}^2 dT^2 + \cdots$$
$$T_n^4 \cong T_{in}^4 + 4T_{in}^3 dT \qquad (2)$$
$$T_n^4 \cong 4T_{in}^3 T_n - 3T_{in}^4$$

where T_{in} is (a) the initial value of T_n for steady state conditions or (b) the temperature at the beginning of time increment Δt during transient cases. Substituting this result into (1), the general equation in matrix form becomes

$$[B_{nm}] \times [T_n] = [D_n]$$
$$\text{where } B_{nm} = -C_{nm} - 4\sigma E_{nm} F_{nm} T_{im}^3, \ (n \neq m)$$
$$B_{nm} = \sum_m C_{nm} + \sum_m 4\sigma E_{nm} F_{nm} T_{in}^3 + 4\sigma \epsilon_n A_{sn} T_{in}^3 + WC_{p_n}/\Delta t, \ (n = m) \qquad (3)$$

$$D_n = S_{sc} A_{p_n} + P_n + q_{atb_n} + q_{res_n} + q_{a_n} + q_{F_n} + \frac{WC_{p_n}}{\Delta\sigma} T_{in} + 3\sigma \epsilon_n A_{sn} T_{in}^4 + \sum_m 3\sigma E_{nm} F_{nm} (T_{in}^4 - T_{im}^4)$$

Since this procedure is an approximation, the error involved may be significant when T_{in} and T_u vary by more than a few degrees. For steady state problems an iterative procedure is required to approach the correct value of T_n. Convergence is not reached until all nodal temperature changes are reduced to within a specified tolerance. Experience has shown that if initial temperature estimates are within 50°C of the converged values, only 2 - 3 iterations are required before the results are virtually constant.

Transient problems employ the same matrix inversion routine except each calculation represents the net energy exchange during a specific time interval. Since the solution of simultaneous equations is implicit, instability of the temperatures is not a problem. Thus, the results of high conductance and (or) low heat capacity do not adversely affect the numerical solution as they do in most explicit techniques. Care, however, must be taken in choosing a time interval. Although instability will not occur, no guarantee exists that the resulting temperatures are correct. For instance, calculations during a normal orbit at one minute intervals may be satisfactory since the environmental heat fluxes do not vary significantly (except perhaps at sunrise and sunset). However, when considering the launch phase,

calculations must be on a second basis due to the rapid rise and attenuation of fairing and free molecule flow heating rates. The short time interval is required both to obtain accurate integrated heat fluxes as well as to minimize significant temperature oscillations on spacecraft skins and externally mounted components (lightweight). The same argument can be applied to sunrise and sunset periods during the orbital phase. The two major considerations used to determine the calculating time are, therefore:

(1) Accuracy in obtaining integrated heat flux, and

(2) Change in nodal temperature during a time increment.

The effect of these inputs depends upon the particular requirements of the problem.

The most straightforward procedure regarding (2) is to permit the program to calculate the time interval based upon a specified permissible temperature change. This method, by necessity, involves an iteration for the time increment determination. At present, the program provides only for a specified calculating time. The value is based primarily on previous experience gained with respect to the particular situation.

III. Discussion of Specific Environments

A. Launch Phase

The thermal environment encountered by the payload during launch consists primarily of radiation from the hot nose cone prior to fairing ejection and free molecule flow heating thereafter. Because of the short time involved (3 to 5 minutes) the concern is generally for spacecraft skins and (or) externally mounted components.

Each surface element (or node) is assumed to view primarily one portion of the fairing whose temperature history is known. The fairing is generally divided isothermally into nose cap, cone, and cylindrical sections.

Upon ejection of the fairing, the infrared radiation source is replaced by aerodynamic or free molecule flow heating. The extent of this heating is based upon the kinetic energy available ($1/2\ \rho v^3$) of the impinging air and the projected area of the corresponding surface normal to the velocity vector. It is conservatively assumed that all of the kinetic energy of the air is imparted to the impinged surface. The analysis in this case depends upon a knowledge of the vehicle's trajectory in addition to the surface projected area.

B. Orbital Phase

1. Solar Input

The solar input may be a constant value per surface node or a time-dependent variable. The variation may be due to change in orientation with respect to the sun as well as eclipse by the earth. The possibility of internodal shading or reflections must be pre-determined since the program employs only net solar flux to a surface.

2. Earthshine and Albedo

Earthshine and albedo generally represent between 15% and 30% of the total energy input to a near earth satellite. At present, constant or average values per orbit are used. Albedo may be combined with the solar input if a transient variation is deemed necessary.

3. Internal Power

Internal power can be read in only as a constant.

IV. Active Control Option

The purpose of the active control option is to evaluate the design feasibility of simple shutter systems. One control temperature with specified limits is taken within the spacecraft. The effective absorptance and emittance as a function of shutter opening must be known. The

results indicate whether the system can handle the imposed extremes in thermal environment.

V. Alternate Transient Solution

In many instances (especially when many nodes are involved) the implicit matrix inversion technique becomes inefficient from the standpoint of computer time. A simple finite different explicit solution has been programmed as an alternative. This option proves advantageous if high conductances and/or low heat capacity are not present to restrict the calculating time interval to extremely small values. The small time interval is necessary to prevent instability of the nodal temperatures. It has been shown with a 25 node problem that the finite difference solution offers no time saving over the matrix inversion.

COMPUTER PROGRAMS FOR SPHERICAL SATELLITES

by

Joseph T. Skladany
Temperature Control Section
NASA Goddard Space Flight Center
Greenbelt, Maryland

COMPUTER PROGRAMS FOR SPHERICAL SATELLITES

BY

Joseph T. Skladany
Temperature Control Section
NASA Goddard Space Flight Center
Greenbelt, Maryland

Introduction

This paper describes briefly two rather specialized computer programs which solve for steady-state temperatures over a sphere. The first program deals with opaque surfaces and allows for skin conduction and black body internal radiation. This program differs from the conventional 3-D heat transfer programs in that it automatically subdivides the sphere into a specified number of nodes and computes for each node, surface area, conductances, radiation shape factors and incident solar flux. The second progam allows for transmission through partially or fully transparent external surfaces and accounts for multiple diffuse reflections at the inner surfaces, but does not include conduction.

The first program was written because a number of GSFC satellites or parts of satellites have been spherical, and it has been used directly or modified to calculate skin temperatures of ECHO-II, and Explorer 17, and of the magnetometers for IMP and OGO. The second program was written specifically for the proposed Rebound satellite, a large ECHO-type balloon which was to be constructed of a laminate of an aluminum mesh and a transparent plastic film.

Nomenclature

- A - Surface area
- A_p - Projected area
- $F_{i,j}$ - Shape factor from node i to node j
- H - Infrared energy incident on interior
- I - Solar energy incident on interior
- K - Conductivity
- P_a - Incident albedo radiation
- P_e - Incident earth emitted radiation
- Q_{cond} Conductance
- R - Radius of sphere
- s - Solar constant
- S_i - Solar input
- T - Absolute temperature

ϕ - Equatorial angle measured from the i axis

t - Thickness of shell

X - Fraction of surface that is opaque

α - Internal solar absorptivity

$\bar{\alpha}$ - External solar absorptivity

ϵ - Internal I.R. emissivity

$\bar{\epsilon}$ - External I.R. emissivity

ρ - Solar reflectivity (internal)

ρ^* - I.R. reflectivity (internal)

τ - Solar transmissivity

τ^* - I.R. transmissivity

σ - Stefan-Boltzmann constant

θ - Polar angle of spherical segment measured from spin axis

θ_s - Angle between spin axis and solar vector

γ - Angle between normal to spherical segment and solar vector

Subscripts

$_i$ - Nodes

$_j$ - Nodes

$_p$ - Transmitting material

$_o$ - Opaque material

Opaque Sphere Program

The sphere is divided into a number of concentric rings about the spin axis as shown in Figure 1. All rings or nodes subtend equal angles at the origin. The surface area of a differential element is

$$dA = R^2 \sin\theta \, d\theta \, d\phi \tag{1}$$

which when integrated over a node gives

$$A_i = 2\pi R^2 (\cos\theta_i - \cos\theta_j) \tag{2}$$

The solar energy absorbed is proportional to the area of the node projected in the direction of the sun. The projection of an elemental area is

$$dA_p = dA \cos\gamma \tag{3}$$

where cos γ can be determined from the dot product of the solar vector and the normal to the elemental area. This expression must be integrated for three distinct zones (see Figure 2).

a. For $0 \leq \theta \leq 90 - \theta_S$ sunlight is incident on every elemental area of each node. For each node the projection is a complete ring whose area is

$$A_{p\,i} = \pi R^2 \cos \theta_S \, (\sin^2 \theta_j - \sin^2 \theta_i) \qquad (4a)$$

b. For $90 - \theta_S < \theta \leq 90 + \theta_S$ the projection is no longer a complete ring and it becomes necessary to limit the integration to sunlit areas only. The projected area can be demonstrated to be

$$\begin{aligned} A_{p\,i} = R^2 \Big[& \cos \theta_i \, (\sin^2 \theta_S - \cos^2 \theta_i)^{\frac{1}{2}} \\ & - \cos \theta_j \, (\sin^2 \theta_S - \cos^2 \theta_j)^{\frac{1}{2}} \\ & + \sin^{-1} (\cos \theta_i / \sin \theta_S) - \sin^{-1} (\cos \theta_j / \sin \theta_S) \\ & + \sin^2 \theta_j \cos \theta_S \cos^{-1} (-\cot \theta_j \cot \theta_S) \\ & - \sin^2 \theta_i \cos \theta_S \cos^{-1} (-\cot \theta_i \cot \theta_S) \Big] \end{aligned} \qquad (4b)$$

c. For $90 + \theta_S < \theta \leq 180$ the nodes do not see the sun and

$$A_{p\,i} = 0 \qquad (4c)$$

In the expressions for the limits of θ for each of the zones, it was assumed that $\theta_s \leq 90^\circ$. For $90 < \theta_s \leq 180$, the program in effect inverts the sphere by a simple transformation of variables to avoid defining new limits of θ for each zone.

The conductance between adjacent nodes, i and i + 1 is

$$Q_{cond} = \frac{2\pi Kt}{\ln \frac{\tan\left(\frac{\theta_{i+1}}{2}\right)}{\tan\left(\frac{\theta_i}{2}\right)}} \qquad (5)$$

where the angles θ_i and θ_{i+1} refer to the centers of the two nodes. This formula can be derived by integration of the expression for conductance between differential areas.

For a hollow sphere, the radiation shape factor is simply

$$F_{ij} = \frac{A_j}{4\pi R^2} \qquad (6)$$

The thermal balance at any node in steady-state is

$$\bar{\alpha}_i A_{p\,i} S + \bar{\alpha}_i A_i P_{a\,i} + \bar{\epsilon}_i A_i P_{e\,i} = A_i \sigma \bar{\epsilon}_i T_i^4 + \sum_j A_i F_{i\,j} \sigma \epsilon_i \, (T_i^4 - T_j^4)$$

$$+ \sum_j Q_{cond_{i\,j}} \, (T_i - T_j) \qquad (7)$$

To solve these simultaneous equations, the T^4 terms are linearized by a Taylor expansion and then matrix methods combined with iterative procedures are used to solve for the temperatures.

It is planned in the near future to publish a more detailed description of this program.

Explorer 17 Thermal Model

The Explorer 17 was not a hollow sphere and hence the computer program had to be modified to include the internal components. The majority of the electronics were mounted on a platform located below the sphere's equator. The thermal model chosen was simply that of a sphere circumscribed about a cylinder as shown in Figure 3. The shape factors were computed by hand and read in with other data.

Transparent Sphere Program

The transparent sphere program solves for the steady-state temperature of a partially transmitting sphere. It is assumed that all reflections are diffuse, that conduction is negligible, and that there is no diffraction as the energy passes through the transparent part of the sphere.

Instead of the thermal balance consisting of one equation per node as in Equation 7, there are now three equations per node. These equations are derived by the Poljak[1] Radiosity Method and are completely general for any enclosure. However, the program is specifically written for a sphere and hence the geometric equations described for the opaque sphere program are included in this program.

---

[1] Eckert, E.R.G. and Drake, R. M., Jr., "Heat and Mass Transfer," McGraw-Hill Book Co., Inc., 1959, p. 405.

The internal energy is divided into I.R. and visible (solar spectrum) components. The net solar energy incident internally on a node is given by

$$I_i = S_i + P_{a\,i} + \sum_j F_{ij} \left[\chi \rho_{o\,j} + (1-\chi)\rho_{p\,j} \right] I_j \qquad (8)$$

These equations are solved simultaneously for I_i by a matrix solution.

The net I.R. energy incident internally on a node is given by

$$H_i = P_i + \sum_j F_{i\,j} \left[\chi \epsilon_{o\,j} + (1-\chi)\epsilon_{p\,j} \right] T_j^4 + \sum_j F_{i\,j} \left[\chi \rho^*_{o\,j} + (1-\chi)\rho^*_{p\,j} \right] H_j \qquad (9)$$

These equations are solved simultaneously for H in terms of T^4 by a matrix solution.

Finally, the thermal balance in steady-state for each node is

$$A_{p\,i} S \left[\chi \bar{\alpha}_{o\,i} + (1-\chi)\bar{\alpha}_{p\,i} \right] + A_i \left\{ \left[\chi \bar{\alpha}_{o\,i} + (1-\chi)\bar{\alpha}_{p\,i} \right] P_{a\,i} + \left[\chi \bar{\epsilon}_{o\,i} + (1-\chi)\bar{\epsilon}_{p\,i} \right] P_i - \left[\chi \rho_{o\,i} + (1-\chi)\rho_{p\,i} + (1-\chi)\tau - 1 \right] I_i \right\}$$

$$= A_i \sigma T_i^4 \left\{ \left[\chi \bar{\epsilon}_{o\,i} + (1-\chi)\bar{\epsilon}_{p\,i} \right] + \left[\chi \epsilon_{o\,i} + (1-\chi)\epsilon_{p\,i} \right] \right\} + \left[\chi \rho^*_{o\,i} + (1-\chi)\rho^*_{p\,i} + (1-\chi)\tau^* - 1 \right] H_i \qquad (10)$$

These equations are linear in T^4 and hence can be solved by a matrix solution to yield the steady-state temperature distribution.

A complete explanation of the derivation of the equations for the temperature of a partially transmitting sphere is being planned as a NASA Technical Note for future publication.

GEOMETRY OF SPHERE

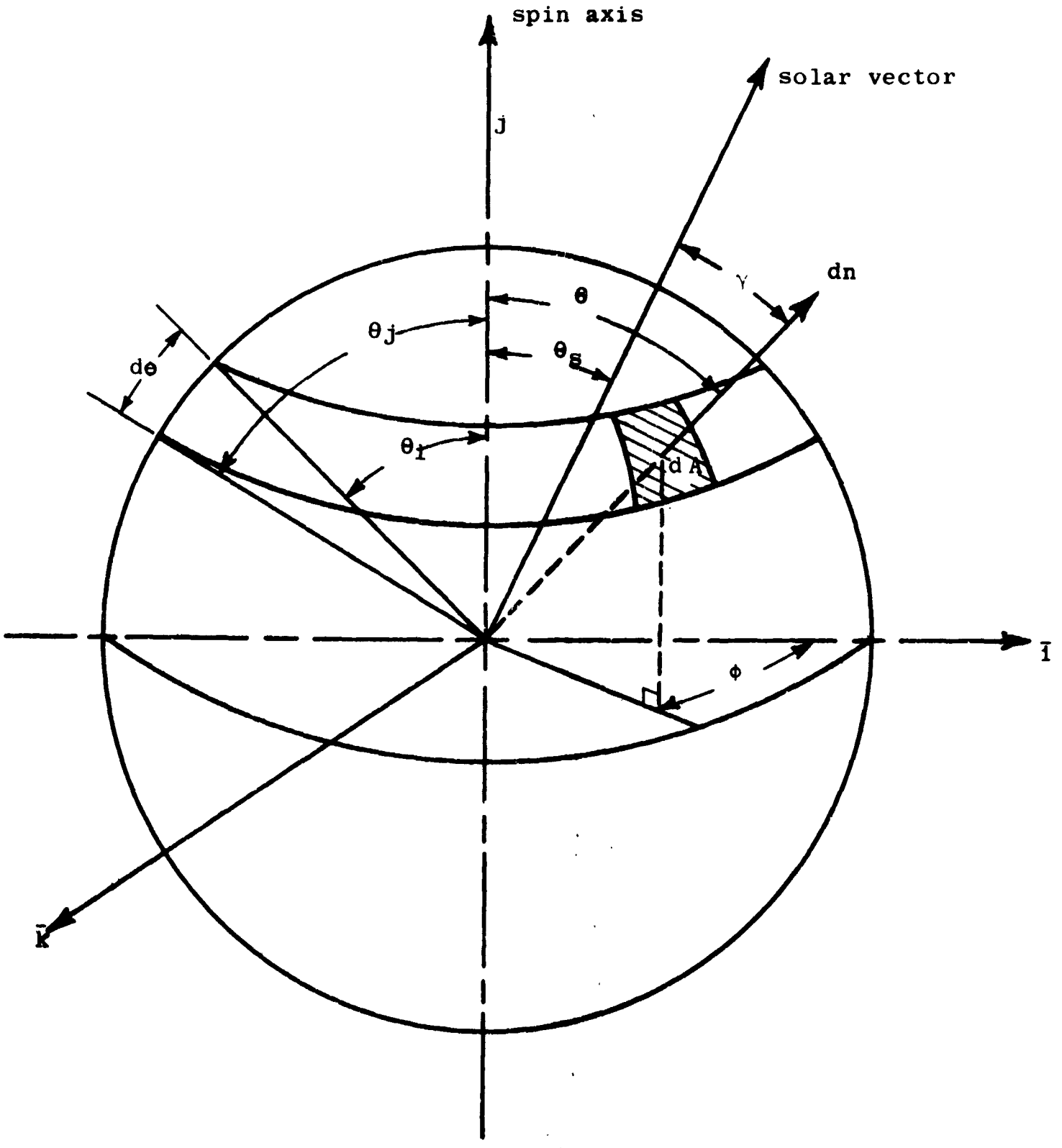

Figure 1

GEOMETRY SHOWING PROJECTED AREA ZONES

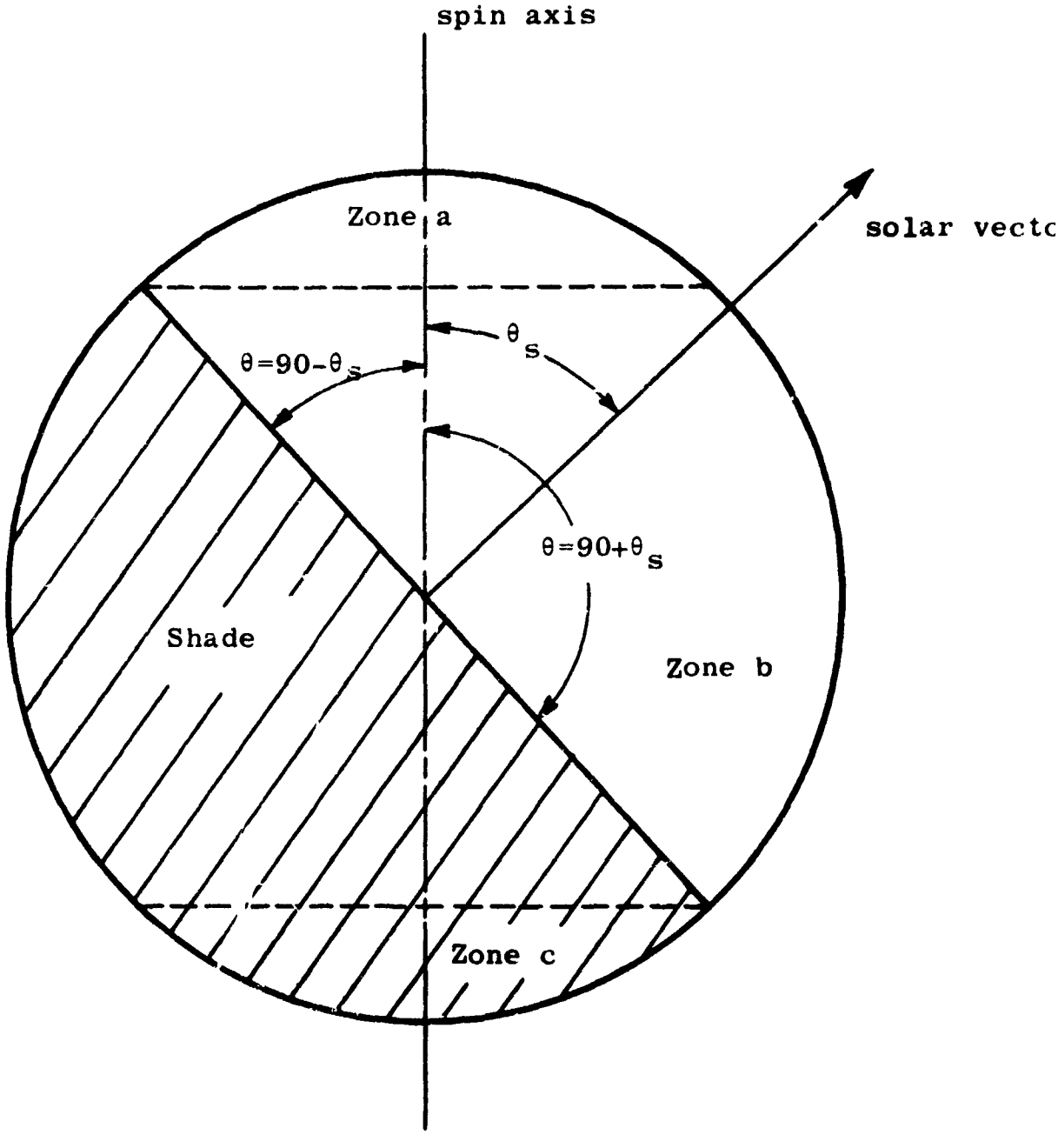

Figure 2

EXPLORER 17 THERMAL MODEL

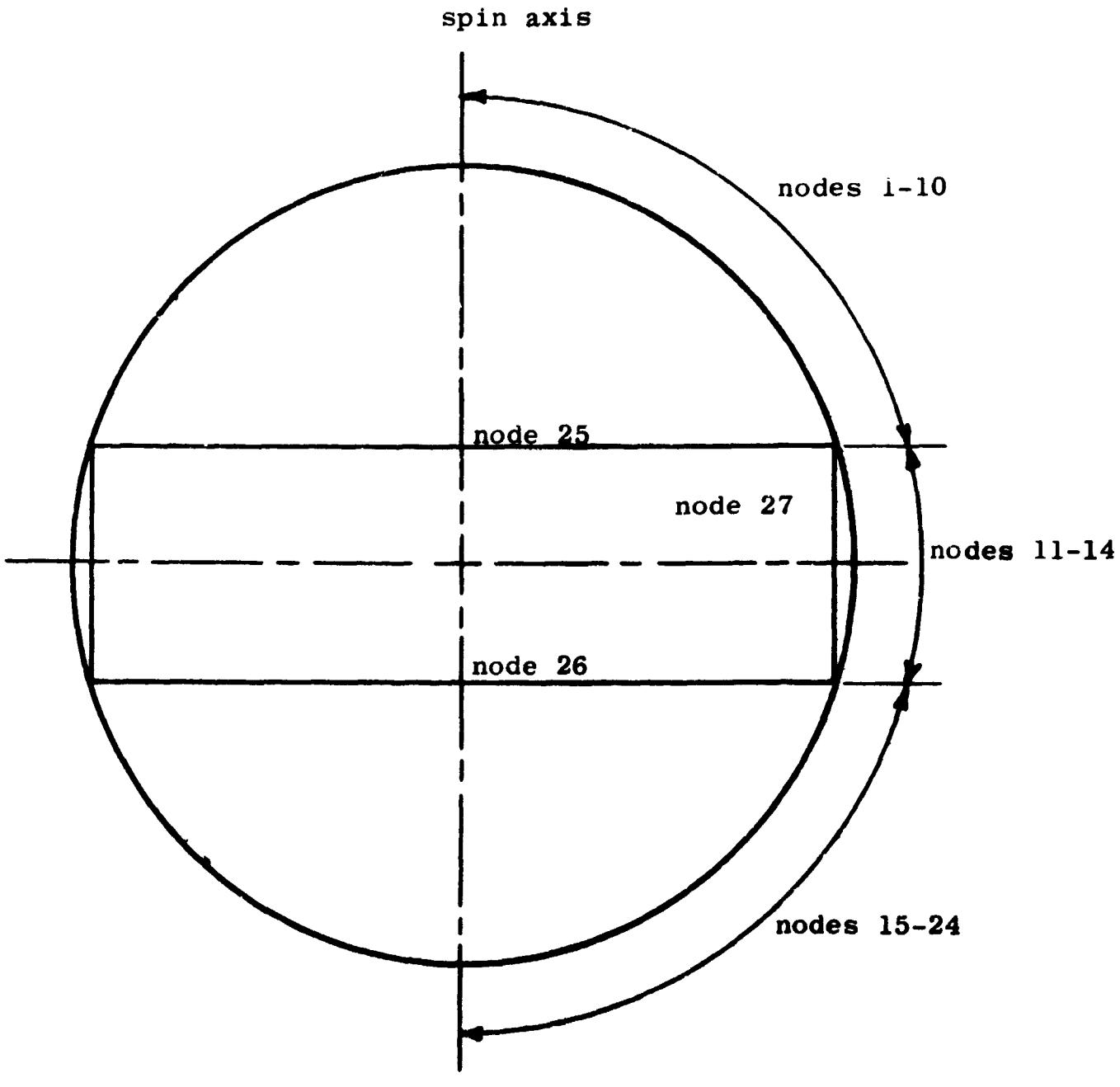

Figure 3

APPLICATIONS OF THE METHOD OF MONTE CARLO TO PROBLEMS IN THERMAL RADIATION

by John R. Howell

Lewis Research Center
National Aeronautics and Space Administration
Cleveland, Ohio

E-2570

ABSTRACT

A summary of the work involving the Monte Carlo method in the solution of problems in thermal radiation transfer is presented, which indicates general methods previously used for solving problems in which radiation is coupled with other modes of energy transfer. Previous work involving radiation in absorbing-emitting media is included.

An example is outlined to indicate the use of the Monte Carlo method in the design of a space radiator. Suggestions are given for solution of a complex case incorporating the effects of coupled conduction, convection and radiation, wavelength dependent and selective surfaces, nonisothermal conditions, and strongly directional or nondiffuse emitting and reflecting surfaces.

A discussion is given of the factors that may affect convergence, running time, and accuracy of the Monte Carlo solutions and of the advantages and disadvantages of this approach for practical problems. Also discussed are the case of programming for complex problems and the probable machine time requirements of the method.

INTRODUCTION

In many thermal radiation problems, integral equations of a type that are amenable to a Monte Carlo solution appear. One example of current interest from a design standpoint is a space radiator system. A segment of such a system might be as shown in figure 1.

A number of analyses of such a system using conventional approaches (refs. 1 to 4, for example) have been performed, but these are limited by certain common factors. The general formulation consists of using "interchange" ("shape", "view", or "configuration") factors, which are derived through an auxiliary analysis to give the fraction of energy leaving a given area element and arriving at another. Inherent in such factors is the assumption of a diffuse surface, which follows the cosine law for emitted and reflected energy.

These fractions of arriving energy are then summed by an appropriate integration, and the net energy flux for each area element is determined. Although it is possible to account for such factors as wavelength dependent properties, temperature dependent properties, and coupling with conduction or convection in the system studied with this type of analysis, it becomes quite cumbersome to evaluate the multiple integral terms that appear. These terms may involve integration over three dimensions and the wavelength interval of interest.

Recently, a number of papers have appeared in the open literature applying the method of Monte Carlo to problems involving thermal radiation exchange (refs. 5 to 8). Reference 5, which is concerned with radiant transfer through absorbing-emitting media, discusses the case of the wavelength- and temperature-dependent radiation absorption coefficient. The advantage of this method, as pointed out by this paper, is the simple evaluation of an otherwise difficult-to-solve set or integral equations.

In reference 6, the case of transients in the temperature of an absorbing-emitting gas with simultaneous heat conduction is treated extensively. In references 7 and 8 a Monte Carlo technique is used to solve for the steady-state, axial heat flux distribution in a rocket nozzle, considering the effects of flow and convection. In reference 8 real equilibrium propellant properties were used, and temperature, pressure, and wavelength effects on the propellant radiation absorption coefficient are demonstrated.

The latter three papers all involve the solution of a set of nonlinear integro-differential equations, generally using a Monte Carlo technique for evaluation of radiation integral terms. A standard method such as Newton-Raphson is used for evaluation of the remaining set of equations, which are put in finite-difference form.

SAMPLE MONTE CARLO PROGRAM

In essence, the Monte Carlo technique removes the evaluations of multiple integrals from the computer program and replaces it with a simple summation. As an example of this approach, we may write the energy balance on a volume element dV_R of a typical radiator fin (fig. 1) as

$$A_x k \nabla^2 T + 2 \int_{\lambda} \int_{A} \alpha_{\lambda,a} \epsilon_{\lambda,e} e_{\lambda,a} F_{a-e} \, dA_a \, d\lambda = 2 \int_{\lambda} \epsilon_{\lambda,a} e_{\lambda,a} \, dA_a \, d\lambda \qquad (1)$$

where the first term is the energy conducted into the volume element, the second term is the radiant energy absorbed by the two exposed surface elements of dV_R (assuming symmetry about the plane of the fin), and the term to the right of the equality is the energy radiated from the two exposed area elements. For an element on a radiator tube, a convection term must be added.

If the integral term can be evaluated separately, the complete equation can be written in finite difference form with the integral replaced by a constant for each iteration. The coupled set of equations that results (one for each element considered) can then be solved by any of a number of standard techniques. A new temperature distribution results that can be used to reevaluate the integral terms. This procedure is continued until the temperatures converge, that is, until the old and new temperatures are the same.

The remainder of this section will be devoted to the evaluation of the integral terms by the Monte Carlo procedure, leaving the methods of solution of the entire matrix of equations and the attendant problems of convergence and accuracy to be settled by the knowledge, experience, and intuition of the interested programmer.

Monte Carlo Procedure

The procedure to be presented is a simple and straightforward "engineering" approach to the problem. It is aimed at giving the general methods that can be applied with no attempt at giving the more complex but often faster running "shortcuts" in programming with which the literature on Monte Carlo abounds.

The method for this type problem reduces to this: a number N_{dA} of "bundles" of energy are assumed to be emitted from each area element on the radiator. The energy per bundle, C_b, is taken as constant for all bundles within the system to simplify bookkeeping, and it can also be specified as a program input. The rate of bundles to be emitted from a given element must then be given by

$$N_{dA} = \frac{\left[\int_\lambda \epsilon_\lambda e_\lambda \, d\lambda\right] dA}{C_b} \tag{2}$$

If the direction of emission of the bundle is (η,θ) as shown in figure 2, then for a surface with directional emissivity ϵ_η independent of wavelength, the direction of an individual bundle is given by

$$R_1 = \frac{\int_0^\eta \epsilon_\eta \cos\eta \sin\eta \, d\eta}{\int_0^{\pi/2} \epsilon_\eta \cos\eta \sin\eta \, d\eta} \tag{3}$$

$$\theta = 2\pi R_2 \tag{4}$$

where R_1 and R_2 are numbers chosen at random from a set of numbers evenly distributed in the range $0 \leq R \leq 1$. The derivation of equations (3) and (4) is given in reference 5. These equations assume an emissivity that is symmetrical about the normal to the surface such as we might expect for a real etched or plated surface. For a surface with a constant ϵ_η, equation (3) reduces to

$$\cos \eta = \sqrt{R_1} \tag{5}$$

If ϵ_η is a nonanalytic function, equation (3) may be integrated numerically to find a curve of η as a function of R_1, which may then be curve fit to put a function, perhaps of the form

$$\eta = A + BR_1 + CR_1^2 + \ldots \tag{6}$$

directly into the machine.

Directional effects might be examined for their possible use in increasing radiator efficiency in this manner. Directional properties for a grooved surface with very strong directional effects are given in reference 9. Such grooving could be used to minimize interchange of radiation between segments of the radiator by directing the radiation preferentially toward space.

Returning to the problem at hand, we may specify the wavelength of the bundle from the equation

$$R_3 = \frac{\int_{\lambda_{min}}^{\lambda} \epsilon_\lambda e_\lambda \, d\lambda}{\int_{\lambda_{min}}^{\lambda_{max}} \epsilon_\lambda e_\lambda \, d\lambda} \tag{7}$$

where λ_{min} and λ_{max} are the limits of the wavelength range of interest. For ease of use, we may again fit a curve of the form of equation (6) to R_3 as a function of λ for use in the program.

It should be noted that ϵ_η has been assumed independent of wavelength and ϵ_λ independent of direction of emission. If this were not so, equation (3) would have to be carried out for many values of λ, and equation (6) would then give a family of curves with λ as the parameter for use in the final program.

Similarly, a family of curves with η as parameter would result from equation (7).

It is seen from the relations derived previously that η, θ, and λ may be found by picking three random numbers R_1, R_2, and R_3 and using them in simple relations. If the direction of emission is known, simple geometry determines whether the bundle will be radiated to space or will strike another point on the radiator surface. For example, if the element of bundle emission is on the fin, it can be seen from figure 3 that for x taken as the distance to the center of the nearest tube, the energy bundle must be lost to space if

$$\cos \eta > \frac{r}{x} \tag{8}$$

However, if the inequality is not satisfied, the bundle will not necessarily strike a surface. Such simple tests are useful if a large fraction of bundles are lost to space, as they save many useless calculations of final position of the bundle.

If the bundle does strike another surface, it may be either reflected or absorbed. To determine this, another number R_4 is chosen and compared to the spectral absorptivity α_λ evaluated at the bundle wavelength. If $R_4 > \alpha_\lambda$, the bundle will be reflected; otherwise, it will be absorbed.

If it is reflected, the new direction must be chosen again by selecting at random from the correct distribution of possible angles. For a diffusely reflecting surface, these are given by equations (4) and (5). For a specular surface, we need only to find the incident angle of the bundle by geometry, and then the angles of reflection are given by

$$\left.\begin{aligned} \eta_{\text{refl.}} &= \eta_{\text{incident}} \\ \theta_{\text{refl.}} &= \theta_{\text{incident}} + \pi \end{aligned}\right\} \tag{9}$$

For a directional surface, the direction of reflection will in general depend on the angle of incidence. A family of curves with the angle of incidence η' must then be specified of the form

$$R_6 = \left[\frac{\int_0^{\eta} \rho_{\eta',\eta} \cos \eta \sin \eta \, d\eta}{\int_0^{\pi/2} \rho_{\eta',\eta} \cos \eta \sin \eta \, d\eta} \right]_{\eta'} \tag{10}$$

where $\rho_{\eta',\eta}$ is the reflectivity in direction η for energy incident from η'. As a practical matter, such data is scarce. One source is reference 10 for an idealized grooved surface.

The reflected bundle is now followed through any successive reflections until it is either absorbed at a surface or lost to space. Each bundle emitted from each element is followed in the same way.

Absorptions at each area element are tallied as they occur. Multiplying the number of bundles finally absorbed by the energy per bundle gives the total radiant energy absorbed at each area element, and we have thus completed evaluation of the integral term in equation (1).

If solar radiation is to be considered, the direction of incidence must be specified, and sufficient bundles are fired at our radiator to equal the incident solar energy. The wavelength of each incident bundle is again chosen by equation (8) using solar emissivities and temperatures. The bundles are followed as outlined previously.

Running time for such a program is difficult to predict. It would certainly depend on many factors; however, the major ones are probably the astuteness of the original temperature distribution guess and the number of energy bundles followed. For this type of program, the running time would be nearly proportional to the number of bundles followed. For the mathematically similar but more cumbersome rocket nozzle program of reference 8, four to five iterations took less than 10 minutes time, following about 75,000 energy bundles on the final few. A Newton-Raphson technique gave good convergence of the set of equations for each iteration. On the IBM 7094, the four to five iterations brought convergence to within 0.1 percent for all temperatures in the distribution. The program outlined here would almost certainly run faster because the multiple absorptions in the nozzle propellant are not present, and these absorptions represent a major fraction of the running time.

Advantages and Disadvantages of the Method

The main work involved in programming this method is the initial evaluation of the functions describing wavelength and directional dependence. These may involve numerical integration, which needs to be carried out only once. The remainder of the programming then consists of setting up a series of "do" loops around the simple algebraic equations derived above.

Many techniques are available (ref. 11) for estimating error in Monte Carlo calculations, but accuracy can usually be increased by following more energy bundles (decreasing the energy per bundle). Often it is difficult to predict or deduce the error present in a standard multiple numerical integration.

The advantages of the Monte Carlo method for these programs might be summarized as

(1) The ability to handle complex problems in a simple and straightforward manner

(2) The simplicity of the resulting computer program, with the attendent ease of checking

(3) The ability to control to some extent and to accurately estimate the probable errors in the solutions

There are also certain disadvantages. It is possible that for certain problems sufficient accuracy cannot be obtained from the straightforward methods outlined without excessive computer times. More sophisticated approaches would then be required, with some loss of the advantages outlined previously. These approaches are well developed in reference 11.

Because of the simplicity of the equations and the independence of each occurrence along the path of a bundle, it is sometimes difficult to pinpoint or even detect the presence of program errors. Judgements made are usually on the basis of the final summations, which may show little obvious effect of error unless gross mistakes are present. Standard approaches generally provide a number of possible intermediate checkpoints, lending some feeling of security to the programmer.

CONCLUSIONS

The Monte Carlo method may offer considerable savings in programming complexity and time for thermal radiation problems in which variations with wavelength and direction are encountered in surface radiative properties. The method appears to offer short computer running times even where complex variations occur.

SYMBOLS

A	area
C_b	energy per Monte Carlo bundle
e_λ	Planck spectral energy distribution
F_{a-e}	view factor between area elements a and e
k	thermal conductivity
N_{dA}	rate of bundles emitted from a given surface element
r	outside radius of tube on tube and fin radiator
R	random number from evenly distributed set in range 0 to 1
T	absolute temperature
V	volume
x	normal distance from area element on fin to centerline of nearest tube
α	surface absorptivity
ϵ	surface emissivity
λ	wavelength
η, θ	angles defined in fig. 2
$\rho_{\eta',\eta}$	reflectivity in angle η for energy incident at angle η'

Subscripts:

λ	spectrally dependent
a,e	surface area element index, absorbing or emitting element, respectively
η, θ	dependent on angle η or θ

REFERENCES

1. Callinan, J. P., and Berggren, W. P.: Some Radiator Design Criteria for Space Vehicles. Jour. Heat Transfer (ASME Trans.), ser. C, vol. 81, no. 3, Aug. 1959, pp. 237-244.

2. Sparrow, E. M., and Eckert, E. R. G.: Radiant Interaction Between Fin and Base Surfaces. Jour. Heat Transfer (ASME Trans.), ser. C, vol. 84, no. 1, Feb. 1962, pp. 12-18.

3. Haller, Henry C., and Stockman, Norbert, O.: A Note on Fin-Tube View Factors. Jour. Heat Transfer (ASME Trans.), ser. C, vol. 85, no. 4, Nov. 1963, pp. 380-381.

4. Pay, Carol J., and Stockman, N. O.: View Factors and Limits of Visibility for Radiant Interchange Between Differential Plane and Cylindrical Surfaces Having Parallel Generating Lines. To be published as NASA Technical Note.

5. Howell, J. R., and Perlmutter, M.: Monte Carlo Solution of Radiant Heat Transfer in a Nongrey Nonisothermal Gas with Temperature-Dependent Properties. (To be publ. in A.I.Ch.E. Jour.)

6. Fleck, Joseph A., Jr.: The Calculation of Nonlinear Radiation Transfer by a Monte Carlo Method. Methods in Computational Physics, Vol. 1, Academic Press, 1963, pp. 43-65.

7. Howell, John R., Strite, Mary Kern, and Renkel, Harold: Heat Transfer Analysis of Rocket Nozzles Using Very High Temperature Propellants. Preprint 64-62, AIAA, 1964.

8. Howell, John R., Strite, Mary Kern, and Renkel, Harold: Heat Transfer in Rocket Nozzles Using High Temperature Propellants with Real Properties. To be published as NASA Technical Report.

9. Perlmutter, Morris, and Howell, John R.: A Strongly Directional Emitting and Absorbing Surface. Jour. Heat Transfer (ASME Trans.), ser. C, vol. 85, no. 3, Aug. 1963, pp. 282-283.

10. Howell, John R., and Perlmutter, Morris: Directional Behavior of Emitted and Reflected Radiant Energy from a Specular, Gray, Asymmetric Groove. NASA TN D-1874, 1963.

11. Cashwell, E. D., and Everett, C. J.: A Practical Manual on the Monte Carlo Method for Random Walk Problems. Rep. LA-2120, Los Alamos Sci. Lab., Dec. 1957.

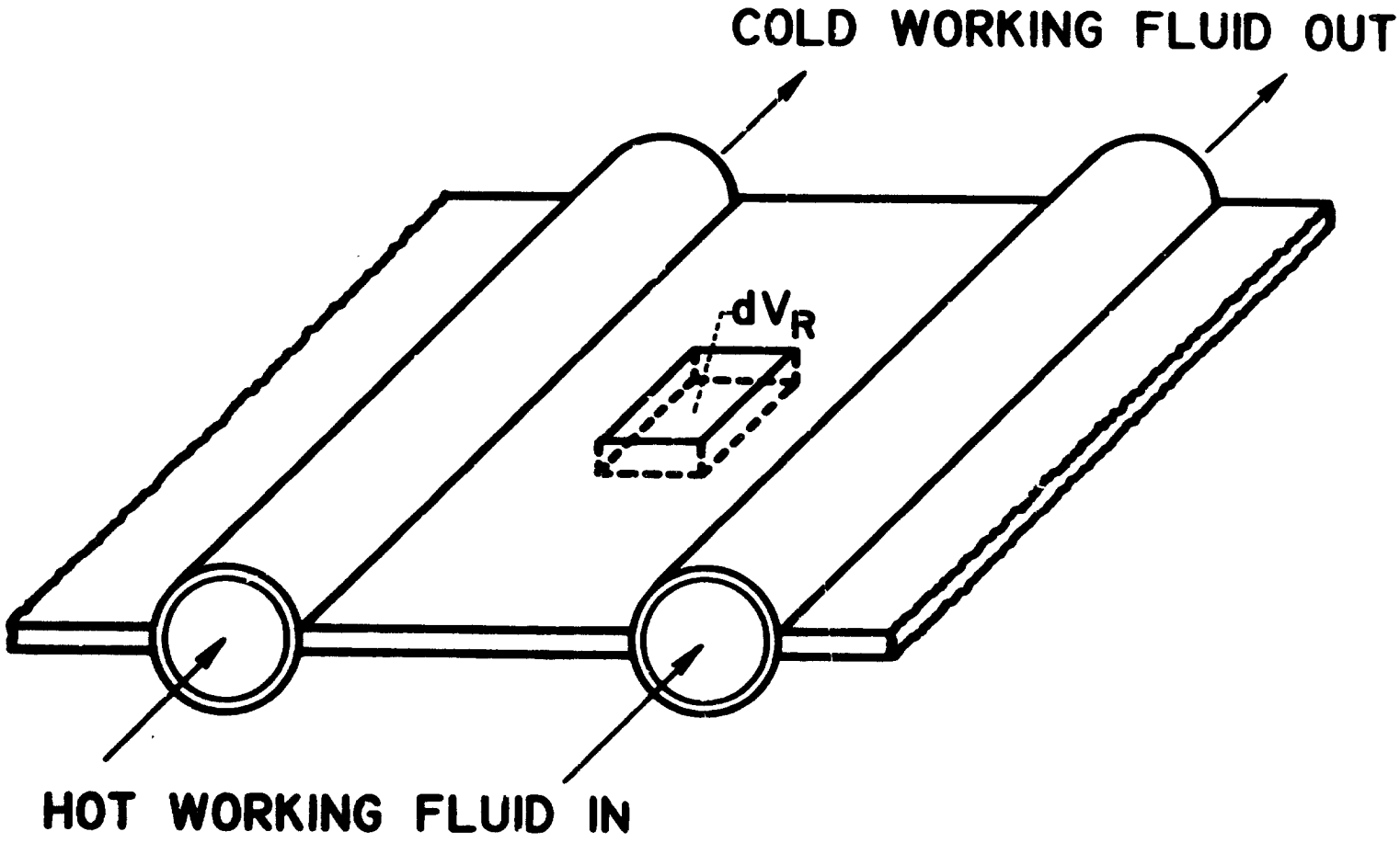

Fig. 1. - Fin-tube space radiator segment.

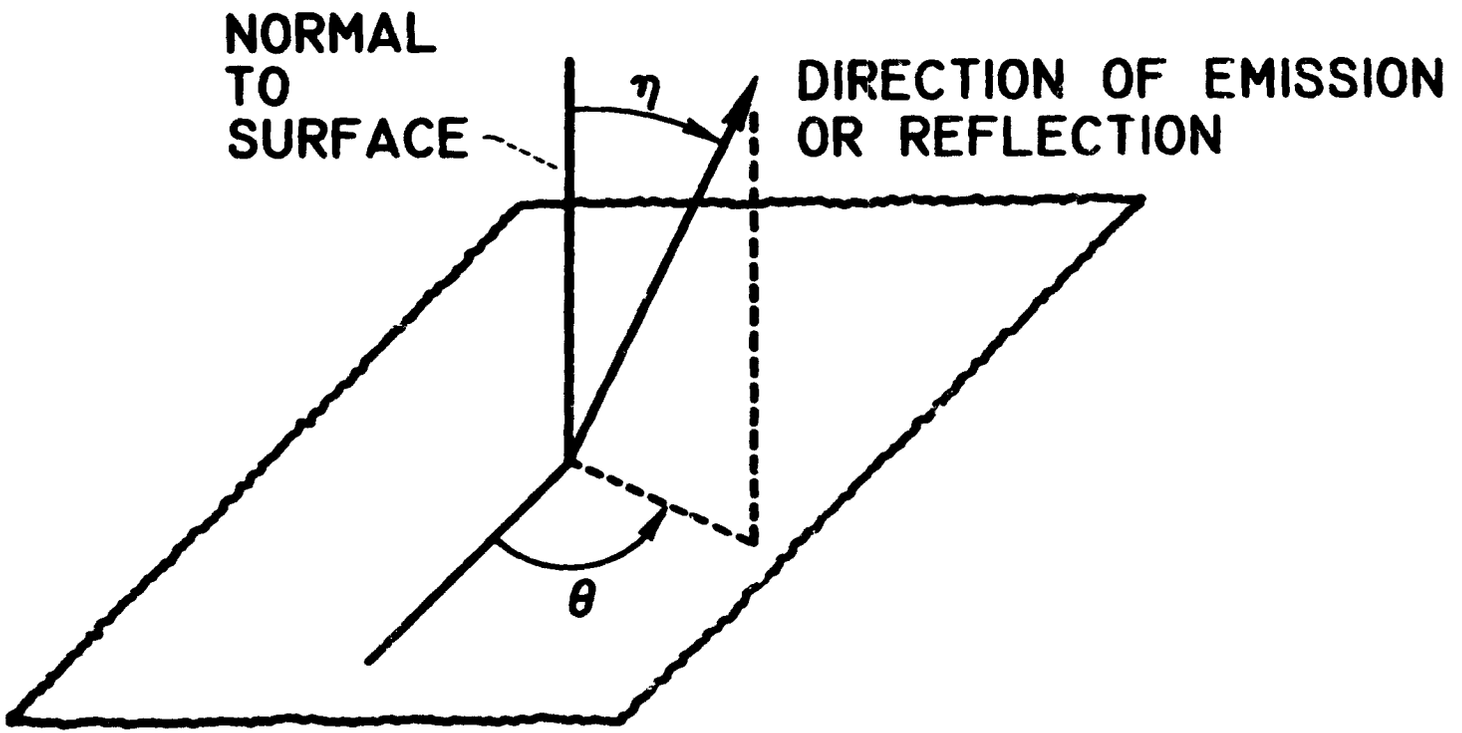

Fig. 2. - Geometry of bundle emission.

E-2570-I

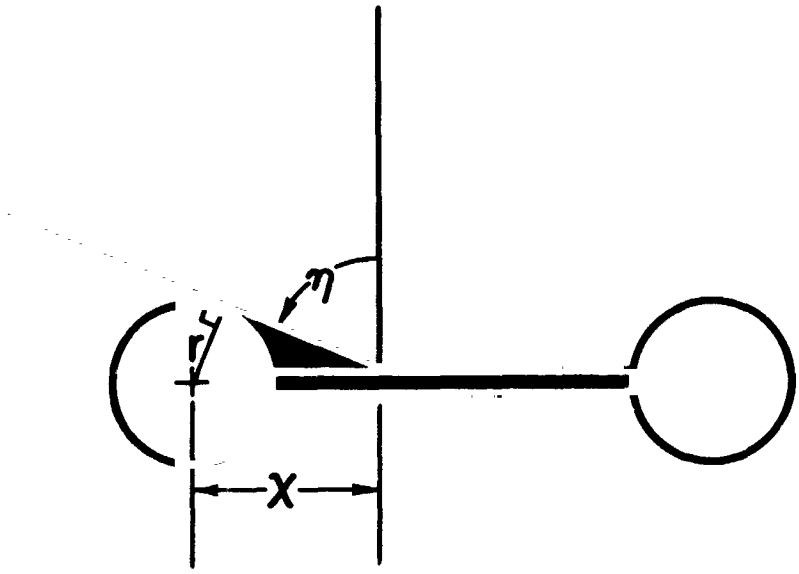

Fig. 3. - Criterion for loss to space.

ORBITING SATELLITE SURFACE TEMPERATURE PREDICTION AND ANALYSIS

I. Introduction

Temperature prediction of spacecraft orbiting the moon, earth or other planets is an essential Manned Spacecraft Center capability. Existing methods [illegible] was found, however, were either too simplified or specialized for MSC requirements. A contract was, therefore, let with Midwest Research Institute in Kansas City, Missouri, to develop a computer program to determine spacecraft heat loads and/or thin skin transient temperatures while orbiting the moon, earth or other planets. It is this computer program, which has recently been completed, that I'd like to introduce. The computer program is written for the IBM 7094 computer and is in the Fortran II language.

II. Spacecraft Thermal Balance

First to give some insight into what are some of the major considerations in determining the thermal balance of an orbiting spacecraft, figure 1 shows the principal external heat loads. The q sun represents solar thermal radiation coming from the sun and directly impinging upon the vehicle. The q albedo represents that quantity of solar radiation from the sun that is reflected off the planet being orbited and then impinging upon the orbiting vehicle. Lastly, the q planet is that thermal radiation from the planet orbited that impinges upon the vehicle.

When the vehicle is on the far dark side of the planet, however, it can be seen that the vehicle would not receive any q sun or q albedo; therefore another consideration is the sun-shade points.

III. Major Features and Capabilities

Before proceeding further with the fundamentals of the program, however, I would like next to outline some of the major features and capabilities of the program. They are as follows:

1. The program has the capability of handling up to 200 elements; each has its own thickness, initial temperature, and thermal properties.

2. The program also has the capability to consider eight different coatings and eight different substrate materials. The thermal properties of each may be temperature dependent.

3. A spinning or fixed vehicle orientation may be considered. The fixed orientation may be with respect to the sun or the planet being orbited.

4. Internal heat may be considered as a function of time. The program has the capability to handle eight different internal heat tables.

5. Constant or variable planet temperatures may be considered. This feature is a most important consideration for a lunar orbital mission. The significance will be shown later for a hypothetical lunar mission.

IV. Assumptions

In order to meet the projects objectives, it was necessary to introduce certain simplifying assumptions. I feel that it is worthwhile at this time to introduce these assumptions for it is up to each individual user or potential user to evaluate the validity of the assumptions for each intended application.

1. Conduction between elements, and convection between the vehicle and its surroundings are neglected. When MSC feels conduction between elements could be a significant factor, the program is used only to compute the incident heat loads and then these outputs are loaded as input into a transient conduction type program.

2. No radiant interchange between elements is considered.

3. All thermal radiation is considered to be diffused.

4. The vehicle's absorptivity to reflected solar radiation is assumed to be equal to the vehicle's absorptivity to direct solar radiation.

5. Internal heat is assumed to be uniformly distributed over the element.

6. The solar constant is assumed to be independent of the vehicle's orbital position.

7. On the sunlit side of a variable temperature planet, the planet surface temperature is assumed to vary according to Lambert's cosine law. The planet temperature on the dark side of a variable temperature planet is, however, assumed constant.

V. Celestial Mechanics

So far nothing has been said about input data. A general outline of the type input required shall therefore be presented next. It is believed that the input is quite simple and logical.

To compute the heat loads to an orbiting vehicle, four basic questions must be considered. They are:

1. What is the location of the vehicle surface element on the vehicle?

2. Where is the vehicle with respect to the planet being orbited?

3. What is the celestial location of the vehicle with respect to space?

4. What is the sun's location with respect to the planet being orbited?

Vehicle Coordinate System

The first question is not applicable to a spinning satellite; however, for an oriented vehicle, the incident heat flux can vary considerably from one surface position to another. For example, looking at figure 2, the element on the side of the planet oriented vehicle shown in the upper left hand corner receives radiation from the planet whereas the element on top does not. Consequently, a system to answer the first question (What is the location of element analyzed?) is required for the thermal analysis of an oriented vehicle.

A meaningful vehicle coordinate system is set up by replacing the complex configuration with a spherical mathematical model shown in the upper right hand corner of figure 2. The elements on the sphere are selected so they have the same space orientation as the corresponding vehicle elements.

For a planet or moon oriented vehicle, the surface positions on the sphere are defined with respect to the coordinate system illustrated in the lower left hand corner of the figure. For the sun oriented case, the surface positions on the sphere are defined with respect to the coordinate system illustrated in the lower right hand corner. For a fixed orientation, the surface elements location is defined by the angles λ and ϕ as shown and are required input data for each element. This system can be likened to defining a position on earth where any position on earth can similarly be defined by giving the proper longitude and latitude.

Planet Coordinate System

Before the impinging heat loads emitted or reflected by the planet can be computed, the second question (Where is the vehicle with respect to the planet being orbited?) must be answered. The answer to this question can be obtained in terms of the planet coordinate system shown in figure 3, using Kepler's equations. The input required by the program to compute internally the vehicle's position with respect to the planet consist only of the semi-major axis (a), semi-minor axis (b) of the orbital ellipse and the true anomaly (ϕ) at the initial time. The three variables are shown in the top right hand corner of the slide which shows the orbit rotated into the plane of the screen, and the X_p and Y_p axes superimposed onto the orbit plane. As shown for a spinning or fixed orientation, the planet coordinate system is the same.

Celestial Coordinate System

The third question (What is the celestial location of the vehicle with respect to space?) involves defining the orbit with respect to space. This question can be answered in terms of the celestial coordinate system. The vehicle's orbit can be conventionally related to the celestial coordinate axes by three angles which are required input data. These angles are shown in figure 4 where Ω is the right ascension of the ascending node, ω is the argument of perifocus, and i is the inclination of the orbital plane.

Any reference system could have been selected for the celestial coordinate system; however, the basis of selection was that it be compatible with standard astronomical references to minimize input data compilation time and effort. With this as a criteria for selection of a celestial coordinate system three systems, geocentric, modified heliocentric and the selenographic were chosen to describe orbits about the earth, a planet other than earth, and the moon respectively.

For earth and planets other than earth, the two celestial coordinate systems used are pictured in figure 5.

For the moon the third celestial coordinate system selected is illustrated by figure 6.

Sun's Position

The only question that remains now to be answered is: What is the location of the sun with respect to the planet being orbited? This can be answered in terms of two angles, the right ascension of the sun (RA) and the declination (DEC). Both angles are required input data to the program and are defined by figure 7.

Since we were careful in our selection to choose a celestial coordinate system that would be compatible with standard astronomical references, we can obtain from the Ephemerus the RA and DEC for the moon, earth or any other planet for any particular date.

VI. Hypothetical Test Case

Case I

A hypothetical lunar mission was run using the described program. For this particular lunar orbital mission, the spacecraft was planet oriented and the variable planet surface temperature feature of the program was used. The mission data was selected in order that the sun would be very near to being in the orbital plane.

Pertinent orbit data consisted of the following:

Altitude 10 NM to 190 NM.

Inclination = 13°.

Right ascension of ascending node = $.87^{\circ}$.

Argument of perifucus 270°.

True anomaly at initial time = 0°.

The temperature time history of differently oriented and painted surface elements reveal several interesting characteristics.

The results shown in figure 8, a white element cools initially even though it is almost facing directly into the sun. A similarly oriented black element shown in the same slide, however, rises to a peak at = 60°, then gradually drops as it turns away from the sun. This is true since the white element reflects a considerable amount of solar energy, whereas the black energy will absorb the majority of solar radiation that impinges upon its surface.

In the next figure (9) the temperature curves of a black and white element facing the moon are very similar since black and white elements absorb long wavelength radiation almost equally. Also of interest shown in the figure is the hump in the black element's curve at about = 100° and = 260°. This is caused by the fact that both elements are briefly irradiated by the sun just before entering the moon's shadow and just after leaving its shadow. However, the hump shows up only in the black element's curve since it absorbs the solar radiation more readily.

Comparison of both black elements in figure 10 reveals at = 0° the element facing the moon is almost as hot as the element facing away from the moon and almost looking directly at the sun. This demonstrates that at low lunar orbits, the planet heat can be as significant as solar heat.

Case II

Finally, to learn the effects of not considering the moon's surface temperature gradient, a similar run was made of Case I; however, this time the moon was taken as a constant temperature planet. The results shown in the final figure (11) reveal the "constant moon temperature" curve Δ is a flat curve that averages out the maximum and minimum peaks of the "variable moon temperature" curve O. As you can see, we have a significant variation (about 100°R) caused by neglecting the moon's surface temperature gradient. These results confirm the importance of the variable planet temperature method in analyzing lunar missions.

Robert A. Vogt
Manned Spacecraft Center

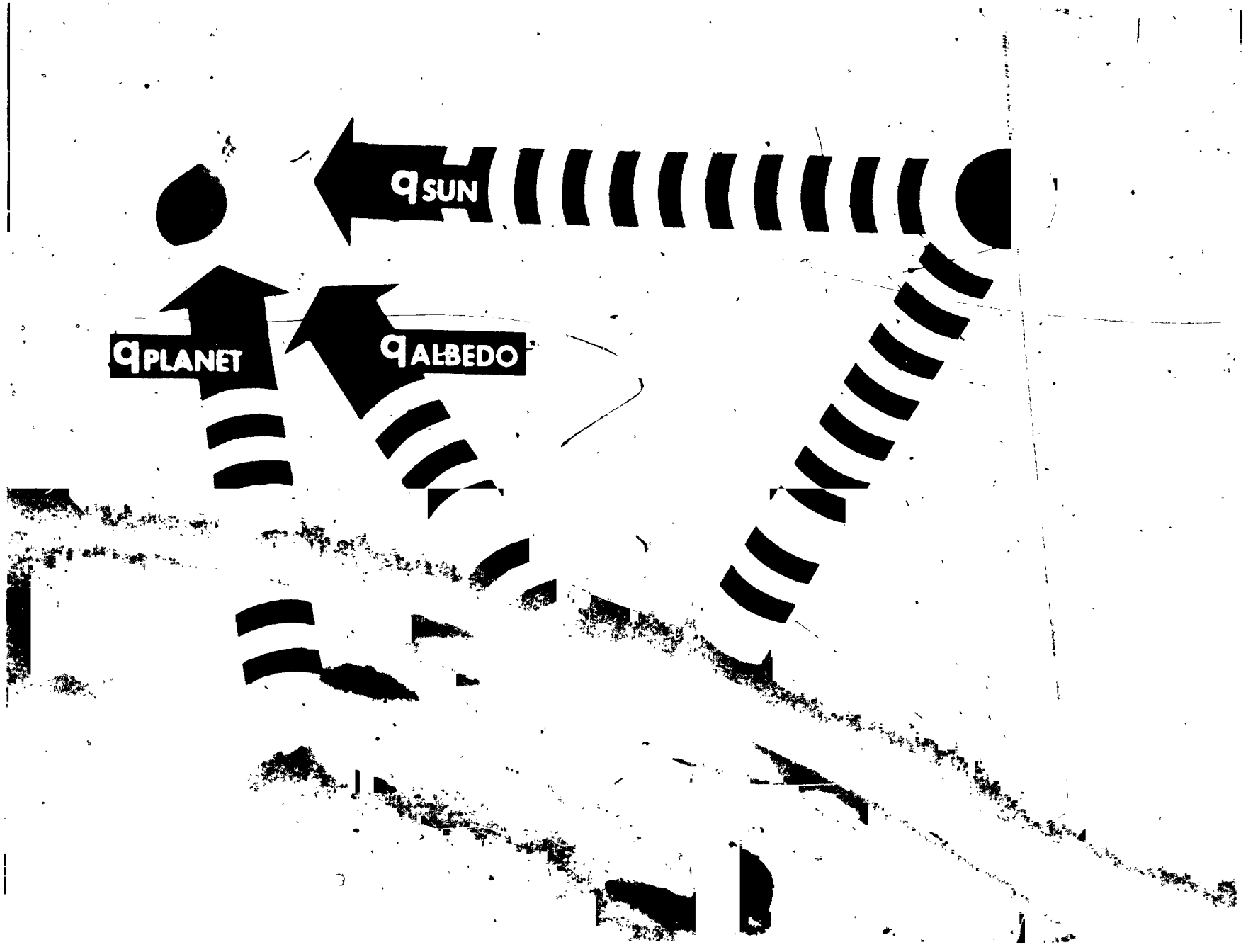

1 Principal External Heat Loads

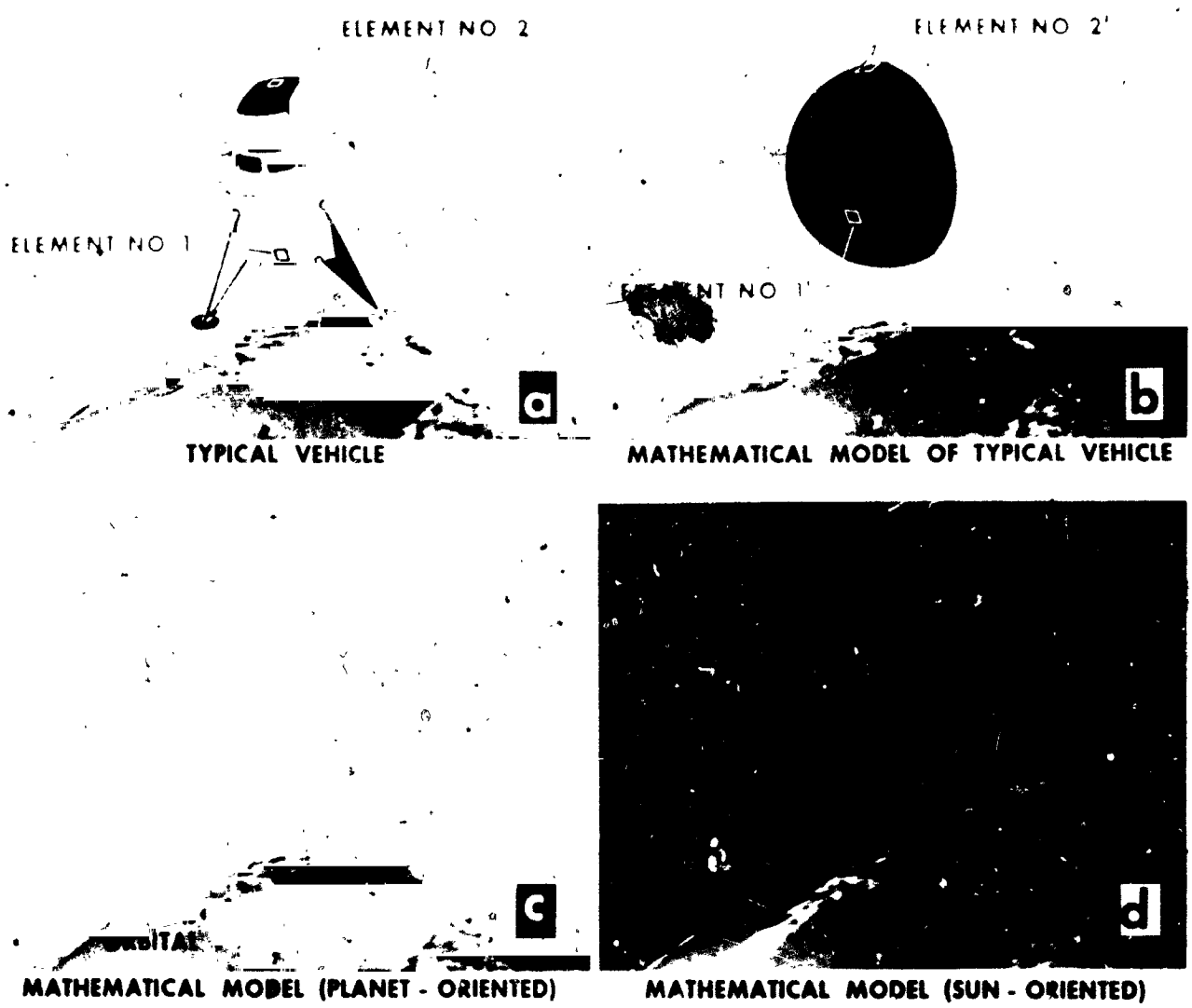

Fig. 2 - Vehicle Coordinate System for a Typical Spacecraft

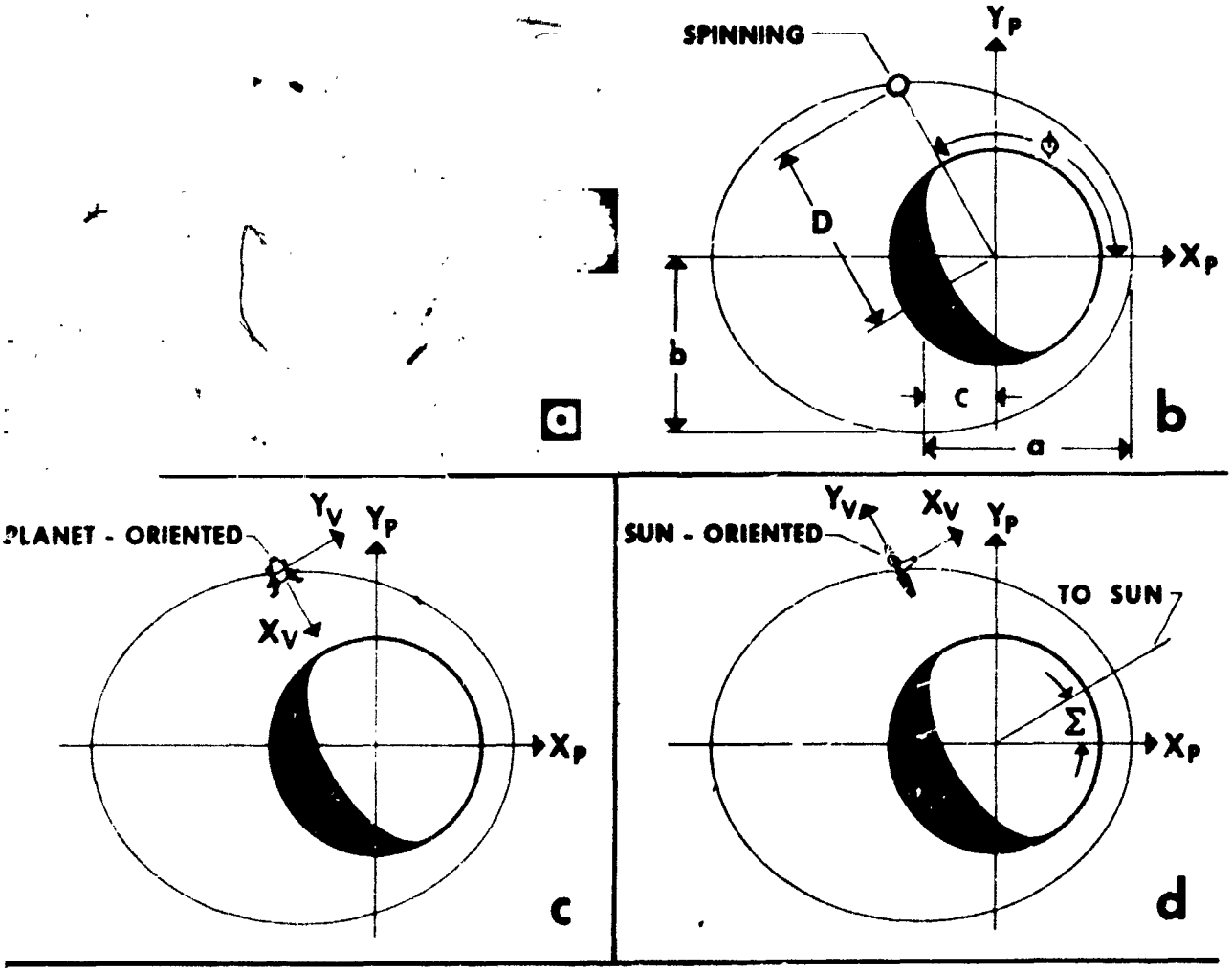

Fig. 3 - Planet Coordinate Systems for Spinning and Oriented Vehicles

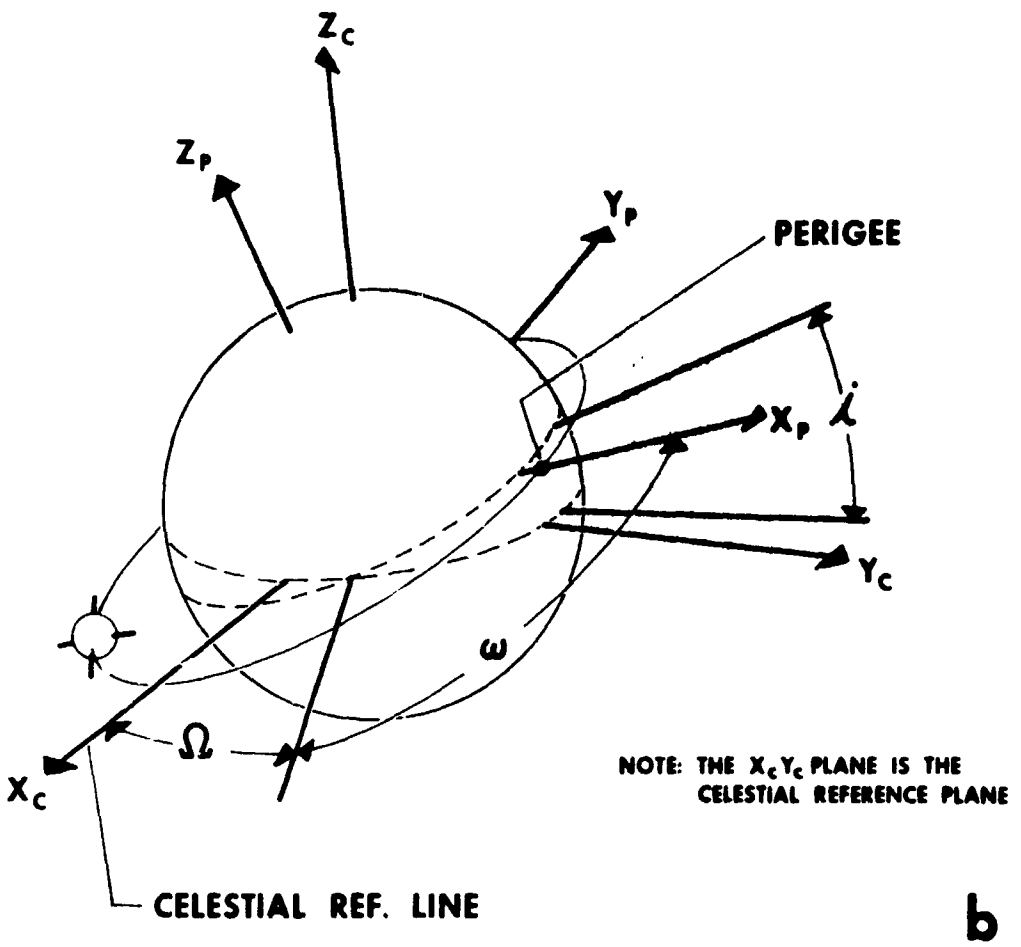

Fig. 4 - Relationship between Orbit and General Celestial Coordinate System

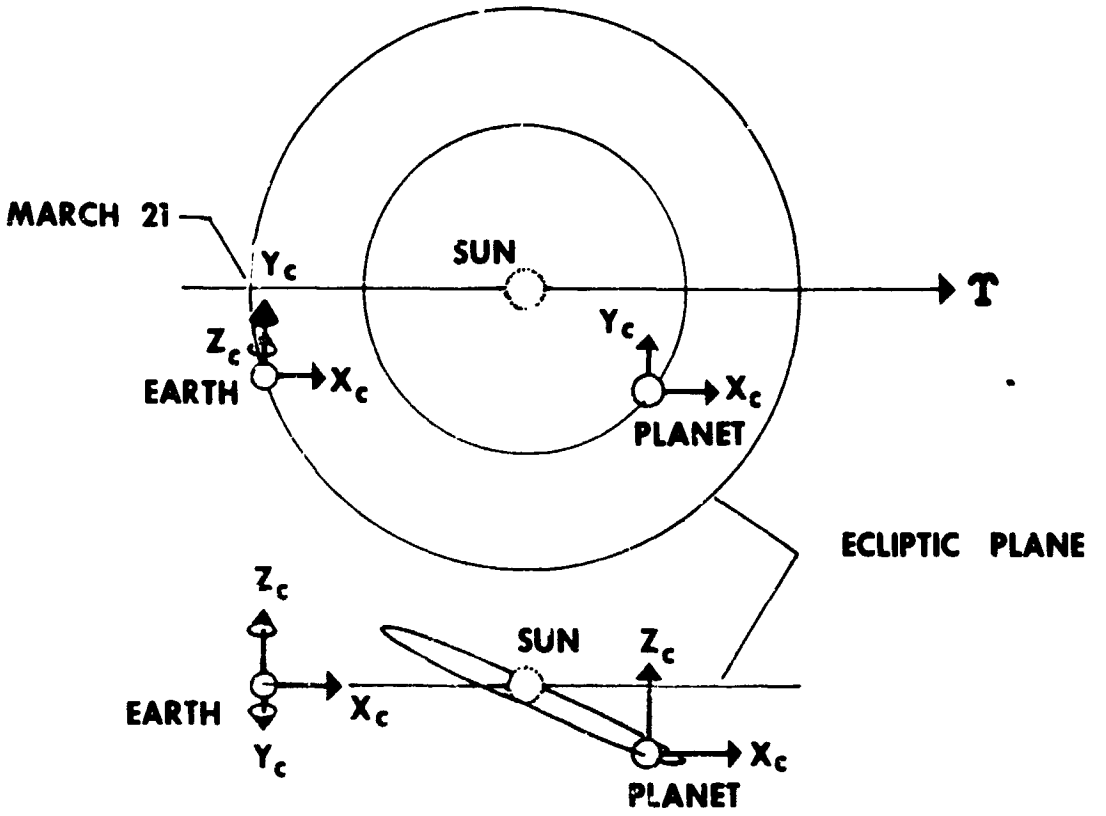

NOTE: EARTH'S $X_c Y_c$ AXES LIE IN ITS EQUATORIAL PLANE
PLANET'S $X_c Y_c$ AXES ARE PARALLEL TO THE ECLIPTIC PLANE

Fig. 5 - Celestial Coordinate System for Earth (Geocentric) and Other Planets (Modified Heliocentric)

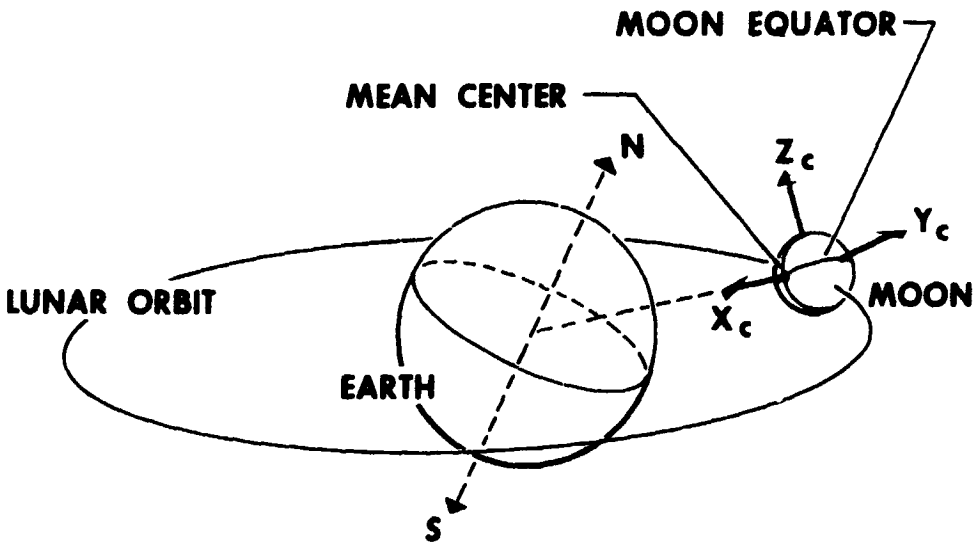

Fig. 6 - Celestial Coordinate System for the Moon (Selenographic)

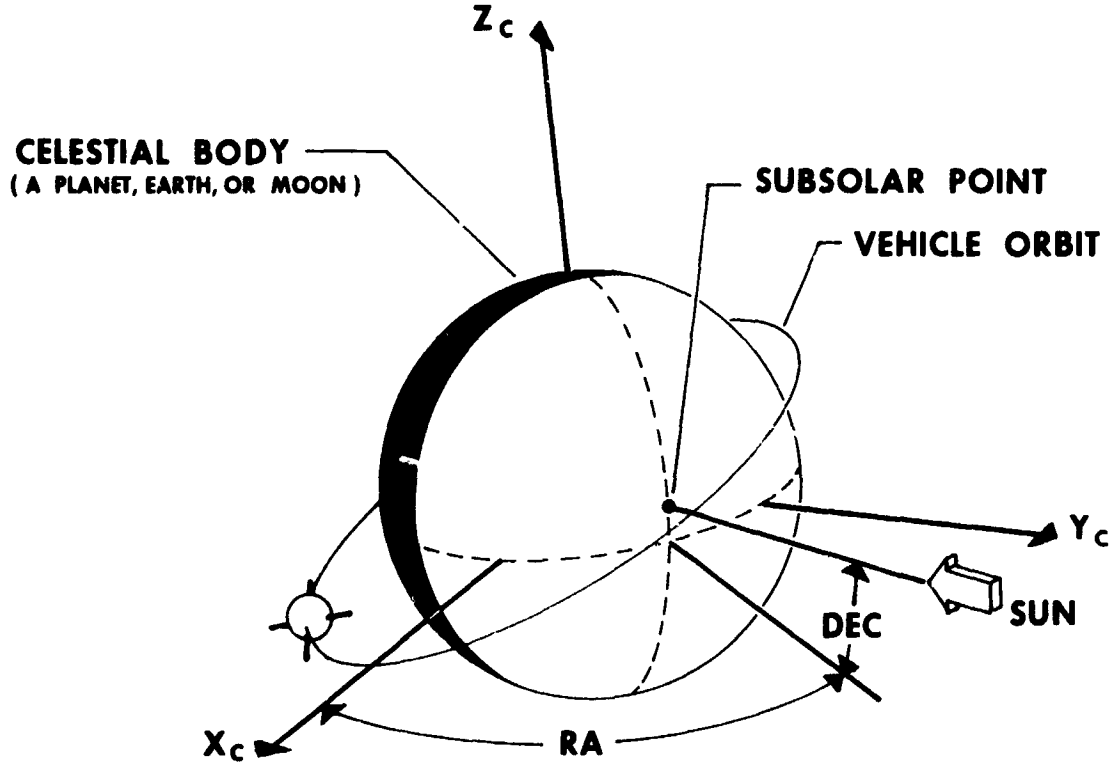

Fig. 7 - Sun's Position Relative to the Celestial Coordinate System

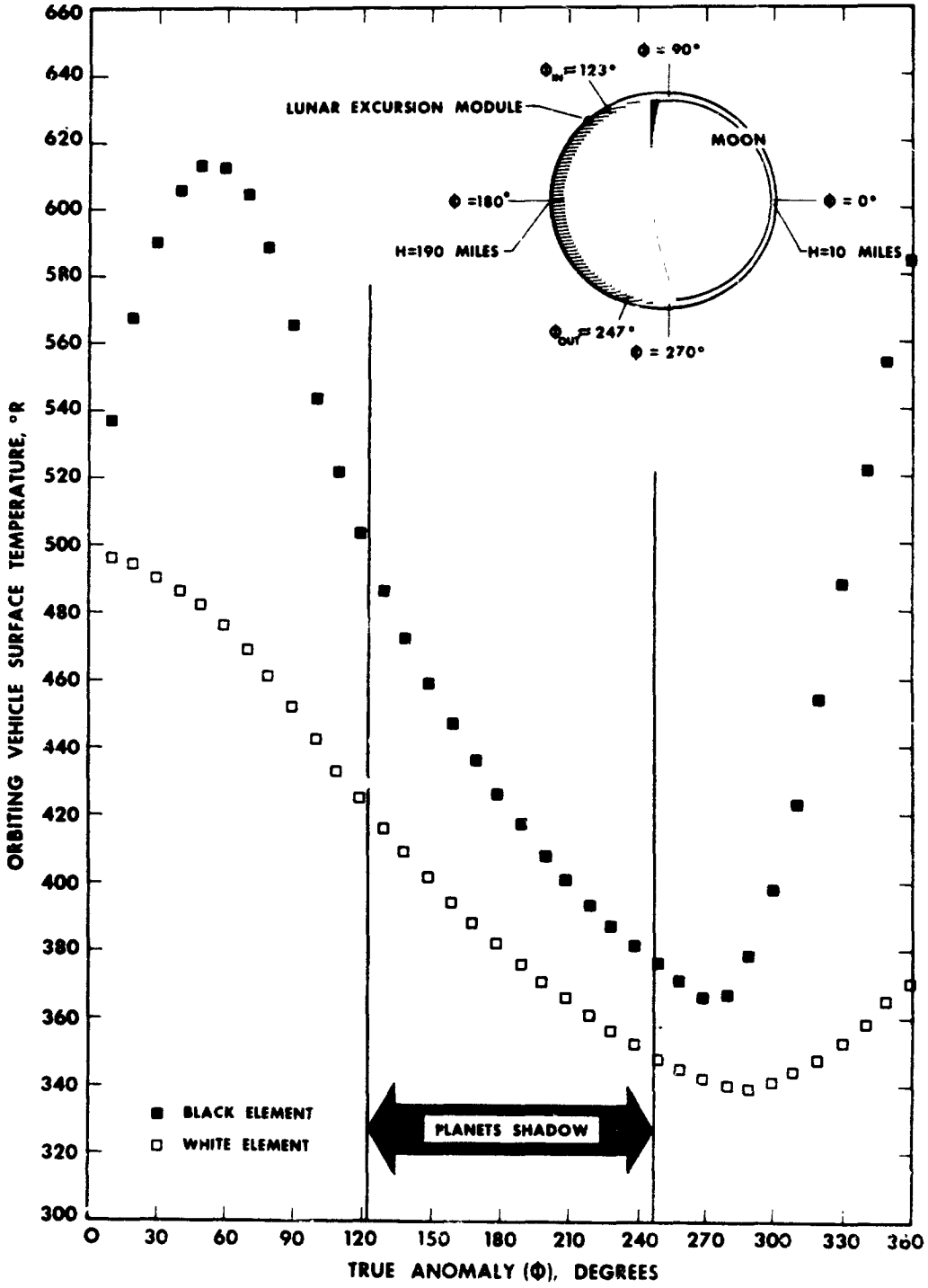

Simulated Lunar Excursion Module; Elements Face Away from the Moon

NASA-S-64-3199

SIMULATED LUNAR EXCURSION MODULE

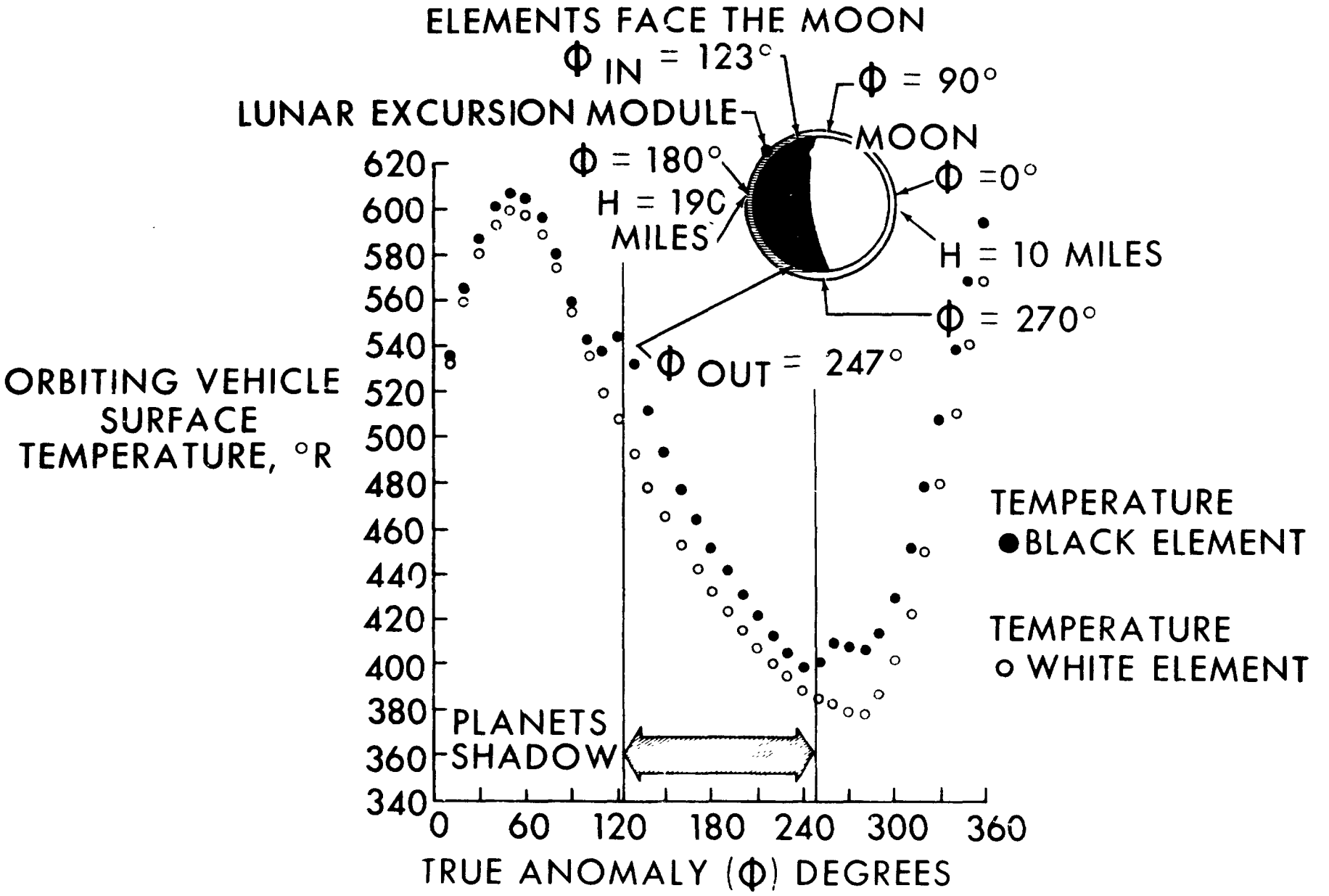

NASA-64-3200

SIMULATED LUNAR EXCURSION MODULE

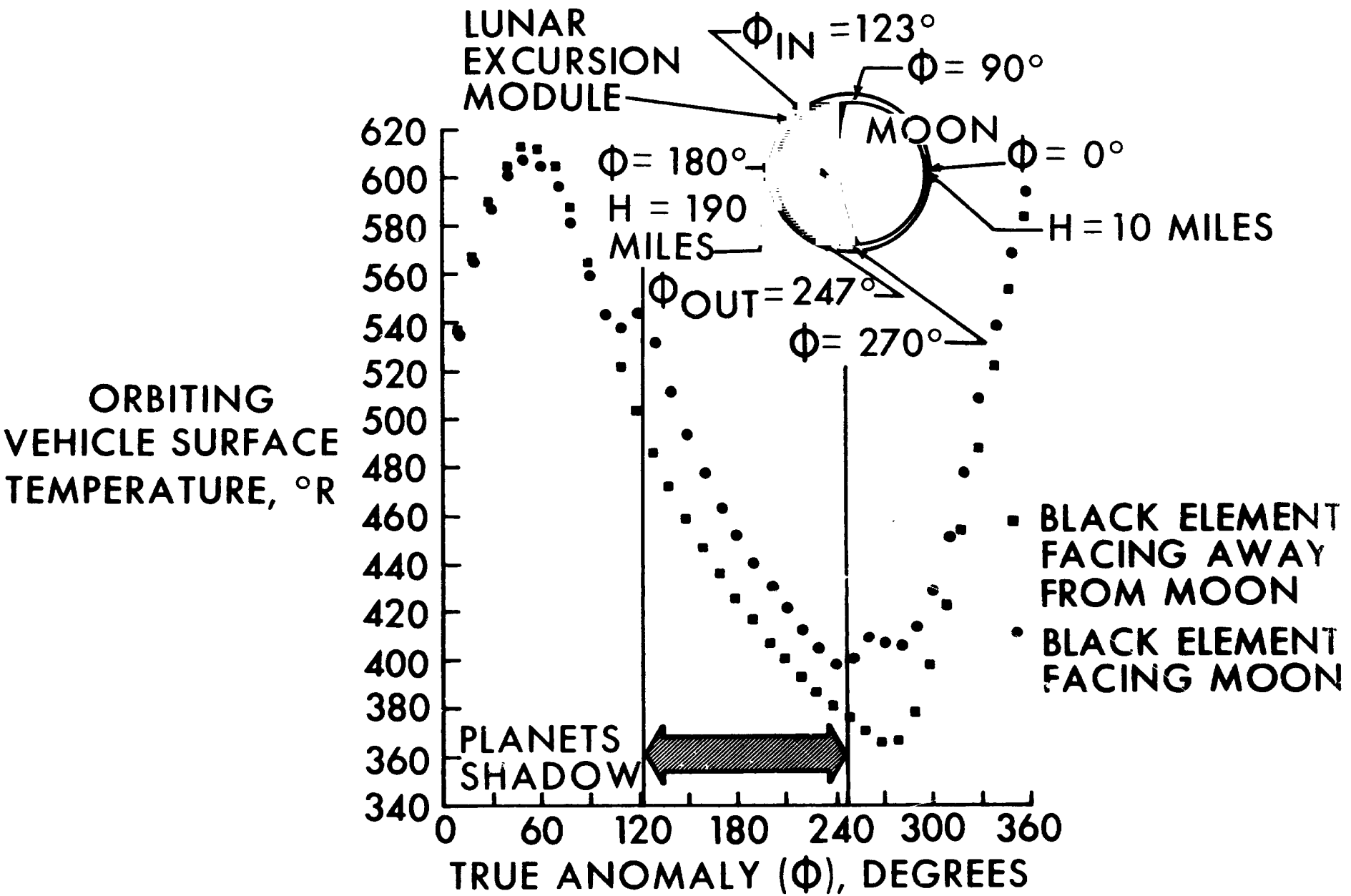

NASA-S-64-3198

SIMULATED LUNAR EXCURSION MODULE

ELEMENTS FACE THE MOON

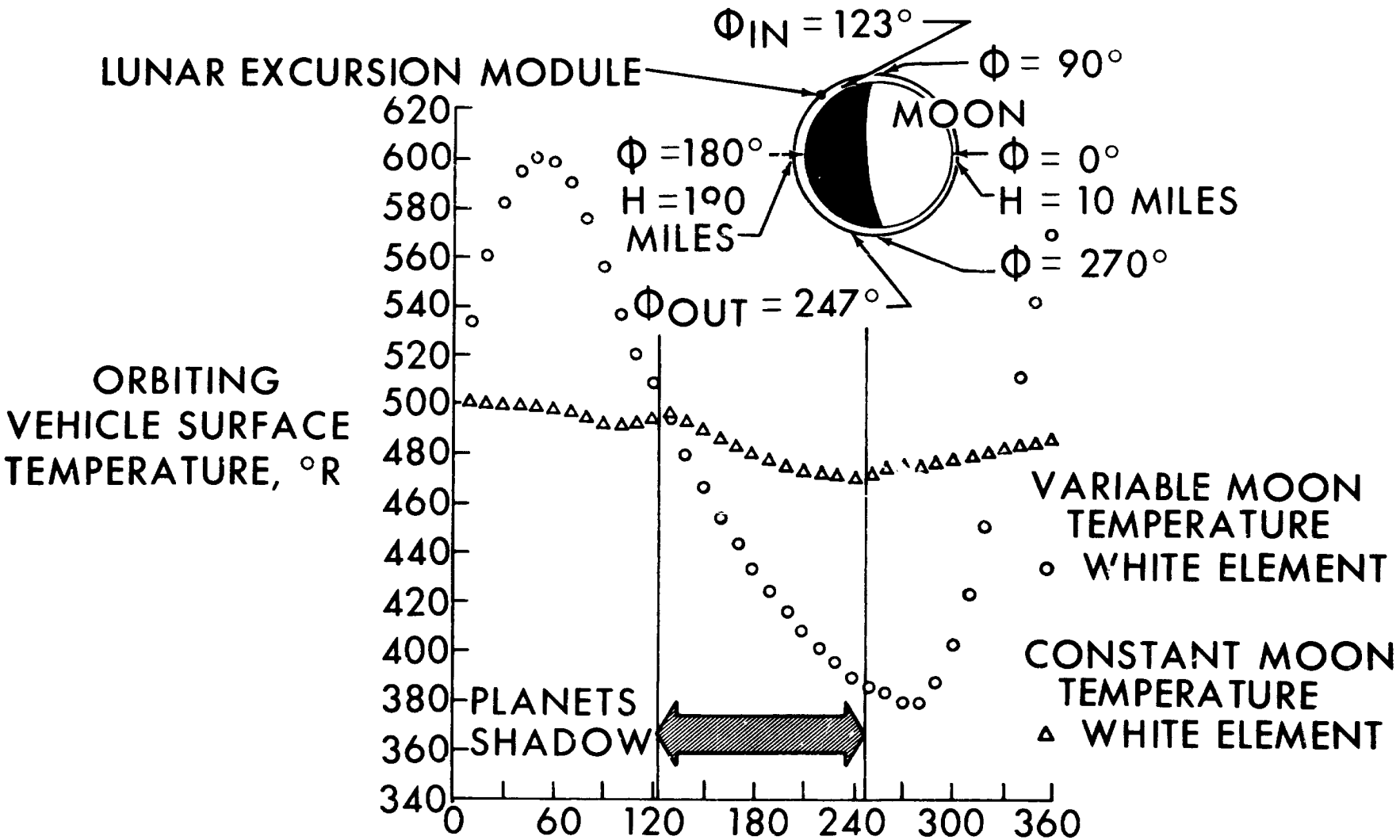

NASA - Langley

SIMPLIFIED COMPUTATION OF EARTH THERMAL AND ALBEDO RADIATION INCIDENT ON A SPACECRAFT

Doyle P. Swofford

ABSTRACT

The integral used for the computation of the earth thermal and albedo flux on a section of a satellite is directly integrable if the projected area is represented by a truncated Fourier series in the aspect angle. A great saving in computer time results from this representation. The series for a general surface of revolution, whose axis coincides with the axis of rotational symmetry of the satellite, is obtained by dividing the surface into elemental conical frustums and averaging the series for a cone over the generating curve.

SYMBOLS

$A_p(\eta)$	projected, or apparent, area of a surface viewed at an aspect angle η
A_T	total area of a surface
a_s	mean solar absorptivity of a surface
e	thermal emissivity of a surface
i_k	coefficient of the kth term in the Fourier cosine series for $A_p/A_T(\eta)$
I_k	kth coefficient of the power series in cosine η which approximates $A_p/A_T(\eta)$
q	heat input to a surface per unit time
r_e	mean albedo of the earth
S	solar radiation constant
T_e	black-body temperature of the earth
(α,ϕ)	angular coordinates of an element of surface area on the earth, with the origin at the satellite
α_o	half the angle subtended at the satellite by the earth
σ	semivertex angle of a cone or frustum
η	aspect angle - the angle between the spin axis of a satellite and the line of view
η_e	value of η at the point on earth directly beneath the satellite
θ_S	angle between the earth-satellite line and the earth-sun line
μ	symbol for A_p/A_T
σ	Stefan-Boltzmann constant

Computation of the heat input to a spacecraft surface due to earth thermal and albedo radiation involves evaluation of a double integral and extensive tabulation of the projected area of the surface. However, a good closed-form approximation for the integral (requiring no numerical integration and no tabulation of projected areas) is obtained by substituting a truncated Fourier series for the projected area.

The two heat input rates are given by

$$q_{\substack{\text{earth} \\ \text{thermal}}} = A_T \epsilon \sigma T_e^4 F(\alpha_o, \eta_e)$$

$$q_{albedo} \cong A_T S r_e a_s \cos \vartheta_S F(\alpha_o, \eta_e)$$

where F, the so-called shape factor, is given by

$$F(\alpha_o, \eta_e) = \frac{1}{\pi} \int_0^{2\pi} \int_0^{\alpha_o} \frac{A_P}{A_T} (\alpha, \phi, \eta_e) \sin \alpha \, d\alpha \, d\phi$$

Expanding the projected area in a Fourier series

$$\frac{A_P}{A_T} (\eta) \cong i_o + i_1 \cos \eta + i_2 \cos 2\eta + i_4 \cos 4\eta$$

By use of trigonometric identities, this series is converted to

$$\frac{A_P}{A_T} (\eta) \cong I_o + I_1 \cos \eta + I_2 \cos^2 \eta + I_4 \cos^4 \eta$$

where

$$\begin{cases} I_o = i_o - i_2 + i_4 \\ I_1 = i_1 \\ I_2 = 2i_2 - 8i_4 \\ I_4 = 8i_4 \end{cases}$$

Taking the scalar product of the unit vectors along the satellite axis and the view line, we get

$$\cos \eta = \cos \eta_e \cos \alpha + \sin \eta_e \sin \alpha \cos \phi$$

Making use of this relation and the series for $\frac{A_P}{A_T}$, we find

$$F(\eta_e,\alpha_o) \cong (1 - \cos \alpha_o)\left[2I_o + I_2 \sin^2\eta_e + \frac{3}{4} I_4 \sin^4\eta_e\right]$$
$$+ (1 - \cos^2\alpha_o)\left[I_1 \cos \eta_e\right]$$
$$+ (1 - \cos^3\alpha_o)\left[I_2\left(\frac{2}{3} - \sin^2\eta_e\right) + I_4 \sin^2\eta_e\left(2 - \frac{5}{2} \sin^2\eta_e\right)\right]$$
$$+ (1 - \cos^5\alpha_o)\, I_4\left(\frac{2}{5} - 2 \sin^2\eta_e + \frac{7}{4} \sin^4\eta_e\right)$$

Thus, the problem is reduced to finding the coefficients I_k in the expansion for $A_P/A_T(\eta)$. For a satellite spinning about its axis of symmetry, the projected areas of some surfaces are given by simple expressions such as these:

$$\mu_{plate} = \left(\frac{A_P}{A_T}\right)_{plate} = \begin{cases} \cos \eta & 0 \leq \eta \leq \frac{\pi}{2} \\ 0 & \frac{\pi}{2} \leq \eta \leq \pi \end{cases}$$

$$\mu_{plate} \cong \frac{1}{\pi} + \frac{1}{2} \cos \eta + \frac{12}{5\pi} \cos^2\eta - \frac{16}{15\pi} \cos^4\eta$$

and

$$\mu_{cylinder} = \frac{1}{\pi} \left|\sin \eta\right| \cong \frac{46}{15\pi^2} - \frac{8}{15\pi^2} \cos^2\eta - \frac{32}{15\pi^2} \cos^4\eta$$

$$\mu_{sphere} = \frac{1}{4}$$

$$\mu_{hemisphere} = \frac{1}{4} + \frac{1}{4} \cos \eta$$

Other surfaces are much more difficult to work with. However, since any surface of revolution can be divided into elemental frustums of cones, finding the I_k's of a cone as a function of its semivertex angle δ will make possible a simple general solution. Dividing the cone into infinitesimal plane elements and integrating the series for the projected area of a plate around the cone from 0 to 2π, the following result is obtained:

$$\mu_{cone} \cong \left[\frac{1}{5\pi} + \frac{6}{5\pi} \cos^2\delta - \frac{2}{5\pi} \cos^4\delta\right] + \left[\frac{1}{2} \sin \delta\right] \cos \eta$$

$$+ \left[\frac{12}{5\pi} - \frac{34}{5\pi} \cos^2\delta + \frac{4}{\pi} \cos^4\delta\right] \cos^2\eta$$

$$+ \left[-\frac{16}{15\pi} + \frac{16}{3\pi} \cos^2\delta - \frac{14}{3\pi} \cos^4\delta\right] \cos^4\eta$$

For a general body of revolution, the projected area is found by summing infinitesimal frustums

$$\mu_{body} = \frac{A_P}{A_T} = \frac{\int \mu_{frust.} \, dA}{\int dA} = \bar{\mu}_{frust.}$$

For a generating curve, $y = f(x)$, revolved about the X-axis, the semivertex angle δ of an infinitesimal frustum is given by

$$\tan \delta = \left|\frac{df}{dx}\right|$$

From this, the I_k's of the infinitesimal frustum can be found as functions of x. Then,

$$(I_k)_{body} = \frac{\int_{x_1}^{x_2} \left[I_k(x)\right]_{frust.} \, dA}{\int_{x_1}^{x_2} dA} = (\overline{I_k})_{frust.}$$

where

$$dA = 2\pi f(x) \sqrt{1 + \left(\frac{df}{dx}\right)^2} \, dx$$

In polar coordinates, revolving the curve $r = r(\vartheta)$ about the axis $\theta = 0$ gives

$$\tan \delta = \left| \frac{r \cos \vartheta + \frac{dr}{d\vartheta} \sin \vartheta}{r \sin \vartheta - \frac{dr}{d\vartheta} \cos \vartheta} \right|$$

and

$$dA = 2\pi r^2 \sin \vartheta \sqrt{1 + \left(\frac{1}{r} \frac{dr}{d\theta}\right)^2} \, d\theta$$

The surfaces of revolution will, of course, be split into sections small enough to justify the assumption of equal temperature throughout a section.

This technique for surfaces of revolution can be applied also to surfaces not physically circular in cross section, but optically so due to their spin.

For a satellite tumbling about an axis perpendicular to the symmetry axis, with some residual spin about the latter, the projected area is given by

$$\mu_{tumbling} = \left[\frac{A_P}{A_T}(\eta)\right]_{tumbling} = \frac{1}{2\pi}\int_0^{2\pi} \mu_{spin}^{(\eta_1)}\, d\phi$$

where

$$\cos\eta_1 = \sin\eta\cos\phi$$

Substituting

$$\mu_{spin}(\eta_1) \cong \sum_{k=0}^{4} (I_k)_{spin} (\sin\eta\cos\phi)^k$$

we get

$$\mu_{tumbling} \cong (I_o)_{spin} + \frac{1}{2}(I_2)_{spin}\sin^2\eta + \frac{3}{8}(I_4)_{spin}\sin^4\eta$$

or

$$\begin{cases} (I_o)_{tumble} = \left[I_o + \frac{1}{2}I_2 + \frac{3}{8}I_4\right]_{spin} \\ (I_1)_{tumble} = 0 \\ (I_2)_{tumble} = -\left[\frac{1}{2}I_2 + \frac{3}{4}I_4\right]_{spin} \\ (I_4)_{tumble} = \frac{3}{8}(I_4)_{spin} \end{cases}$$

MONTE CARLO TECHNIQUES FOR SOLVING TRANSPORT PROBLEMS

by Morris Perlmutter
Lewis Research Center

INTRODUCTION

The Monte Carlo procedure is a model sampling technique. A model is established, and the behavior of sample units in this model is followed. A sufficient number of sample units are followed to obtain a statistical average or macroscopic quantities, which are the quantities of interest.

This technique was used in crude form by Fermi in connection with the building of the first atomic pile. Later, Von Neumann and Ulam developed and used the Monte Carlo procedure extensively in developing the atomic bomb. Since then this technique has gained considerable use in nuclear reactor problems (refs. 1 and 2), and we at the Lewis Research Center have been extending it to thermal radiation (refs. 3 and 4), rarefied gas flows, and plasma flow problems (ref. 5). This technique, which requires a large number of sample histories to obtain solutions with small variances, is receiving greater use because of the development of the high-speed electronic computors.

Method of Obtaining Sample Histories

The sample history is the behavior of a sample unit under the conditions of the model. The sample unit can be an actual physical quantity such as a photon in thermal radiation problems or a molecule in rarefied gas flow, or it can be some idealized nonphysical quantity such as bundle of radiation or a bundle of molecules that behave according to well defined laws. For purposes of illustration let us consider rarefied gas flow through a channel. A similar problem for ionized gas flow through a channel with a magnetic field across the channel is treated in reference 5. (The procedure applied in this sample problem would apply to other situations such as thermal radiation as well.) Our sample history will be that of a sample molecule as it passes through the channel as shown in figure 1. The sample molecule is equally likely to enter at any height x_2 between 0 and 1 for the case of a flat plate channel. To find the height at which the sample molecule enters the channel, a random number is picked between 0 and 1. This random number has an equal likelihood of being anywhere between 0 and 1 and can be generated by use of standard techniques on the high-speed computor. If a Maxwellian gas in equilibrium in the reservoir is assumed, then the distribution of speeds of the molecules entering the channel is given by

$$f_V = 2\beta^4 V^3 e^{-\beta^2 V^2} \tag{1}$$

where f_V is called the probability density distribution of V. Then $f_V\,dV$ is the fraction of all the molecules that enter the channel that have a speed in the range V to $V + dV$. This depends on the parameter $\beta = (2RT)^{-1/2}$ which is a function of the gas temperature T in the reservoir.

A velocity must now be selected for the sample molecule entering the channel from this distribution. There are several methods of picking from this distribution. One method consists of picking two random numbers R_1 and R_2 and setting R_1 equal to V. In this case every V would be equally likely. Therefore, it is necessary to reject some of the values of V so that the sample distribution will agree with f_v. This is done by using this value of V to find f_v. If f_v is less than R_2, then $R_1 = V$ is rejected (fig. 2) and a new set of random numbers is selected. If f_v is greater than R_2, then $V_1 = R_1$ is used. Thus after a large number of sample molecules are picked, the chosen velocities will satisfy the distribution given by equation (1). There are many different techniques for picking from a distribution, and these are given in the references. In a similar manner we can pick a direction from the appropriate distribution for the sample molecule entering the channel. These are given for a Maxwellian gas by $f_\theta = \theta/2\pi$ and $f_\psi = 2 \cos \psi \sin \psi$ where ψ is the cone angle and θ is the polar angle as shown in figure 1 (ref. 3). The molecule is followed until it has a collision with another gas molecule. The frequency distribution for path length to collision can be given by

$$f_l = \frac{1}{L} e^{-l/L} \tag{5}$$

where l is the path length of the sample molecule and L is the average path length of all the molecules at that location; the path length to the collision is picked from this distribution. The new molecule path must then be picked, and the molecule is followed in this manner until it leaves the channel.

Obtaining the Mean Properties

The mean properties are obtained by dividing the height of the channel into increments of width Δx_2 at several locations along the length of the channel (fig. 2). The amount of some quantity Q that is carried by a single molecule across Δx_2 at that axial position is given by

$$\dot{M} \int_0^\infty Q V_1 f \, dV = \rho \overline{V_1 Q} = \frac{C_L}{\Delta x_2} \left(\sum^{S^+} Q - \sum^{S^-} Q \right) \tag{6}$$

where M is the mass of a molecule and C_L is the number of molecules each sample molecule represents. The terms $\sum^{S^+} Q$ and $\sum^{S^-} Q$ are the sums of the Q contained in each sample molecule passing Δx_2 in the positive or negative axial direction, respectively. The number of these molecules is given by S. If the axial flow is desired, then $Q = 1$ and equation (6) reduces to

$$\rho \bar{V}_1 = M \int_0^\infty V_1 f \, dV = \frac{C_L}{\Delta x_2} (S^+ - S^-) \tag{7}$$

If the mass flow in the x_2 or vertical direction is desired, then $Q = V_2/V_1$ and equation (6) becomes

$$\rho\bar{V}_2 = M\int_0^\infty V_2 f\, dV = \frac{C_L}{\Delta x_2}\left(\sum^{S^+}\frac{V_2}{V_1} - \sum^{S^-}\frac{V_2}{V_1}\right) \tag{8}$$

If the density is desired, then $Q = 1/V_1$ and equation (6) reduces to

$$\rho = M\int_0^\infty f\, dV = \frac{C_L}{\Delta x_2}\left(\sum^{S^+}\frac{1}{V_1} - \sum^{S^-}\frac{1}{V_1}\right) \tag{9}$$

In this manner macroscopic flow properties in the channel can be obtained by summing these Q properties as the molecules pass the designated cross sections.

In a similar manner the shear stress or drag on the wall can be calculated. The shear stress on the wall in the x_1 direction P_{x_1,x_2} is given by

$$-P_{x_1,x_2} = \left(M\int_0^\infty V_1 V_2 f\, dV\right)_w = \frac{C_L\left(\sum^{Sq} V_1\right)}{D\,\Delta x_1}$$

That is, by summing the V_1 components of velocity of all the sample molecules hitting an elemental area Δx_1 on the wall (fig. 1) we can find the shear stress or drag at the wall at that location. If the molecules are reflected diffusely, they will not contribute to the shear stress. Some results obtained in references 5 and 6 are shown in figures 2 to 4.

Figure 3 shows the axial flow through a flat plate channel for a collisionless gas. Different channel lengths over width l were used. The solid lines are the analytical solutions (ref. 5), and the points are the Monte Carlo results (ref. 6). The cross-sectional measurements were made at the entrance $x_1 = 0$, one quarter down the channel $l/4$ and the midpoint of the channel $l/2$. The height of the channel was divided into 20 increments. The results are symmetrical around $l/2$ and also around $x_2 = 1/2$.

The densities are shown in figure 4. Again the back half of the channel is not shown because of the relation

$$\left(\frac{\rho}{\rho_L}\right)_{x_1} + \left(\frac{\rho}{\rho_L}\right)_{l-x_1} = 1$$

In figure 5 the wall shear results are presented. There is good agreement between the Monte Carlo and the analytical results.

One major drawback of this technique is the large amount of computor time required because of the fact that to obtain small variations in the average quantities a large number of trials are needed. However, various techniques have been developed that allow shorter running times to be obtained. Also, the high-speed computors are constantly being improved. This Monte Carlo procedure is relatively new and will probably be used a great deal more in the future for solving problems on widely different subjects. It has already been found very useful in solving problems that would be highly intractable using more standard procedures.

REFERENCES

1. Kahn, Herman. Applications of Monte Carlo. RM-1237-AEC, The Rand Corp., Apr. 27, 1956.

2. Cashwell, E. D., and Everett, C. J.: A Practical Manuel on the Monte Carlo Method for Random Walk Problems. LA-2120, Los Alamos Sci., Lab., 1957.

3. Howell, J. R., and Perlmutter, M.: Monte Carlo Solution of Thermal Transfer Through Radiant Media Between Gray Walls. Jour. Heat Transfer (Trans. ASME), ser. c, vol. 86, no. 1, 1964, pp. 116-130.

4. Howell, J. R., and Perlmutter, M.: Monte Carlo Solution of Radiant Heat Transfer in a Nongray Nonisothermal Gas with Temperature Dependent Properties. (To be publ. in A.I.Ch.E. Jour.)

5. Perlmutter, M.: Monte Carlo Solution of a Highly Rarefied Ionized Gas Flowing Through a Channel with a Transverse Magnetic Field. Paper to be Presented at Int. Symposium on Rarefied Gas Dynamics, Toronto (Canada), July 14-17, 1964.

6. Perlmutter, M.: Flow and Heat Transfer Between Heated Plates of Finite Width in a Free Molecules Flow Environment. Proposed NASA TN.

CHANNEL MODEL

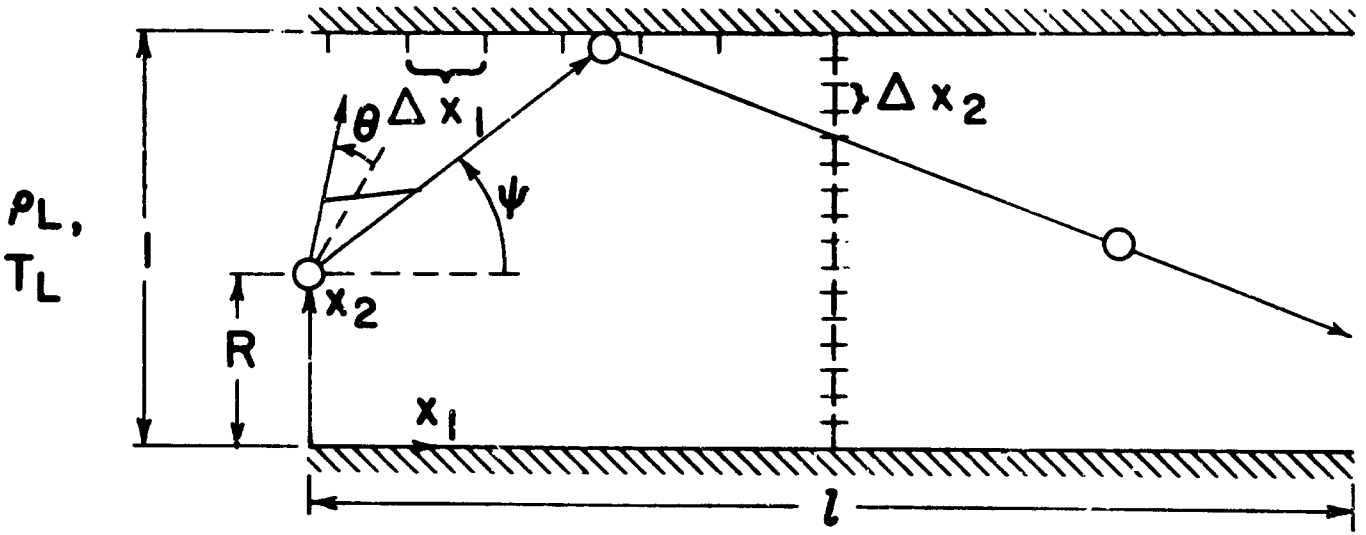

Figure 1

SAMPLING TECHNIQUE

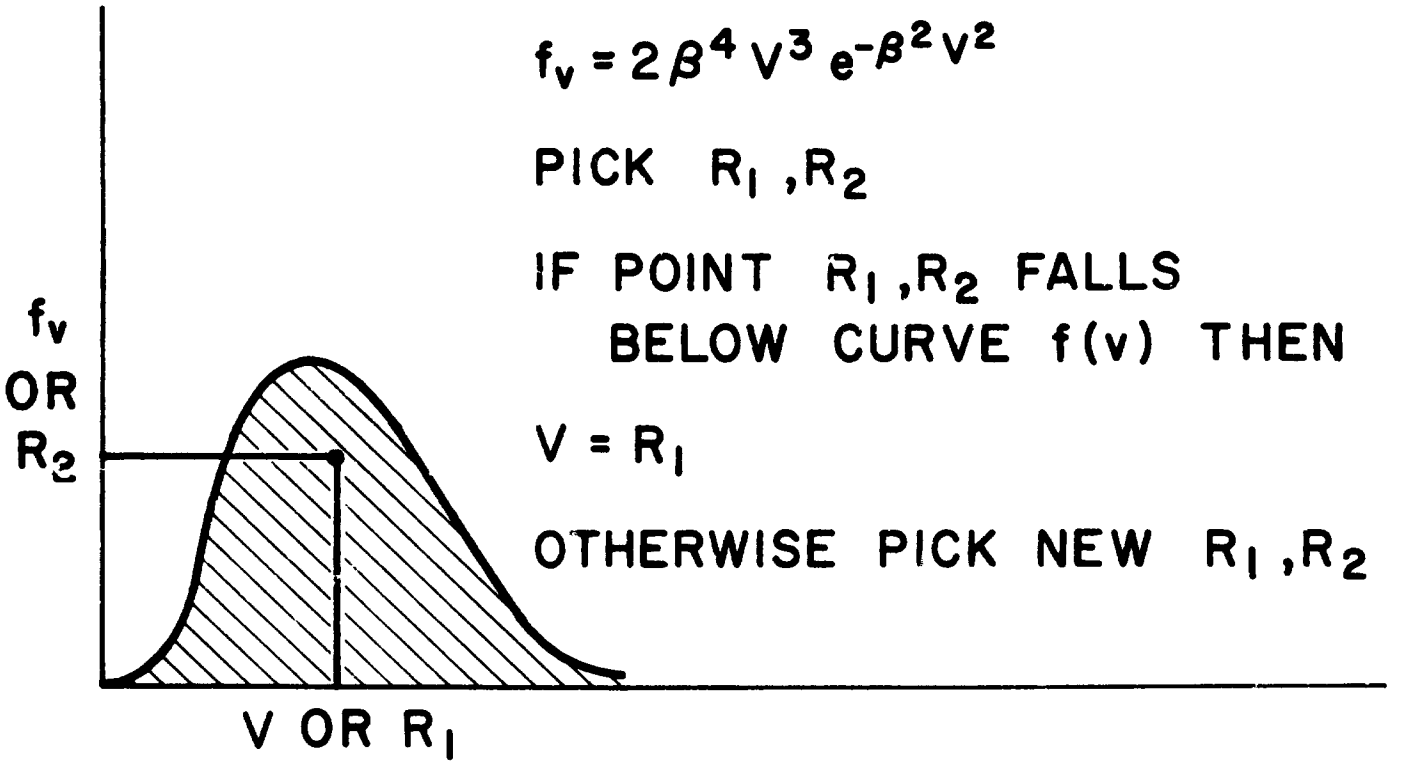

Figure 2

E-2570-II

AXIAL MASS-FLOW PROFILE

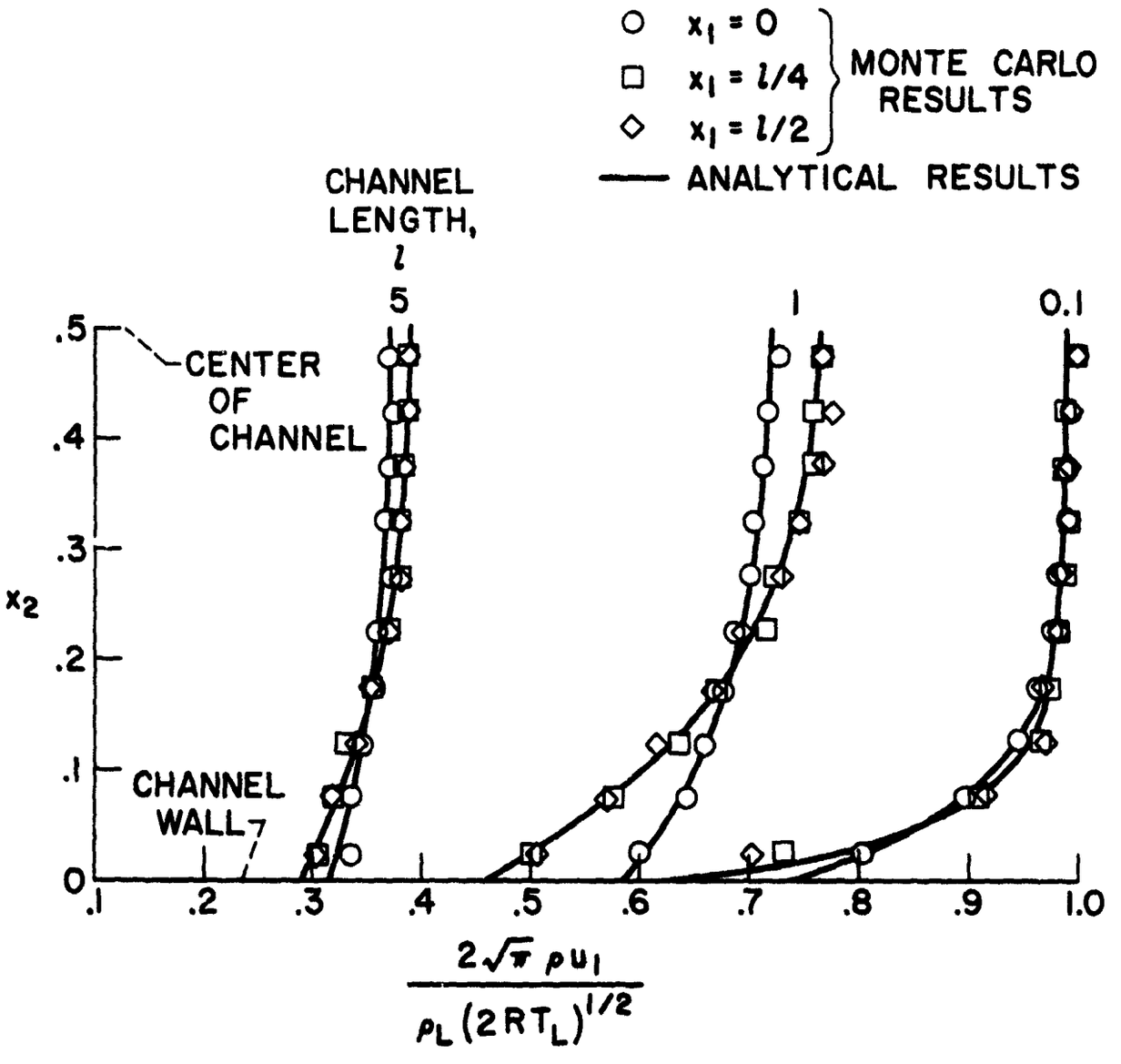

Figure 3

DENSITY DISTRIBUTION IN CHANNEL

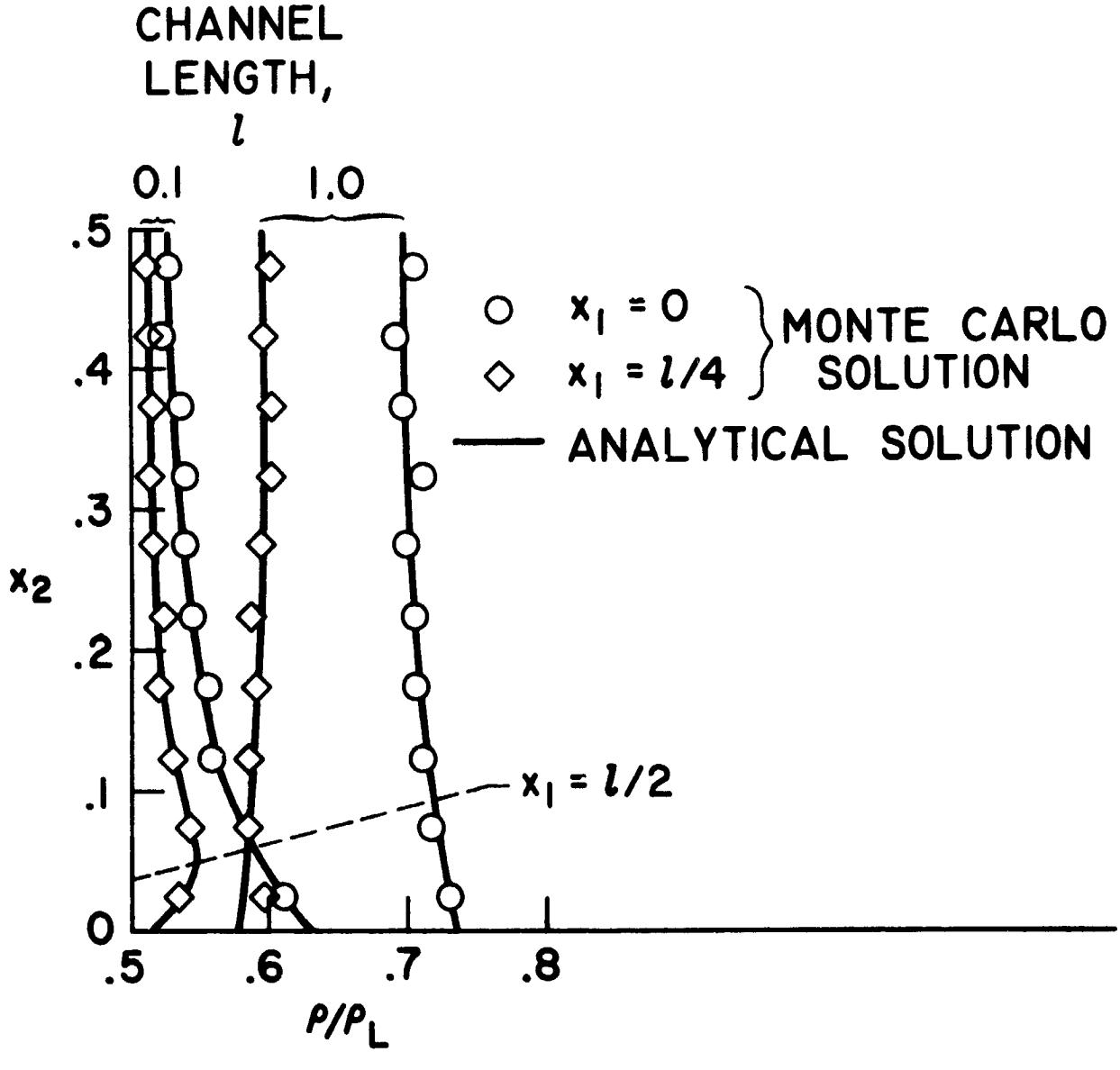

Figure 4

WALL SHEAR DISTRIBUTION

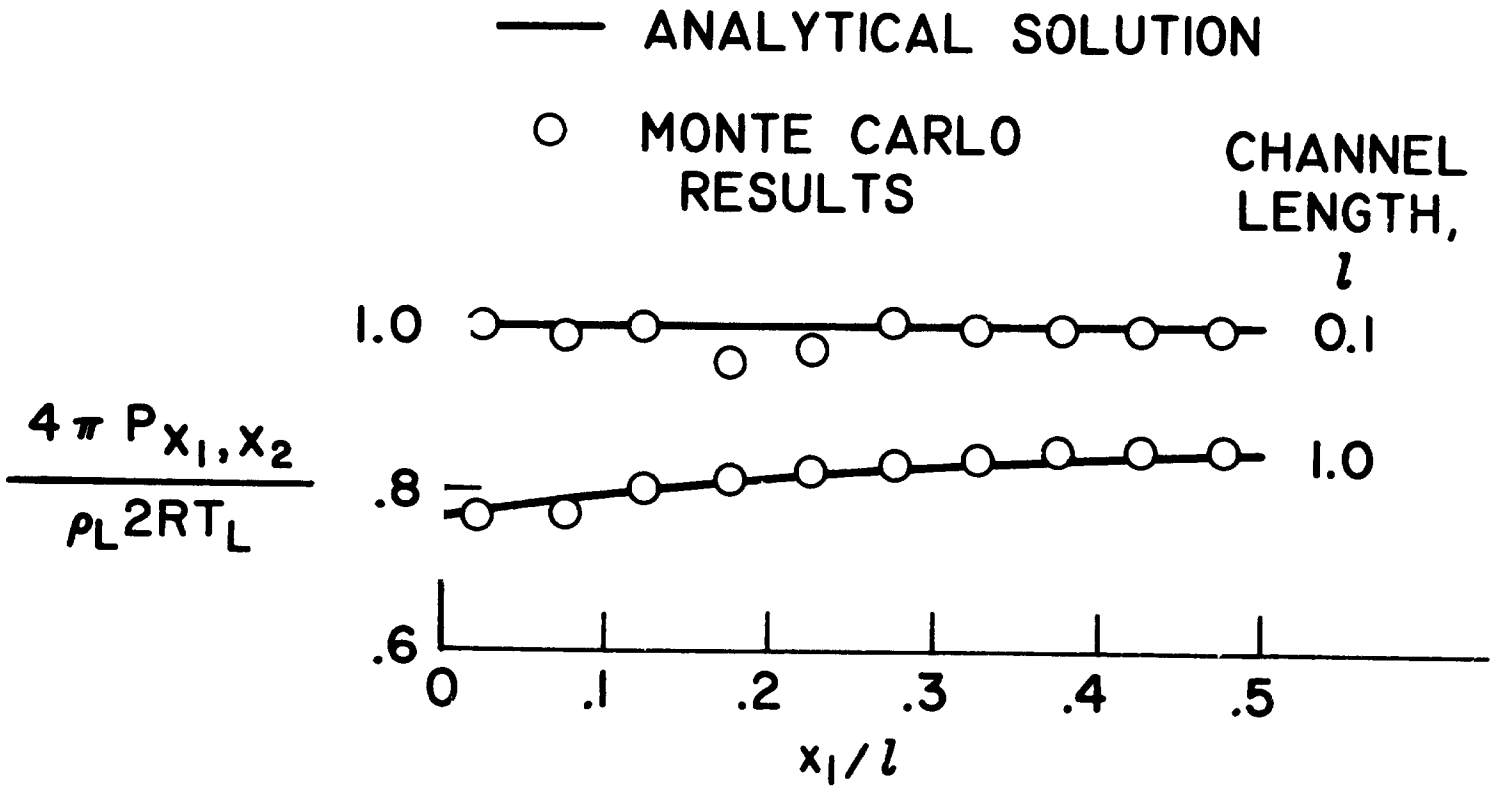

Figure 5

DISCUSSION OF THE GENERAL ELECTRIC PROPOSAL TO DEVELOP A COMPUTER PROGRAM TO SELECT THERMAL COATINGS FOR PASSIVE TEMPERATURE CONTROL OF SATELLITES

by

Robert E. Kidwell, Jr.
NASA Goddard Space Flight Center
Greenbelt, Maryland

DISCUSSION OF THE GENERAL ELECTRIC PROPOSAL TO DEVELOP A COMPUTER PROGRAM TO SELECT THERMAL COATINGS FOR PASSIVE TEMPERATURE CONTROL OF SATELLITES

by

Robert E. Kidwell, Jr.
NASA Goddard Space Flight Center
Greenbelt, Maryland

Scope of G. E. Proposal

The General Electric Company, Missiles and Space Division, submitted a proposal to NASA for the development of an IBM 7094 computer program which would select the exterior surface coatings for passively controlling spacecraft temperatures. G. E. claims that the "trial and error" procedures currently used can be accomplished more rationally and can therefore be programmed for a digital computer. In the ASME paper, 63-HT-41, which was presented at the ASME-AIChE Heat Transfer Conference at Boston in August, 1963, Costello, Harper, and Cline, described the procedures that have been used at G. E. to develop a coating selection program subject to the following restrictions:

1. Steady-state conditions prevail,
2. Heat transfer occurs by radiation only,

3. Temperatures are optimized at only one interior point in the spacecraft, and
4. Only the solar absorptance of the external coatings is varied to optimize temperature. The emittance must remain constant at initially specified values.

General Electric proposes to develop a generalized program in three steps:

1. The program would vary both solar absorptance and hemispherical emittance to obtain the optimum coating patterns;
2. Temperatures would be optimized at more than one interior point; and
3. The equations would be modified to account for both conduction and radiation heat transfer.

In the development of the general program, the scope would be restricted to steady-state heat transfer. Since the thermal designs of most spacecraft are based primarily on nearly equilibrium conditions, the proposed program could have wide application. An obvious extension of the proposed program would be to account for transient temperatures.

Examples

To illustrate how the present program works, two examples are discussed. The first is very simple and the second is a little more complex.

Case I. - Consider a simple spacecraft which can be represented by equations describing the heat transfer at two locations or nodes. One node would represent the internal compartment which contains the electronic modules, batteries, etc. and the second node would represent the skin of the spacecraft. It is assumed that the internal compartment is isolated thermally from the skin, as in the case of the Vanguard Satellites, so that the predominant mode of heat transfer is by radiation. The temperature of the internal compartment is a function of: (1) a/e of the external surfaces of the skin, and (2) the average per orbit of the solar and planetary heat fluxes incident on the skin. Consider finally three orbits that represent typical and extreme environments. The internal temperature, T, in degrees absolute to the fourth power is simply a linear function of the a/e of the surface coatings as shown in Figure 1. If T_d is the desired temperature, then

an a/e can be selected so that the maximum difference between T_d^4 and T^4 for the three orbits is a minimum.

A selection criterion can be stated formally by defining a parameter Δ_j such that

$$\Delta_j = (T^4 - T_d^4)^2$$

where j represents a particular orbit. For a given a/e, one would obtain three values of Δ_j, one for each orbit. The optimum coating would have an a/e such that the maximum value of Δ_j for a given a/e would be a minimum, as shown in Figure 2, where Δ is plotted as a function of a/e.

The procedure for applying the selection criterion in a way that can be programmed for a computer can be visualized by referring again to Figure 2. The first step would be to assume a trial a/e, to compute the three Δ_j's and to select the maximum Δ_j. The next step would be to make an incremental change in a/e such that the new maximum Δ_j would be less than the previous value. The process would then be continued until no further decrease in the maximum Δ_j could be obtained.

Case II - Consider next a cylinder in a polar orbit near the earth with the axis of the cylinder parallel to the velocity vector and with one side of the cylinder always facing the earth. It is assumed that there are 10 possible orbital conditions based on launches at 8, 10, 12, 2, and 4 o'clock in summer or winter. Temperature is to be controlled at one internal point which is radiatively coupled to the skin. To show the advantages of a coating pattern over one uniform coating, the optimum a/e's are shown in Figure 3 for 1, 2, 4, and 8 surface nodes. Included in Figure 3 is the maximum deviation in ^{o}F of the internal temperature from the desired temperature. It is noted that when 8 surface nodes are used the maximum temperature deviation is reduced considerably compared to the deviation for one node. In addition, the coating pattern for the eight node case appears to be rather unusual. It would have been interesting to compare this solution to an independent solution by conventional methods using the same number of nodes.

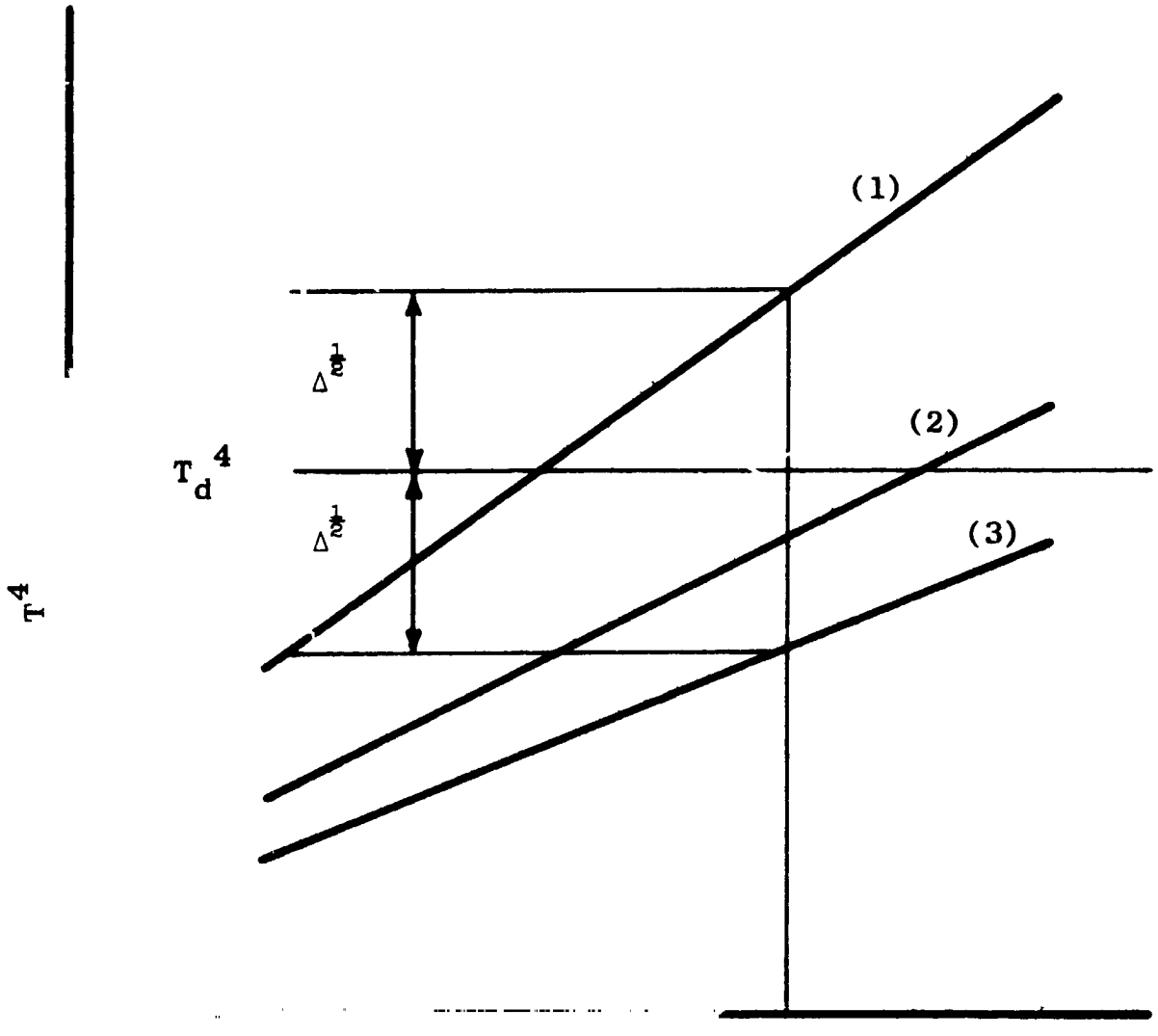

FIGURE 1 - Case I T^4 vs a/e

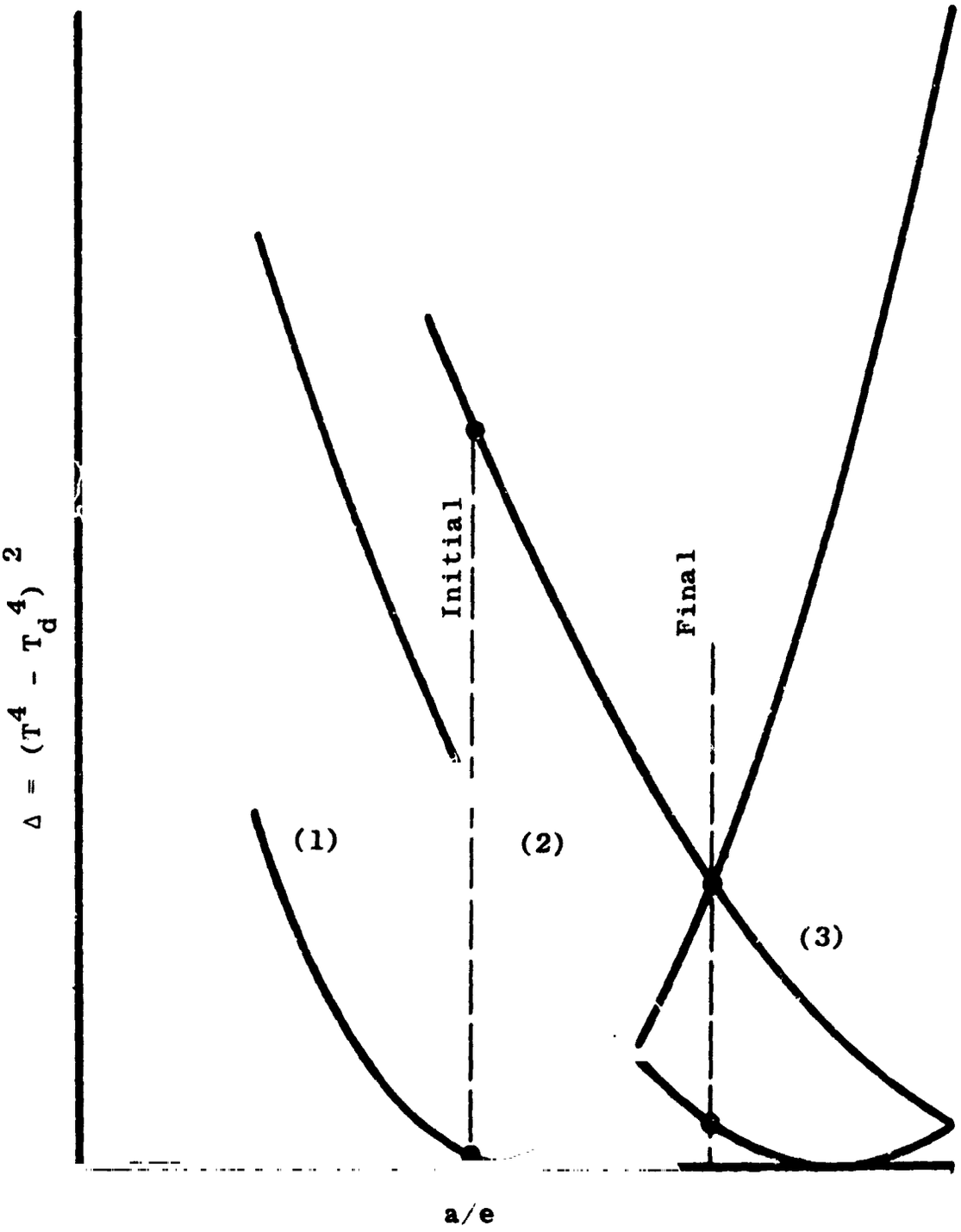

FIGURE 2 - Case I Δ vs a/e

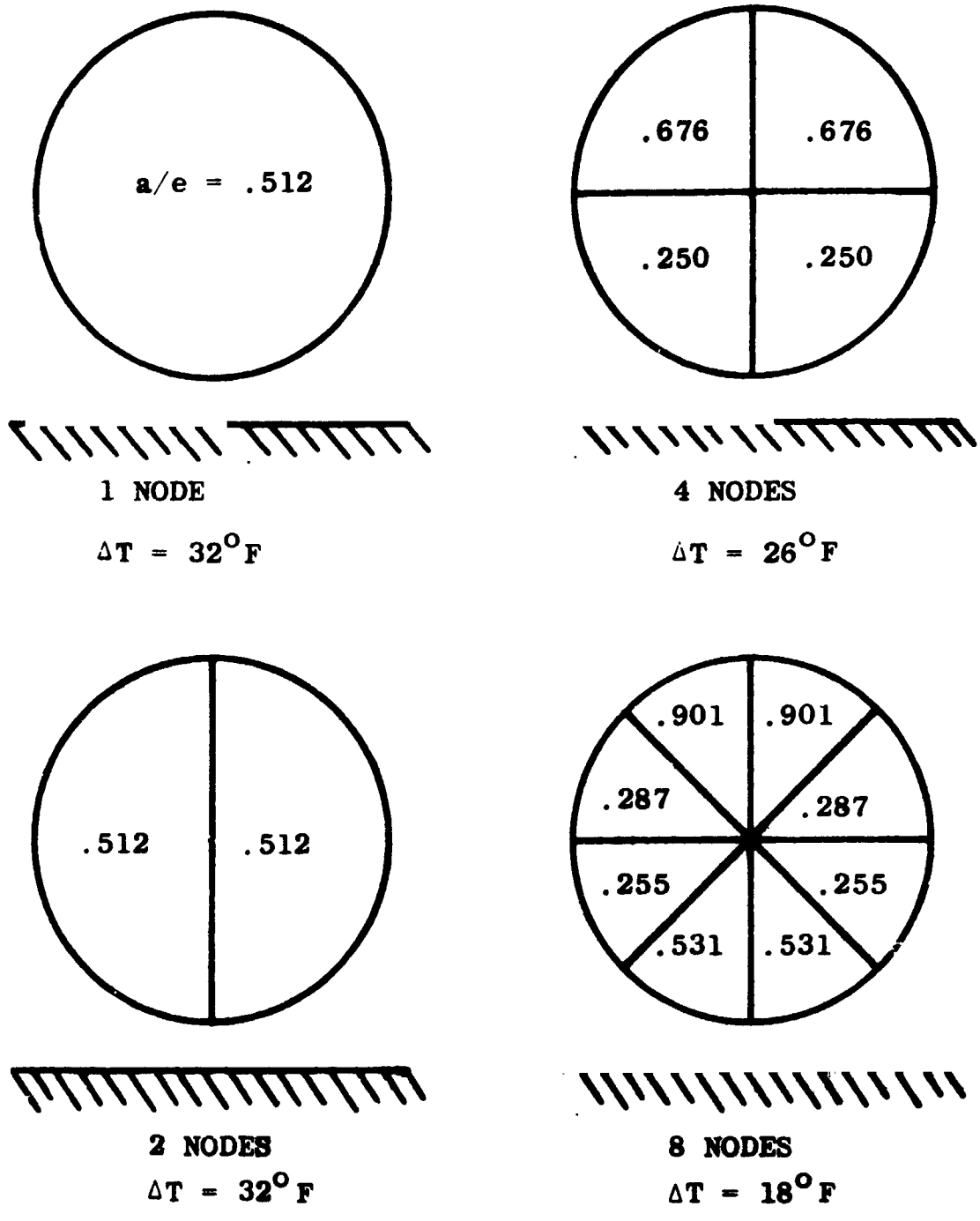

FIGURE 3 - Case II a/e and ΔT for 1, 2, 4, and 8 surface nodes. $\Delta T = (T - T_d)_{max}$

Comments on the Proposal

There are a number of advantages which could be derived from a coating selection program. The program would save the engineering time in the coating selection phase of the thermal design. In addition, it would save the time lost between the many trial solutions that are run on the computer. For example, in the present trial and error procedure for coating selection, several steps are required. First, it is necessary to decide what coatings are to be applied hypothetically to each surface. Then it is necessary to punch new input data cards for the heat transfer computer program and to submit the deck to the computer. Without priorities over other work for the computer (and priorities are extremely difficult to obtain) several hours or more are lost before the solutions can be analyzed to determine what adjustments should be made in the coating pattern for the next trial.

Another advantage of a selection program is that a computer has infinite patience. It can be required to compare and select from hundreds of numbers whereas an engineer tends to become fatigued. It is therefore quite probable that a computer could arrive at a better thermal design when there

are seemingly unlimited combinations to be considered.

There are two reservations about the proposed program. First, how does one program a computer to perform a function in which so much intuition, judgment, and experience is required? And second, how much machine time would be required to run such a program?

In both the ASME paper and the Proposal, none of the essential details were given concerning the method used to determine how to change the coating pattern for each trial so that a minimum number of steps would be required to converge on an optimum solution. Therefore, it is difficult to tell what obstacles must be overcome in developing the general program without actually doing most of the same work independently. However, it is not nearly as difficult to think of ways that most of the trial and error procedure could be programmed for a computer for any type of satellite thermal design problem without necessarily achieving optimum coatings in an efficient manner.

It is difficult to know how to account for tolerances in the coating properties, or to decide rationally whether an optimum coating pattern involving delicate materials

would be preferred over a less optimum coating pattern in which only reliable materials would be required.

At the present time, it is convenient to break up problems so that the computer time for any one run is limited to a few minutes. Longer runs must be made at night. For a 50 node problem with about 24 orbital conditions, which is typical for Goddard satellites, the running time for one trial is in the order of a few minutes. It is obvious that a coating selection program would require much longer times.

Although reservations have been expressed, it is believed that the possible advantages outweigh any of these reservations, and that the general coating selection program should be developed.

(On June 19, 1964, contract NASw-960 was awarded to G.E. to develop the program)

Spacecraft Heat Transfer Analysis

J. A. Plamondon
Jet Propulsion Laboratory

INTRODUCTION

Two somewhat related but yet distinct topics are presented below. First, some of our thoughts, at the Jet Propulsion Laboratory, on the position of computing as a tool for developing the thermal design of a spacecraft are given. The purpose in doing this is to stimulate discussion on the subject of the computer by presenting one approach to how computing might fit into thermal design. Second, a new general type heat transfer program that was recently acquired from Arthur D. Little, Inc. is briefly described. The program is called, "The Method of Zones for the Calculation of Temperature Distribution."

DISCUSSION OF COMPUTING

Over the past few years - actually from the early days of the Jet Propulsion Laboratory's involvement in space projects - those who have been close to spacecraft thermal control, directly or indirectly, have been concerned over the position that the digital computer should hold in the overall effort of spacecraft thermal design.

There is a general awareness of the importance of the digital computer and of analysis, in general, in a thermal design effort. At the same time, it is also very clear that analysis and, in particular, complicated analysis involving the digital computer is not precise, and therefore, cannot be relied upon by itself to establish the final thermal design of a spacecraft. Solutions obtained from the digital computer are simply not accurate enough, or at most, our confidence in their accuracy is not sufficient, for them to be the sole basis of final design certification. Collaboration of the experimental and the analytical is essential to establish confidence in the suitability and reliability of a design. Nevertheless, the computer, in spite of its shortcomings, does appear to have great potential, perhaps more potential than any other single tool available to the temperature control engineer.

The usual technique for using computers to solve complicated heat transfer problems is to lump into nodes, zones, and so forth, incremental volumes to form a network analog or model of the heat flow paths present in the physical problem. The computer, of course, then analyzes this computational model. This is fine; but in the process of transcribing a real problem into a computational model, the important question arises of how well this process can be carried out for very complicated problems, and consequently, how much confidence can be placed in computed data?

The difficulties encountered in computational modeling can probably be considered as arising from two sources; the modeling of the heat flow paths

present in the hardware, and the assigning of numerical values to describe the lumps and the interactions between lumps. For geometrically simple problems, the lumping or formation of a heat flow model is a relatively straightforward process with most computer programs having analytical guide lines. However, when the geometry of a problem is complicated, computational modeling becomes difficult and simple analytical guide lines become almost meaningless. The lumping process becomes partly intuitive and accurate representation becomes heavily dependent upon engineering understanding, judgement, and experience. This leads to uncertainties and a corresponding lack of confidence in computed results. In the area of assigning numerical values to describe the lumps and their interactions, the main problem is of a different nature and centers around obtaining reliable thermo-physical data; for example, obtaining reliable joint conductance information. Problems in this area will certainly diminish as a result of current and future thermo-physical research.

In addition to those problems associated with the modeling of hardware, uncertainties are also introduced because of the equations upon which we base our calculations; for example, it is known that the physical idealizations which are generally ascribed to the behavior of radiation interchange are very liberal. This type of uncertainty will also diminish with future research on the physical behavior of heat transport. The last type of error which is encountered in computed data results from numerical inaccuracies in computation; however, this type of error can be controlled since it is mathematical in nature, involving numerical analysis.

Faced with uncertainties of the type just described, it is legitimate to question the possible usages of the digital computer in thermal design and, of course, the consequential advantages of its utilization.

In reviewing the development scheduling of a spacecraft, it appears that the use of the computer should be initiated as early as possible. Certainly, it should be initiated no later than the completion of preliminary design when mission objectives and general spacecraft configurations are somewhat defined in terms of probable size, shape, power, and so forth. The purpose would be to investigate, as early as possible, the feasibility of preliminary design concepts as they relate to a particular spacecraft's configuration and mission. The results from such early analytical investigations do not have to be very accurate or very detailed; all that would be sought is verification that preliminary design concepts do indeed produce desired trends. For example, suppose that preliminary estimates call for a particular type of temperature control hardware such as louvers; it certainly would be desirable to analytically verify, early in the development schedule, that the louvers are really needed and, if so, that they produce the desired degree of control. Furthermore, and perhaps just as important, it would be very desirable to know early in design the criticality of such a device to parametric, thermal variations so as to know what conditions lead to marginal and unreliable operation. Early analytical investigations in which complicated spacecraft thermal interactions are accounted for, offer the opportunity of uncovering critical thermal problems so as to allow a maximum of time for their solution or to permit alterations in configuration and/or mission objectives with the least amount of disturbance. It should be pointed out that such early investigations can only be carried out analytically since experimental hardware is not available, and that only through the use of the computer can the necessary sophistication be brought to bear; by this is meant the multiplicity of thermal interactions. Further development in the methodological use of the digital computer must be carried out in order that such early investigations can be performed with reasonable confidence.

Upon confirmation of preliminary design concepts and corrections thereof, the simple computational models used can then be refined to conform more and more closely with actual spacecraft hardware in order to perform detailed thermal investigations. However because of the uncertainties associated with computer analysis, it is essential that refinements in computational modeling be carried out in conjunction with experimentation. The inclusion of the experimental with the analytical forms an iterative process or procedure. With somewhat refined computational models, parametric studies can be undertaken to determine the importance of various thermal elements making up the model. For example, the thermal influence of a particular joint thought to be important could be analytically studied to determine its influence. If found to be important, an experiment could be developed to determine fairly precisely the magnitude of the conductance across the joint. The experimental result would then be incorporated into the computational model. This sort of iteration procedure can be repeated, using the computational model itself to determine its own shortcomings through parametric study, until a fairly representative model evolves in the sense that the heat transfer within a piece of hardware is well understood. Utilization of the computer in this manner aids in directing and giving credence to certain test programs; that is, it aids in determining just what areas are really important to test. Verification of the computational model of course requires experimental correlation of its ability to predict steady-state and simple transient conditions. Once correlation has been established, it would then be possible to investigate all thermal events occurring during the course of a mission, which is something that is entirely impractical to carry out experimentally. Another thing that is impractical experimentally, but easily done analytically, is failure mode studies in which various possible failures can be studied to determine their effect.

The potential advantages of better integrating the digital computer into the design effort lie basically in obtaining concrete design information at an earlier time in the over-all development schedule. Without analysis upon which we can place a high degree of confidence, concrete design information must necessarily wait for hardware development, fabrication, and delivery before experimental information can be obtained. Design changes at this point can only be justified when catastrophic failure or unsolvable situation is expected. Thus, the temperature control engineer must live with his problem with little or no chance of sidestepping it through hardware redesign. What we are seeking in temperature control is earlier decision capability in order to better integrate thermal considerations into other aspects of hardware design. To do this, we must be able to obtain thermal information, accurately founded, at a pace consistent with other design activities. There appears to be no way, other than analysis.

Current plans are to investigate possible ways in which the digital computer can best be used within the framework of its current uncertainties. A particular configuration will be analyzed in order to define the difficulties encountered in using the computer and to find ways around these difficulties. In this investigation, testing will be used as a complement to analysis in the manner described previously. The object for analysis will be the Arthur D. Little thermal scale models. The ADL models have been thoroughly tested and the accuracy of the results is almost unquestionable. Plans call for using the computer along with complementary testing to predict the thermal condition of the models. For this effort, none of the ADL model test results will be used as inputs for analysis. They will be used only as a standard for comparison with analytically obtained predictions. In this way, it is planned that ways of sidestepping some current uncertainties in analysis will be found. This will in turn lead to ways of better exploiting the potential of the computer.

METHOD OF ZONES

Next, a new heat transfer program which was recently acquired from Arthur D. Little, Inc. and which is called, "The Method of Zones for the Calculation of Temperature Distribution," will be described. There are two reports on this program, so the description will be brief. The first report covers the methodology of the approach used in the program. The second part is a description of how to use the program covering the input and output format and a program listing.

The "Method of Zones" is an improved method for obtaining solutions to spacecraft associated heat transfer problems involving radiation and conduction. The program is one of the few general type heat transfer programs specifically designed for spacecraft heat transfer problems. The approach used in the program is not that of simply lumping parameters to form a nodal network analogous to an electrical circuit as in most general heat transfer programs. Rather, the approach consists of breaking a problem into zones of finite area for two-dimensional situations and into finite volumes for three-dimensional situations. The approach retains the essential characteristics of boundary value techniques in that each zone is characterized by prescribing conditions to the boundaries of each zone. The boundary conditions can represent a known heat input or output rate, or an unknown heat input or output rate expressed in terms of an unknown boundary temperature function such as T^4. The generalized heat diffusion equation is written for each zone and is integrated over the volume of the zone. The integration is performed by introducing the volumetric mean temperature of the zone. The integration of the diffusion equation results in an instantaneous heat balance equation which involves the heat fluxes over the boundaries of the zone and the rate of change in the mean temperature of the zone; that is, we have a differential equation expressed in terms of the time rate of change in mean temperature and the heat fluxes over the boundaries. The differential equation itself is no different than one would find in the typical lumped parameter program. The difference results from relating the input and output fluxes in the differential equation to the boundary conditions of the zone. This is done by deriving approximate formulas, based upon an assumed parabolic temperature distribution in the zone, in which the fluxes at the boundaries are expressed in terms of the boundary's mean temperature and the zone's mean temperature. If the boundary conditions are ignored, the program degenerates into the typical lumped parameter program. Each zone is, thus, mathematically characterized by a set of equations consisting of one differential equation for the mean temperature of the zone and a number of boundary equations (algebraic) for the temperature of the boundary. The equations are solved in a manner normal to other general heat transfer programs in that the differential equation is solved implicitly; however, the boundary equations are solved explicitly. The higher order of approximation resulting from the parabolic assumption permits a complicated system to be subdivided into fewer parts than is necessary when conventional methods are used.

In the report on the program, three simple examples are given to illustrate the application and accuracy of the method. Criteria are also given which enable zone sizes to be chosen properly in practical applications. The criteria are derived by comparing calculations made by the method of zone with exact results obtained for simple cases.

The numerical procedure, which is a modified Gauss-Seidel procedure, for solving the difference equations at each time step is discussed, and experience by ADL with convergence of the procedure is reviewed. The program also includes checking procedures which are based on the principles of reciprocity and conservation of energy. These provide an initial check on the consistency of the input through the reciprocity principle, and a running check on the solution of a problem through the conservation of energy principle. Capability is built into the program and is controllable by the user for stopping the computer should the conservation of energy check show that the numerical solution is not being carried out to desired accuracy.

As far as the user is concerned, the input and output formats of the program are as simple as any the writer has seen. However, all information supplied to the program must be supplied in duplicate in order that the reciprocity principle can check for input consistency. One of the important advantages in the program results from the way the equations are written. Being written in terms of flux instead of temperature, permits the utilization of Oppenheim's network method for diffuse inter-reflections or Bobco's corollary for specular inter-reflections involving planar surfaces.

ORBITER HEAT FLUX COMPUTER PROGRAM

W.A. Hagemeyer
Jet Propulsion Laboratory

Abstract

A two-phased contract is currently underway to develop 1) a set of parametric curves of absorbed heat flux for specific geometries, and 2) a generalized computer program whose output is absorbed heat flux on the surfaces of a planet orbiting spacecraft. The absorbed heat fluxes include the effects of blockage by and reflections from adjacent spacecraft surfaces, assuming all surfaces to be diffuse.

The final computer program will calculate fluxes on any of ten arbitrarily positioned plane surfaces, with any surface properties, planetary radiation characteristics, solar intensity, and orbital parameters. Outputs will be heat fluxes versus time, geometrical configuration factors, and radiant flux interchange factors.

This effort started roughly in May of 1963 when JPL was in the midst of its Voyager Studies. Thermal Control was actively involved in that study, seeking to provide guidelines for basic vehicle configuration. The transit problem was felt to be fairly well understood, and effort was directed at determining the peculiarities involved in making a deep space probe into an orbiter.

At this point, it might be worth while to mention some of the constraints to the Voyager as they apply to the thermal design. JPL spacecraft are typically fairly regular polygons with the electronics connected to the flat faces of this polygon, which then constitutes

what is called the spacecraft bus. This, plus the fact that cylinders can be represented by flat surfaces, allowed us to restrict the study to flat surfaces. Mission requirements of importance were dual planet capability (Venus or Mars), solar panel or RTG power source, landing capsule, and a scientific payload which would want to scan the planet. Obviously a solar panel power source required sun orientation for the solar panels and probably the spacecraft bus, while an RTG would allow planet orientation. Therefore, both situations had to be evaluated.

Our first estimation was that the added heat fluxes near a planet would be critical, especially in the case of Venus. This conclusion was reinforced by some preliminary numbers extracted from Reference 1.

A survey of the literature (Reference 2) indicated that no published effort had been expended in the direction of accounting for shading of orbiter radiator surfaces by portions of the vehicle. It was felt that this might be a reasonable way to eliminate some unwanted heat fluxes. Alternatively, this approach might allow adding some heat flux during periods of spacecraft quiescence. These heat fluxes, in order to be successfully used, must include the energy reflected from the adjacent surfaces. To provide the capability to more readily evaluate these effects, a contract was let to generate a computer program which would provide the required heat flux information. The required flux information will consist of the following fluxes: solar, planet albedo, and planetary infrared, including blockage by

and reflections from adjacent spacecraft surfaces. Secondary information output will be incident solar, planet albedo, and planetary infrared fluxes, view factors, and radiant flux interchange factors.

The contract consists of two phases. The first is a parametric study of particular orbiter configurations. The second is to prepare a generalized computer program for generating the required heat fluxes for any configuration of flat surfaces.

In the parametric study, the basic configuration studied consists of two or three adjacent sides of a rectangular box as shown in Fig. 1, surface 1 being the primary radiator surface, surfaces 2 and 3 being secondary surfaces. Fig. 1 also delineates the dimensions used to describe the configuration. This configuration is then considered to be either sun oriented or planet oriented in three particular orbits as shown in Fig. 2. Specific positions considered in each orbit are shown in Fig. 3. For all the above conditions, eight attitudes are considered varying from 100km to 30,000km, a/b and c/b (see Fig. 1) vary from 1/4 to 1 while $\phi = 90°$ and $\lambda = \beta = 90°$, and the surface properties of the primary surface and the secondary surface are fixed.

Several of the other parameters are varied at only one altitude at the sub-solar point in order to indicate the trends of these changes.

This parametric information will be tabulated with bounding values plotted. It is intended that this data will provide preliminary design information for the up-coming planetary orbiters.

The generalized computer program will have as inputs any arbitrary set of orbital parameters, planetary characteristics, solar intensity,

number and orientation of radiator surfaces, and a specification of either sun or planet orientation. Using these inputs, the program will generate the required heat flux information as mentioned previously in addition to giving the points of entry and exit from the planet shadow. These heat flux outputs, as well as the radiation interchange factors can then be inserted directly into a temperature computation program to develop a complete temperature profile for the vehicle in orbit.

References

1. ASD Technical Report 61-119, Part 1, December 1961.

2. JPL Literature Search No. 522, April 29, 1963, Thermal Design of Non-Spinning, Planet, or Inertially Oriented Satellites.

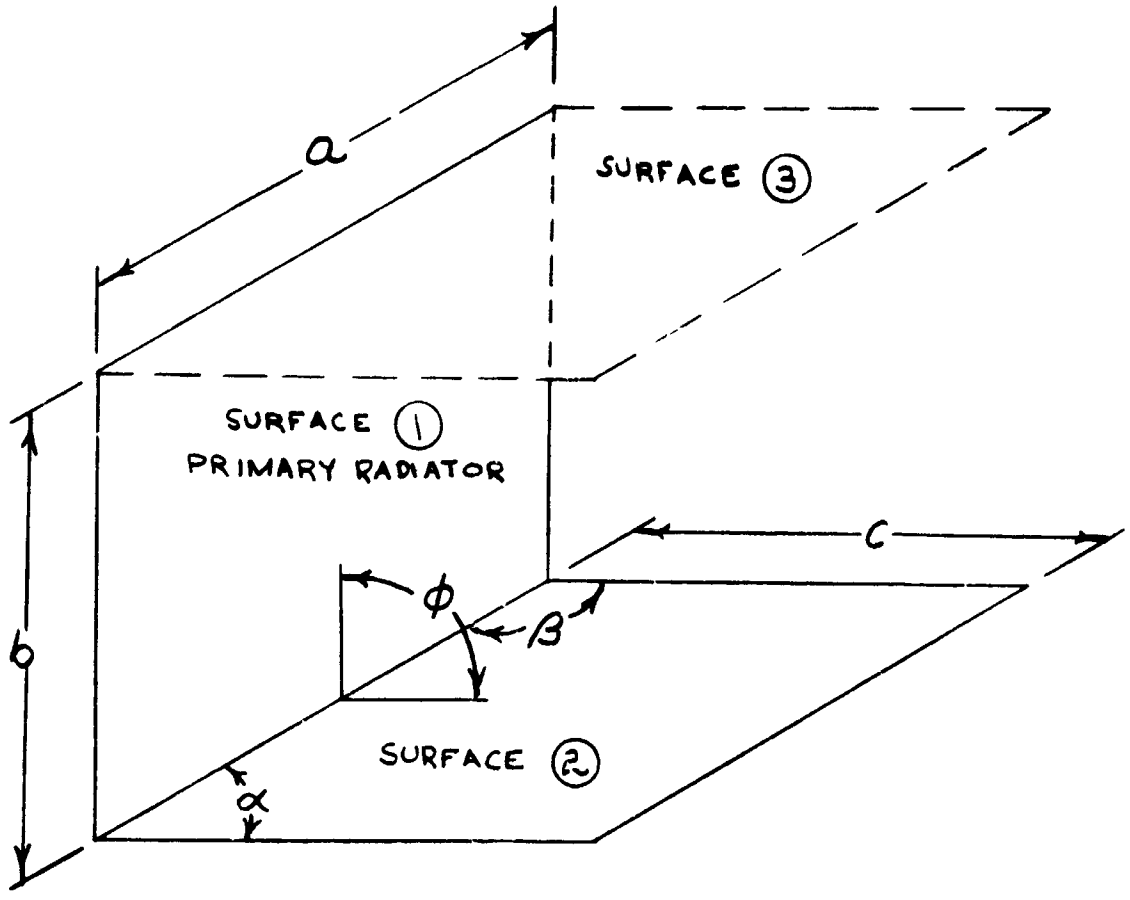

FIGURE 1 ~ CONFIGURATION

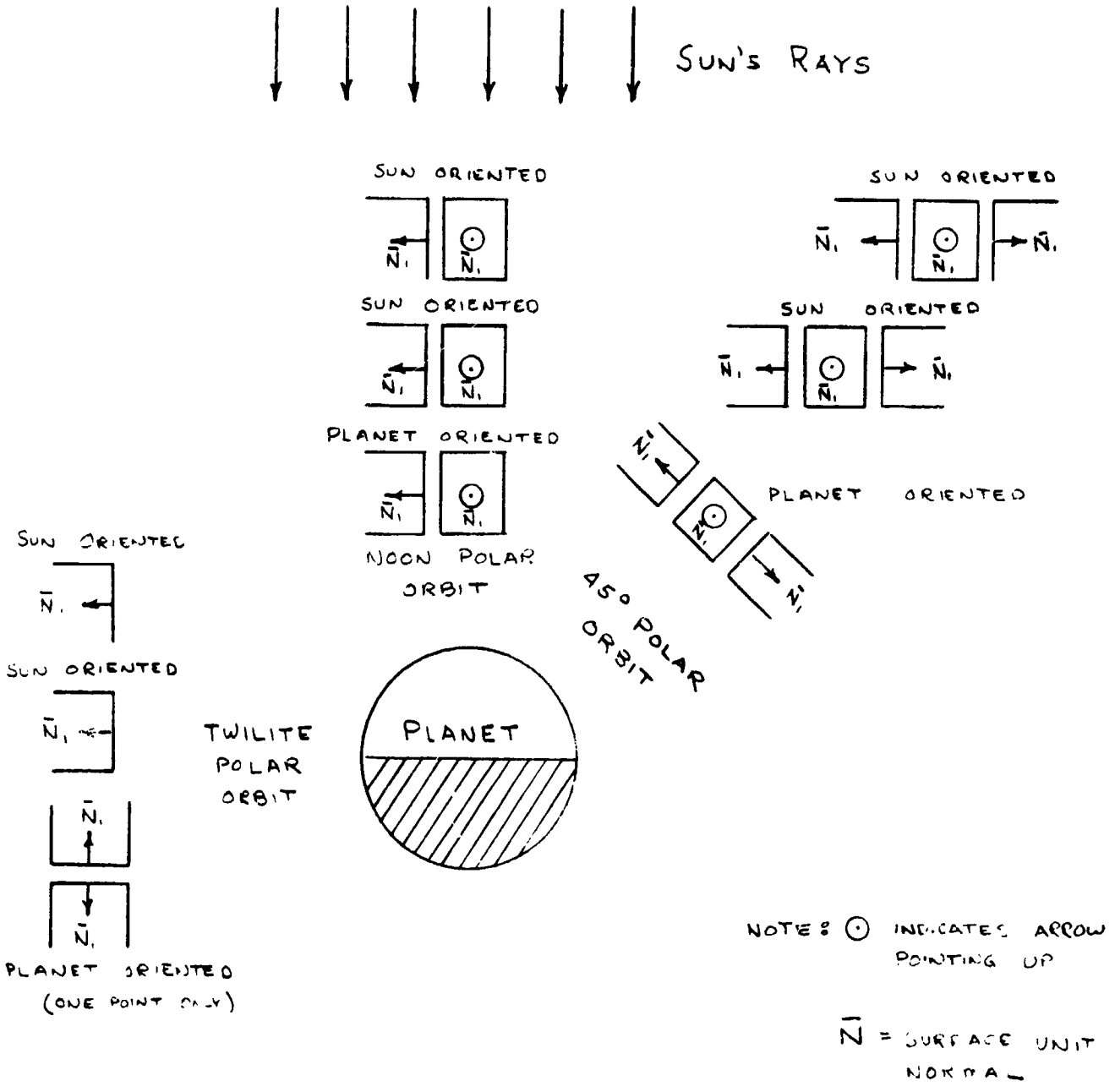

FIGURE 2 ~ ORIENTATIONS

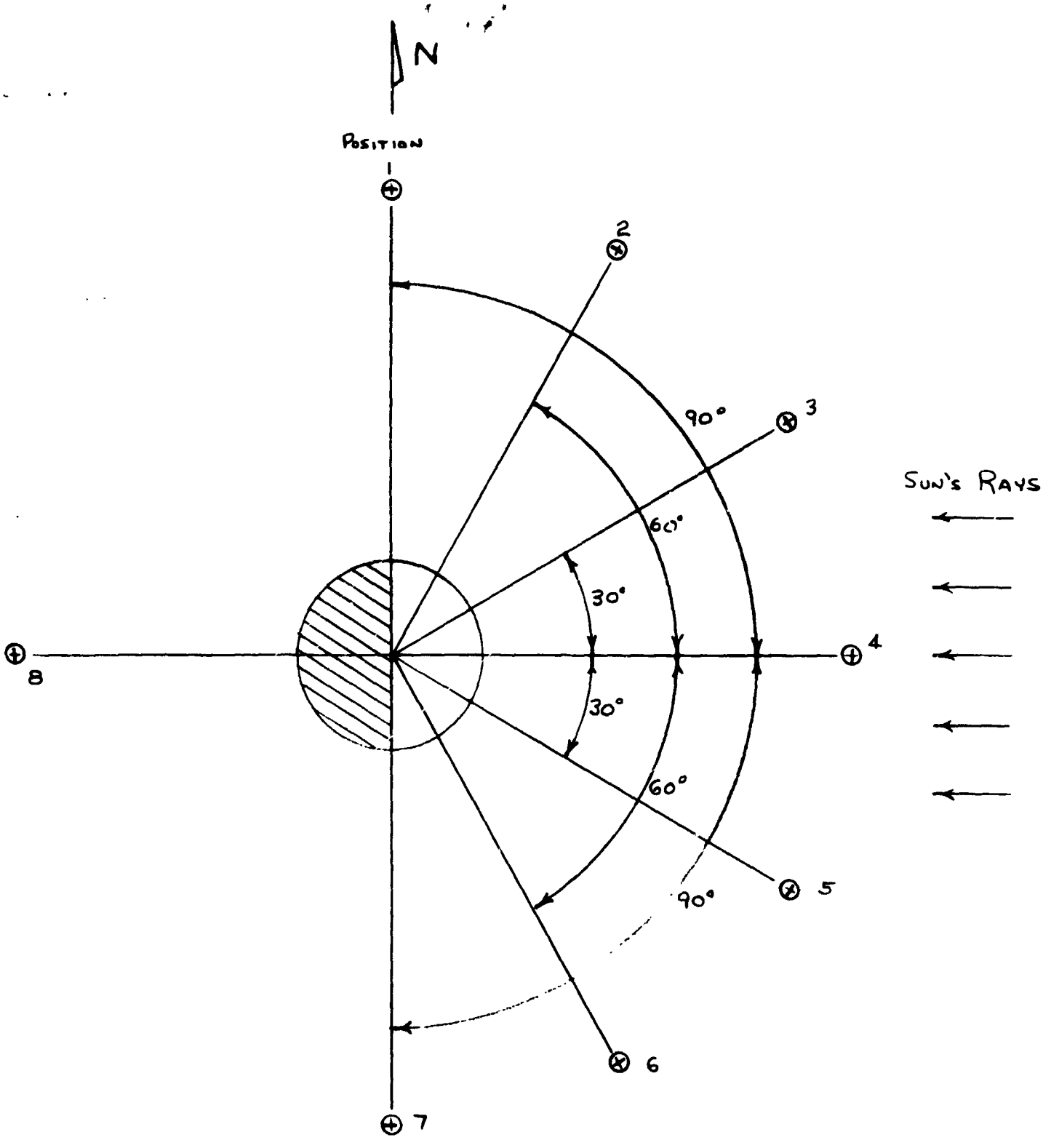

NOTE: THIS SET OF POSITIONS IS ROTATED CLOCK-WISE WHEN VIEWED FROM ABOVE THE NORTH POLE FOR THE 45° AND TWILITE ORBITS.

FIGURE 3 ~ POSITIONS

BASIC APPROACH

IN

JPL COMPUTER PROGRAMS

Frederick N. Magee

Jet Propulsion Laboratory

Pasadena, California

Numerical analysis methods for the solution of spacecraft heat transfer problems were not used to a significant degree at the Jet Propulsion Laboratory as of March, 1962. The computer program at the Laboratory at that time had been prepared for another application some years earlier and had been found to be unsatisfactory for spacecraft calculations. Since it was known that considerable effort in this area had been invested by various industrial concerns, it seemed appropriate to examine and compare their methods to assure that the utmost advantage was taken of this experience. Uppermost in mind was the fact that the personnel who would derive the greatest utility from this tool were unacquainted with computer programs. Therefore, the absolute minimum of familiarization time was necessary and the routine selected should not be so completely automatic as to make it merely a "numbers game".

The following criteria were established as a basis for evaluation:

1. Simplicity--simplicity should be sacrificed only at the expense of actual computation time or accuracy. Even then trade-offs should be carefully examined.
2. Input formats should be highly systemized. Clear, concise form sheets together with a code key chart to follow.
3. Assure that data input interpretations by the key punch operator are minimized.
4. Double storage of any input data will permit external checking by a simple sub-routine.
5. Output format should always include a print-out of the input data.

The routine format finally chosen was that employed by the Hughes Aircraft Co. essentially due to the program simplicity and the fact that explicit and implicit (transient and steady-state) solutions could be obtained from the same input data "package".

The input package consists of:

1. Problem identification.
2. Time information.
3. Initial temperatures (T).
4. Heat capacitance (G).
5. Heat generated (internal) (Q).
6. Conductive heat connection (C).
7. Radiation heat connection (S).
8. Geometry data (how nodes are interconnected).

The program capacity is of the order of 500 "nodes" and to date problems of 250 to 300 nodes have been run without difficulty.

Necessity forced the development of additional features as our experience increased and specific needs were recognized.

The transient program can now monitor the temperature of any desired node and output the quantity of heat required to maintain it within a specified temperature range. At a predetermined signal temperature a trigger can be activated to change certain thermal characteristics (such as conductivity, emissivity, absorptivity, heat capacitance) when necessary.

These features provide considerable latitude in examining the many complex problems inherent in the spacecraft thermal spectrum.

I cannot say with great certainty that the following basic question has been answered, but here is my humble attempt:

Why computing?

Ultimately to be able, through analysis, to define the complete temperature spectra of a spacecraft through all phases of its flight within the conventional limits of engineering accuracy. The two advantages are greatly reduced schedule time and cost. It is recognized that this goal is ambitious but should we aspire to less we would be remiss in attending our professional obligation.